ABSTRACT

Title of Document: INSULIN-LIKE GROWTH FACTOR-1 SIGNALING IN ENGINEERED ARTICULAR CARTILAGE

Diana Meeae Yoon, Ph.D., 2008

Directed By: Associate Professor John P. Fisher, Fischell Department of Bioengineering

Articular cartilage can easily become damaged or diseased and it does not have the ability to heal itself. A tissue engineering approach to regenerate cartilage is to integrate chondrocytes, the primary cell in cartilage, with biomaterials and biomolecules. Currently, there is limited knowledge on how all these factors influence the expression of upstream insulin-like growth factor-1 (IGF-1) signaling molecules. In an effort to better understand how IGF-1 and phenotypic, type II collagen, expression can be modified by altering construct properties, chondrocytes were embedded in alginate hydrogels. Increasing alginate concentration resulted in an upregulation of IGF-1 expression and by increasing cell density further enhanced IGF-1 expression. Additional changes in chondrocyte signaling were observed when exogenously delivering IGF-1 to the constructs. IGF-1 expression decreased while the receptor for IGF-1 (IGF-1R) expression as well as type II collagen increased in the presence of excess IGF-1 indicating that it has a key role in IGF-1 and

chondrocyte interaction. An extracellular matrix molecule, such as hyaluronic acid (HA), provides anchorage sites for chondrocytes and therefore the influence of HA on IGF-1 signaling was also investigated. The incorporation of HA created a dual affect by entrapping exogenously delivered IGF-1 as well as directly interacting with chondrocytes. As a result, the IGF-1 expression levels varied depending on HA concentration and there was also a lack of correlation with IGF-1R expression. The upregulated expression of type I collagen, a fibroblastic marker, by chondrocytes indicated that HA can overcome the beneficial affects of IGF-1. These *in vitro* works were also compared to an *in vivo* study. Alginate/HA constructs with embedded chondrocytes were pre-cultured with IGF-1 and then subcutaneously implanted into mice. Similar levels of type II collagen were observed for the constructs. However, by increasing the HA content a decrease in IGF-1 synthesis occurred with an increase in type I collagen staining. Pre-incubating the samples with IGF-1 led to a further decrease in IGF-1 production but was able to reverse the affects of HA on type I collagen expression. This research demonstrates that construct properties can alter endogenous IGF-1 signaling and overall shows the importance of understanding these details when engineering an articular cartilage construct.

INSULIN-LIKE GROWTH FACTOR-1 SIGNALING IN ENGINEERED ARTICULAR CARTILAGE

By

Diana Meeae Yoon

Dissertation submitted to the Faculty of the Graduate School of the
University of Maryland, College Park, in partial fulfillment
of the requirements for the degree of
Doctor of Philosophy
2008

Advisory Committee:
Associate Professor John P. Fisher, Chair
Assistant Professor Jose Helim Aranda-Espinoza
Professor William E. Bentley
Professor Peter Kofinas
Professor David M. Mosser

© Copyright by
Diana Meeae Yoon
2008

Dedication

I dedicate this work to my Appa and Umma.

Acknowledgements

I would like to thank my advisor, Dr. John P. Fisher, for giving me the opportunity to work in his lab. I really appreciate your guidance during my graduate career and also providing a tremendous amount of new research experiences that I will forever remember. Also, I would like to thank my committee members for their advice and support in the completion of this work. I am very greatful to Dr. Sabine Francke-Carroll, John J. Murone, and Emily C. Hawkins for their endless help in teaching me histology. Thanks to Dr. Srinivasa R. Raghavan for allowing me to use your lyophilization equipment. To Dr. A. Hari Reddi and Shane Curtiss at the University of California Davis Medical Center (UCDMC) – Center for Tissue Regeneration and Repair, I appreciate all of your help and guidance during the *in vivo* study. Additionally, thank you to the Orthopaedic Laboratory at UCDMC for being so welcoming and friendly during my stay in California. To all the members in the Tissue Engineering and Biomaterials Laboratory, thank you for all your helpful criticisms and suggestions especially during the late night lab sessions. A special thanks to the Fischell Department of Bioengineering for awarding me the Fischell Fellowship in Biomedical Engineering to help fund my graduate career. To all the friends that I have met along the way, I would not have been able to complete this journey without all the fun and laughter that you all have brought into my life. Finally to my parents and sister, thank you for your love and continuous support throughout all of my endeavors.

Table of Contents

Dedication ii
Acknowledgements iii
Table of Contents iv
List of Tables vii
List of Figures viii
1 Introduction 1
2 Background – Engineering Articular Cartilage 4
2.1 Articular Cartilage and Chondrocyte Signaling* 4
2.1.1 Introduction 4
2.1.2 Biology of Articular Cartilage 6
2.1.3 Basic Principles of Cellular Signaling 8
2.1.4 Native Effectors on Chondrocyte Signaling 9
2.1.4.1 Extracellular Matrix 9
2.1.5 Signaling Molecules of Chondrocytes 11
2.1.5.1 Growth Factors 12
2.1.5.2 Catabolic Growth Factors/Cytokines 22
2.1.6 Tissue Engineering Approaches to Regulate Signaling 25
2.1.7 Summary 29
2.2 Polymeric Scaffolds for Tissue Engineering Applications* 31
2.2.1 Introduction 31
2.2.2 Natural Polymers for Scaffold Fabrication 31
2.2.2.1 Polysaccharides 32
2.2.2.2 Polypeptides 36
2.2.3 Synthetic Polymers for Scaffold Fabrication 38
2.2.3.1 Polyesters 38
2.2.3.2 Other Synthetic Polymers 43
2.2.4 Scaffold Design Properties 46
2.2.4.1 Fabrication 46
2.2.4.2 Micro-structure 48
2.2.4.3 Macro-structure 49
2.2.4.4 Biocompatibility 50
2.2.4.5 Biodegradability 51
2.2.4.6 Mechanical Strength 52
2.2.5 Summary 52
3 Effect of Construct Properties on Encapsulated Chondrocyte Expression of Insulin-like Growth Factor-1* 58
3.1 Introduction 58
3.2 Materials and Methods 59
3.2.1 Cartilage Extraction and Chondrocyte Isolation 59
3.2.2 Chondrocyte Encapsulation in Alginate and Culture 60
3.2.3 Alginate Water Content 61
3.2.4 Cell Viability 61
3.2.5 Histological Preparation 62
3.2.6 Chondrocyte Distribution Analysis 62

3.2.7 RNA Isolation 63
3.2.8 Quantitative Reverse Transcriptase Polymerase Chain Reaction (qRT-PCR) 63
3.2.9 Western Blotting 64
3.2.10 Statistical Analysis 65
3.3 Results 65
3.3.1 Physical Characterization of Encapsulated Chondrocytes in Alginate Beads 65
3.3.2 IGF-1 mRNA Expression 67
3.3.3 Type II Collagen mRNA Expression 68
3.3.4 IGF-1 and Type II Collagen Protein Expression 69
3.4 Discussion 69
3.5 Conclusion 72
4 Effects of Exogenous IGF-1 Delivery on the Early Expression of IGF-1 Signaling Molecules by Alginate Embedded Chondrocytes* 84
4.1 Introduction 84
4.2 Materials and Methods 86
4.2.1 Cartilage Extraction and Chondrocyte Isolation 86
4.2.2 Chondrocyte Encapsulation in Alginate and Culture 87
4.2.3 RNA Isolation 88
4.2.4 DNA Isolation and Quantification 88
4.2.5 Histology 88
4.2.6 Histochemical Staining 89
4.2.7 Immunohistochemistry 89
4.2.8 Quantitative Reverse Transcriptase-Polymerase Chain Reaction (qRT-PCR) 90
4.2.9 Statistical Analysis 91
4.3 Results 91
4.3.1 Physical Characterization of Embedded Chondrocytes 91
4.3.2 mRNA Expression of Endogenous IGF-1 Signaling Molecules 92
4.3.3 mRNA Expression of Phenotypic Matrix Proteins 93
4.3.4 IGF-1 and Type II Collagen Protein Expression 94
4.4 Discussion 95
4.5 Conclusions 99
5 Hyaluronic Acid Interferes with IGF-1 Signaling Among Alginate Embedded Chondrocytes 111
5.1 Introduction 111
5.2 Materials and Methods 113
5.2.1 Materials 113
5.2.2 Methods 114
5.2.2.1 Cartilage Extraction and Chondrocyte Isolation 114
5.2.2.2 Chondrocyte Encapsulation and Culture 114
5.2.2.3 RNA Isolation 115
5.2.2.4 DNA Isolation and Quantification 115
5.2.2.5 Histology 116
5.2.2.6 Histochemical Staining 116

5.2.2.7 Immunohistochemistry 116
5.2.2.8 Quantitative Reverse Transcriptase-Polymerase Chain Reaction (qRT-PCR) 117
5.2.2.9 Release of IGF-1 in Alginate/HA Hydrogels....118
5.2.2.10 Statistical Analysis....118
5.3 Results....118
5.3.1 Hyaluronic Acid Entanglement in Alginate.... 118
5.3.2 CD44 mRNA Expression.... 119
5.3.3 Endogenous mRNA Expression of IGF-1 Signaling Molecules 120
5.3.4 mRNA Expression of Phenotypic Matrix Proteins.... 121
5.3.5 CD44, IGF-1, Type II Collagen, and Type I Collagen Protein Expression.... 122
5.3.6 Release of IGF-1 in Alginate/HA Hydrogels.... 122
5.4 Discussion....123
5.5 Conclusions....128
6 *In Vivo* Investigation of IGF-1 Delivery Effects on Chondrocytes Embedded in an Alginate/Hyaluronic Acid Hydrogel 141
6.1 Introduction....141
6.2 Materials and Methods....142
6.2.1 Materials 142
6.2.2 Methods.... 143
6.2.2.1 Cartilage Extraction and Chondrocyte Isolation....143
6.2.2.2 Chondrocyte Encapsulation and Culture 143
6.2.2.3 Implantation 144
6.2.2.4 Histology....145
6.2.2.5 Histochemical Staining 145
6.2.2.6 Immunohistochemistry 145
6.2.2.7 Histomorphometrical Analysis 146
6.2.2.8 Statistical Analysis....146
6.3 Results....147
6.3.1 Cell Morphology, Viability, and Proliferation.... 147
6.3.2 Glycosaminoglycan Production 147
6.3.3 Immunohistochemistry Analysis 149
6.4 Discussion....149
6.5 Conclusions....153
7 Summary 160
8 Conclusions 163
9 Future Works....165
10 Bibliography....167
11 Appendix A: Cell-to-Cell Distance Calculation....187

List of Tables

Table 2.1. Abbreviations for proteins involved in chondrocyte signaling.....5

Table 2.2. Properties of degradable natural homopolymers that have been utilized in the fabrication of tissue engineering scaffolds. 54

Table 2.3. Properties of degradable synthetic homopolymers that have been utilized in the fabrication of tissue engineering scaffolds. 55

Table 3.1. Primer and Probe Sequences for Quantitative RT-PCR. 73

List of Figures

Figure 2.1. Integrin signaling pathway of chondrocytes. Integrins interact with ECM proteins to phosphorylate Shc and/or FAK proteins. These molecules lead to the activation of the MAPK, PI3K, p38, and/or JNK pathways. 10

Figure 2.2. Signaling cascade of IGF-1. IGF-1 growth factors activate the β subunits of IGF-1R, which translocates proteins to the integrin to active the MAPK, PI3K, p38, and/or JNK pathway. 14

Figure 2.3. Scheme of the TGF-β superfamily activation pathway. Type I and II receptors integrate together after the adherence to TGF-β proteins. This results in the phosphorylation of R-Smads. I-Smads act as intracellular antagonists to regulate the Smad signaling pathway. Co-Smads aid in the translocation of R-Smads into the nucleus, which affects chondrocyte gene expression. 15

Figure 2.4. The transduction of the IL-1 pathway by chondrocytes. IL-1 can be bound to the IGF-1RII antagonist, which is present within the plasma membrane and in soluble form. Additionally, IL-1ra prevents IL-1 from adhering to its respective receptor, IL-1RI. The activation of IL-1RI results in either the activation of MAPK, JNK, p38, and/or NF-κB pathways. 23

Figure 2.5. Repeating structural unit of degradable natural homopolymers under investigation as scaffold materials for tissue engineering applications. (*Collagen and gelatin have variable sequences, but are predominately glycine, proline, and hydroxyproline. **Silks have a glycine rich sequence, with glycine repeating every second or third amino acid residue. The variable residues are primarily alanine or serine.)....56

Figure 2.6. Repeating structural unit of degradable synthetic homopolymers under investigation as scaffold materials for tissue engineering applications. 57

Figure 3.1. Percentage of water content in 0.8%, 1.2%, and 2.0% w/v alginate bead concentrations. The means and standard deviations are reported (n = 3). 74

Figure 3.2. Percentage of chondrocyte viability when encapsulated in 0.8%, 1.2%, and 2.0% w/v alginate bead concentrations for 25,000 and 100,000 cell density over the 8 d study. The means and standard deviations are reported (n = 3). 75

Figure 3.3. Microscopy images of 2.0% w/v alginate beads with (a) 25,000 chondrocytes/bead and (b) 100,000 chondroctyes/bead at day 1 in two different magnifications. The scale bars are located in the bottom right hand corner of each image. 76

Figure 3.4. Hematoxylin and eosin stained sections of 1.2% w/v alginate bead with (a) 25,000 and (b) 100,000 chondrocyte density encapsulated after 8 and 4 d of culture, respectively. The alginate matrix stained with a light violet hue, while the chondrocytes stained darker purple. The scale bars are located in the top right hand corner of each image. 77

Figure 3.5. Average number of cells per area determined from hematoxylin and eosin stained 1.2% w/v alginate beads at 25,000 and 100,000 chondrocyte densities. Both cell densities investigated are associated with a homogenous cell distribution throughout the alginate bead. The means and standard deviations are reported (n = 3). 78

Figure 3.6. IGF-1 mRNA expression for 0.8%, 1.2%, and 2.0% w/v alginate hydrogels with an initial chondrocyte density of 25,000 cells per bead over 8 d. An increase in IGF-1 mRNA expression by encapsulated chondrocytes occurs for all alginate concentrations from day 1 to 8. The calibrator for all the samples tested for IGF-1 expression is indicated by (◆). The means and standard deviations are reported (n = 3). 79

Figure 3.7. IGF-1 mRNA expression for 0.8%, 1.2%, and 2.0% w/v alginate hydrogels with an initial chondrocyte density of 100,000 cells per bead over 8 d. In general, chondrocytes encapsulated in all alginate bead concentrations increased their mRNA expression of IGF-1 over 8 d. The means and standard deviations are reported (n = 3). 80

Figure 3.8. Type II collagen mRNA expression for 0.8%, 1.2%, and 2.0% w/v alginate hydrogels with an initial chondrocyte density of 25,000 cells per bead over 8 d. Chondrocytes sustain their mRNA expression of type II collagen in various alginate bead concentrations. The calibrator for all the samples tested for type II collagen expression is indicated by (●). The means and standard deviations are reported (n = 3). 81

Figure 3.9. Type II collagen mRNA expression for 0.8%, 1.2%, and 2.0% w/v alginate hydrogels with an initial chondrocyte density of 100,000 cells per bead over 8 d. Phenotypic type II collagen mRNA expression of encapsulated chondrocytes within all alginate bead

concentrations is observed. The means and standard deviations are reported (n = 3). 82

Figure 3.10. Dot blots of intracellular protein samples from a density of 25,000 (A, C and E) and 100,000 (B, D and F) chondrocytes/bead as well as all alginate concentrations, 0.8% w/v (A and B), 1.2% w/v (C and D), and 2.0% w/v (E and F). These samples are taken from day 1, 4, and 8 time points, where (a) indicates IGF-1 protein amounts and (b) shows type II collagen levels.....83

Figure 4.1. The dry weight of alginate beads for the 0, 10, 50, and 100 ng/mL IGF-1 groups. The means and standard deviations are reported (n = 3, ∗ indicates $p < 0.01$). 101

Figure 4.2. Safranin-O/Fast Green stained sections at (a) day 1 for 50 ng/mL IGF-1 group, (b) day 8 for 0 ng/mL IGF-1 group, (c) day 8 for 10 ng/mL IGF-1 group, (d) day 8 for 50 ng/mL IGF-1 group, and (e) day 8 for 100 ng/mL IGF-1 group. Alginate beads are a bright orange color, while the matrix proteins are shown with an arrow (light orange hue), and chondrocytes are shown with double arrows (gray hue). Scale bars are located on the bottom right corner of each image. 102

Figure 4.3. DNA content per bead for all sample groups over the course of 8 days. There is an increasing trend of DNA for all groups during the length of the study. However, no differences in DNA levels were seen between all the groups at each time point. The means and standard deviations are reported (n = 3).....103

Figure 4.4. IGF-1 mRNA expression for all sample groups over 8 days. Results indicate that at day 8, IGF-1 induced samples had lower levels of gene expression compared to the control group. The means and standard deviations are reported (n = 3, ∗ indicates $p < 0.01$). 104

Figure 4.5. IGF-1R mRNA expression for all sample groups over 8 days. An increased level of expression occurred in the experiment groups versus the control group at day 8. The means and standard deviations are reported (n = 3, ∗ indicates $p < 0.01$). The labels ‡ and # indicate no statistical differences among the group. 105

Figure 4.6. IGFBP-3 mRNA expression for all sample groups over 8 days. A decrease in IGFBP-3 expression occurred for all groups by 8 days. The means and standard deviations are reported (n = 3, ∗ indicates $p < 0.01$). The labels ‡ and # indicate no statistical differences among the group. 106

Figure 4.7. Type II collagen mRNA expression for all sample groups over 8 days. Chondrocytes sustained their expression for the experimental groups by day 8, while a decrease in expression occurred for the control group. The means and standard deviations are reported (n = 3, ∗ indicates $p < 0.01$). The labels ‡ and # indicate no statistical differences among the group. 107

Figure 4.8. Type I collagen mRNA expression for all sample groups over 8 days. A higher level of expression occurred in the control group versus the experimental groups by the day 8 time point. The means and standard deviations are reported (n = 3, ∗ indicates $p <$ 0.01). 108

Figure 4.9. IGF-1 immunohistochemistry staining at (a) day 1 for 100 ng/mL IGF-1 group, (b) day 8 for 0 ng/mL IGF-1 group, (c) day 8 for 10 ng/mL IGF-1 group, (d) day 8 for 50 ng/mL IGF-1 group, (e) day 8 for 100 ng/mL IGF-1 group, and (f) a negative staining control. The clusters stained with greater intensity at day 8 compared to the single cells at day 1. Scale bars are located on the bottom right corner of each image. 109

Figure 4.10. Type II collagen immunohistochemistry staining for (a) day 1 for 100 ng/mL IGF-1 group, (b) day 8 for 0 ng/mL IGF-1 group, (c) day 8 for 10 ng/mL IGF-1 group, (d) day 8 for 50 ng/mL IGF-1 group, (e) day 8 for 100 ng/mL IGF-1 group, and (f) a negative staining control. The presence of type II collagen seems to be greater at day 8 for the groups that received exogenous IGF-1. Scale bars are located on the bottom right corner of each image. 110

Figure 5.1. Nanogram DNA levels per bead for all sample groups over the experimental time course of 8 days. There is no significant difference in DNA levels among each of groups at each time point. The means and standard deviations are reported (n = 3). 130

Figure 5.2. The alginate/HA bead dry weights were measured for the following groups during the time course of the experiment: 0, 0.05, 0.50, and 5.00 mg/mL HA. The means and standard deviations are reported (n = 3, ∗ indicates $p < 0.01$). 131

Figure 5.3. Safranin-O and Fast Green stained sections at day 1 and day 8 for 0 mg/mL HA, 0.05 mg/mL HA, 0.50 mg/mL HA, and 5.00 mg/mL HA. Alginate stains into an intense orange color, hyaluronic acid becomes a lighter orange hue, and chondrocytes a shade of gray. Scale bars are located on the bottom right corner of each image. 132

Figure 5.4. CD44 mRNA expression for all sample groups over 8 days. Chondrocytes only expressed CD44 in the groups that contained hyaluronic acid in the alginate beads at day 4 and 8. There was no statistical difference in CD44 expression when there were different hyaluronic acid concentrations. The means and standard deviations are reported ($n = 3$, ∗ indicates $p < 0.01$). 133

Figure 5.5. Chondrocytes in all bead groups expressed IGF-1 at day 1, 4, and 8. Results indicate that at day 8, the 0 and 5.00 mg/mL HA samples had similar as well as the lowest level of IGF-1 expression compared to the 0.05 and 0.50 mg/mL HA groups. The highest level of expression was from the 0.05 mg/mL HA beads, followed by the 0.50 mg/mL HA group. The means and standard deviations are reported ($n = 3$, ∗ indicates $p < 0.01$). 134

Figure 5.6. All the groups expressed IGF-1R throughout the study. By day 8, the IGF-1R expression was lowest for the 0 mg/mL HA group compared to the other samples. The means and standard deviations are reported ($n = 3$, ∗ indicates $p < 0.01$). 135

Figure 5.7. IGFBP-3 mRNA expression for all sample groups over 8 days. A decrease in IGFBP-3 expression occurred for all groups by 8 days. The means and standard deviations are reported ($n = 3$, ∗ indicates $p < 0.01$). 136

Figure 5.8. Type II collagen mRNA expression was sustained throughout the 8 day study for all the sample groups. However, a decreasing trend occurred by all the groups from day 1 to 8. At day 8, the 0 mg/mL HA case had the lowest type II collagen expression compared to the groups that contained hyaluronic acid. The means and standard deviations are reported ($n = 3$, ∗ indicates $p < 0.01$). 137

Figure 5.9. Type I collagen mRNA expression for all sample groups over 8 days. A higher level of expression occurred in the beads that contained hyaluronic acid versus the 0 mg/mL HA group by the day 8 time point. The means and standard deviations are reported ($n = 3$, ∗ indicates $p < 0.01$). 138

Figure 5.10. Immunohistochemistry staining at day 8 for CD44, IGF-1, type II collagen, and type I collagen. The 0, 0.05, 0.50, and 5.00 mg/mL HA groups are all represented here, as well as the negative staining control (NTC). Most of the staining occurred around the cluster of chondrocytes. Scale bars are located on the bottom right corner of each image. 139

Figure 5.11. IGF-1 diffusion through 0 mg/mL and 5.00 mg/mL HA alginate hydrogels. The 0 mg/mL HA released twice as much IGF-1 compared to the 5.00 mg/mL HA gels. The means and standard deviations are reported ($n = 3$, ∗ indicates $p < 0.01$). 140

Figure 6.1. A representative image of how the glycosaminoglycan areas were measured from a Safranin-O/Fast Green stained image. 154

Figure 6.2. H&E image from 0 mg/mL HA group with IGF-1 pre-culture at day 21. Chondrocytes were evenly distributed in the hydrogel and maintained their viability and rounded morphology throughout the experiment.....155

Figure 6.3. Chondrocytes were counted on Safranin-O/Fast Green stained images to determine cell proliferation throughout the study. Cell count per slide area was graphed for all the groups at day 7, 14, and 21. Chondrocytes were able to proliferate in all the cases. However by day 21, the 0.05 mg/mL HA (+) group had the greatest number of chondrocytes per area and the 0 mg/mL HA (-) group had the lowest. The means and standard deviations are reported ($n = 16$; ∗ indicates $p < 0.05$).....156

Figure 6.4. Glycosaminoglycan area was measured from Safranin-O/Fast Green stained samples. The total GAG area was calculated per slide area for each case at each timepoint. At day 21, the GAG area increased with higher HA content. The greatest GAG amount was measured in the 5.0 mg/mL HA group. The means and standard deviations are reported ($n = 16$; ∗ indicates $p < 0.05$).....157

Figure 6.5. The total GAG area per cell count was calculated for each group at day 7, 14, and 21. At day 21, the GAG production per chondrocyte was lowest in the 0 mg/mL HA and 0.5 mg/mL HA groups that were pre-cultured with IGF-1 (+). The means and standard deviations are reported ($n = 16$; ∗ indicates $p < 0.05$).....158

Figure 6.6. Immunohistochemical staining of IGF-1, type II collagen, and type I collagen for all the groups at day 7, 14, and 21. The 0, 0.5, and 5.0 mg/mL HA groups are all represented here, as well as the negative staining control (NTC). The scale bars are located on the bottom right hand corner for each image.....159

1 Introduction

Articular cartilage is located on the surface of articulating joints, such as those found in the knees. Damage of articular cartilage due to trauma and degenerative osteoarthritis often results in permanent injuries. This condition is partially due to the lack of vasculature in the tissue, which limits the ability for cartilage to properly heal. To date, the options for clinical treatment such as arthroscopic lavage, autografting, and allografting provide temporary relief but do not result in complete regeneration of cartilage. These inadequacies have prompted tissue engineers to seek other methods for repairing articular cartilage. To accomplish this task, tissue engineers must be able to harmoniously integrate the three major components of healthy tissues: cells, soluble growth factors and physical matrices for cellular support.

Chondrocytes are the primary cell type in articular cartilage. These cells express type II collagen, a phenotypic extracellular matrix marker, and insulin-like growth-factor (IGF-1), a soluble growth factor shown to increase cartilage matrix synthesis. Chondrocytes can be embedded in a degradable hydrogel to create an implantable tissue engineered construct. Currently, there is limited knowledge on how biomaterial properties affect chondrocyte expression of IGF-1 signaling molecules. Therefore, this research is focused on endogenous IGF-1 signaling by chondrocytes embedded in hydrogels.

Bio-polymers are commonly used as cellular scaffolds because it can provide temporary support for chondrocytes to grow cartilage. By using degradable polymers, newly formed tissue can eventually replace the graft to leave behind naturally developed healthy cartilage. Hydrogels are a common form of biomaterials to use because of their

similarity in water retention to cartilage. Additionally, in hydrogels chondrocytes are able to maintain their rounded morphology, which has been linked to increased type II collagen expression. Chondrocytes are known to remain viable in polymer hydrogels but interestingly material properties on chondrocyte signaling have been minimally studied. Alginate hydrogels were chosen as the biomaterial because it has minimal interaction with chondrocytes due to its lack of amine groups. As a result, individual components can be altered and chondrocytes signaling can be closely monitored in a 3-D environment. Preliminary studies indicate that chondrocytes within alginate hydrogels express IGF-1, while retaining type II collagen expression. Therefore, for this research we proposed the following objectives:

(1) Investigate the effect of alginate concentration and cell density on chondrocyte IGF-1 and type II collagen expression;

(2) Investigate the effect of exogenous IGF-1 concentration on endogenous IGF-1, IGF-1 receptor (IGF-1R), and IGF-1 binding protein-3 (IGFBP-3) expression as well chondrocyte phenotypic stability;

(3) Investigate the effect of hyaluronic acid content on IGF-1 delivery and endogenous IGF-1, IGF-1R, and IGFBP-3 expression as well as type II collagen and type I collagen expression;

(4) Investigate *in vivo* the effect of exogenous delivery of IGF-1 and hyaluronic acid concentration on glycosaminoglycan, IGF-1, type II collagen, and type I collagen protein expression.

Overall, this research will undertake the completion of these objectives to provide a novel approach to regenerate articular cartilage defects, specifically focusing on monitoring the expression of upstream IGF-1 signaling molecules by chondrocytes embedded within alginate hydrogels. By closely understanding how chondrocyte expressions can be controlled by construct properties, this will help improve the tissue engineering approach to regenerate articular cartilage.

2 Background – Engineering Articular Cartilage

*2.1 Articular Cartilage and Chondrocyte Signaling**

2.1.1 Introduction

The proper functionality of healthy tissue requires maintenance. Even after tissue has undergone trauma, it attempts to repair itself. However, there are tissues within the body that are unable to completely regenerate when inflicted with severe stress, such as articular cartilage. The field of tissue engineering can alleviate this problem by providing cells, biological molecules and scaffolding materials to facilitate regeneration of healthy tissue. In order to achieve this task, fundamental mechanisms of cartilage tissue function needs to be understood. Cartilage is composed of components, such as cells, proteins and macromolecules, which all play a role in maintaining the well-being of the tissue. There has been considerable evidence that the interaction of chondrocytes with proteins and extracellular matrix play an important role in the homeostasis of cartilage. This is a continuously evolving area of study as biologists are furiously discovering new details of the cellular signaling pathways involved in the communication of chondrocytes. Recent studies have implicated that alterations in the signaling pathways of chondrocytes can lead to osteoarthritis, a degenerative condition of articular cartilage. We propose that the success of tissue engineers involves understanding the intricacy of chondrocytes signaling mechanisms in order to maintain their proper function while in contact with biomaterial scaffolds. To this end, we first investigate the basic biology of articular cartilage. Then we will examine the activation of signaling pathways that occur by

---

***** This chapter was published as: Yoon DM and Fisher JP. Chondrocyte Signaling and Artificial Matrices for Articular Cartilage Engineering. Advances in Experimental Medicine and Biology. 2006; 585: 67-86.

chondrocytes due to the interaction with proteins (growth factors and cytokines) and extracellular matrix components (type II collagen, glycosaminoglycans and proteoglycans), which are listed in Table 2.1. Finally, we discuss the effects polymers of synthetic biomaterials.

Table 2.1. Abbreviations for proteins involved in chondrocyte signaling.

ACTR	activin receptor
ALK	activin-like receptor
AP1	activating protein 1
BMP	bone morphogenic protein
c-met	hepatocyte growth factor receptor
COX2	cyclooxygenase-2
DAN	differential screening-selected gene aberrative in neuroblastoma
ECM	extracellular matrix
EGF	epithelial growth factor
ERK	extracellular signal-regulated kinase
FADD	fas-activated death domain protein
FAK	focal adhesion kinase
FGF	fibroblastic growth factor
FGFR	fibroblastic growth factor receptor
Flt-1	fms-like tyrosine kinase
GAG	glycosaminoglycan
Grb2	growth factor receptor-binding protein 2
IGF	insulin-like growth factor
IGF-1R	insulin-like growth factor-1 receptor
IGFBP	insulin-like growth factor binding protein
IKK	inhibitor of NF-κB kinase
IL	interleukin
IL-1ra	interleukin-1 receptor antagonist
IL-1RacP	interleukin-1 receptor associated protein
IL-R	interleukin receptor
IRAK	interleukin-1 receptor activate kinase
IRS	insulin receptor substrate
I-κB	inhibitor of kappa B
JNK	c-Jun N-terminal protein kinase
KDR	kinase insert domain-containing receptor
MAPK	mitogen-activated protein kinase
MEK	mitogen-activated protein kinase kinase
MH2	mad homology 2
MMP	metallanoproteases
MyD88	adaptor protein
NF-κB	nuclear transcription factor-kappaB

NIK	NF-κB-inducing kinase
NRP-1	neutropilin-1
PDGF	platelet-derived growth factor
PDK	phosphatidylinositol 3-kinase-dependent kinases
PGE_2	prostaglandin E_2
PI3K	phosphatidylinositol 3-kinase
PKC	protein kinase C
Ras	rat sarcoma guanine triphosphatase
SH2	src homology 2
Shc	src homology 2 domain containing transforming protein 1
SOS	son-of-sevenless
Sox9	sex-determining region Y-related gene
Src	sarcoma
STAT	signal transducer and activator of transcription
TACE	tumor necrosis factor-converting enzyme
TGF	transforming growth factor
TNF	tumor necrosis factor
TNF-R	tumor necrosis factor receptor
TRADD	tumor necrosis factor receptor-associated death domain protein
TRAF	tumor necrosis factor receptor-associated factor
VEGF	vascular endothelial growth factor

2.1.2 Biology of Articular Cartilage

Articular cartilage is an avascular, alymphatic tissue that is predominately found on the surface of articulating joints [1, 2]. Its function is to provide protection and enable articulation of subchondral bone, allowing the joint to undergo compressive forces as well as smooth movement [3, 4]. This functionality may be attributed to the zonal architectural composition of articular cartilage, which is composed of extracellular matrix (ECM) components and chondrocytes. There are four subsections of articular cartilage known as the superficial, middle, deep and calcified zones [1, 4-6].

The main ECM components in articular cartilage are collagen, glycosaminoglycans (GAGs) and proteoglycans. Structural integrity of articular cartilage is sustained partially by the relationship of all the ECM components. The predominant

collagen found in articular cartilage is type II collagen, which provides an interconnected network of support through the mobile restriction of GAGs and proteoglycans [2, 4, 6-8]. Articular cartilage has two main types of GAGs: chondroitin sulfate and keratin sulfate [2, 9]. Proteoglycans are large protein core molecules that have numerous amounts of GAGs attached to it, comprising up to 95% of their composition [9]. Aggrecan and hyaluronic acid are the most prevalent proteoglycans in articular cartilage and are partially responsible for maintaining the integrity of articular cartilage under compressive forces [6, 9, 10]. Other smaller proteoglycans in articular cartilage include decorin, biglycan and perlecan [1, 2, 5, 11]. Glycosaminoglycans and proteoglycans are both negatively charged, allowing for continuous hydration of the tissue [4]. Thus, the water content in articular cartilage can comprise about 75% of the total weight [2, 4, 12]. This high water content, as well as a lack of vascularization of articular cartilage necessitates diffusion the leading mechanism for nutrient and waste exchange between chondrocytes and the synovial fluid.

The extracellular matrix is the structural component of articular cartilage that provides a framework for cell viability and function. Chondrocytes, which are the primary cell in articular cartilage, comprise only 5% of cartilage volume [2, 4, 13]. They have a unique physical appearance in that they maintain a spherical morphology. Chondrocytes also provide the necessary homeostasis for healthy articular cartilage by communicating with both the ECM and soluble proteins within and surrounding the tissue [4]. These interactions are controlled by protein receptors, which are located within the plasma membrane of chondrocytes. Each receptor has specific affinity for their respective ligand, which is crucial to cellular signaling.

Like most tissue, articular cartilage can become diseased or damaged. One of the most common articular cartilage diseases is known as osteoarthritis. In this state, articular cartilage is more fibrous and contain higher levels of type I collagen and type X collagen versus type II collagen [8, 12, 14, 15]. Additionally, the appearance of chondrocytes seems to be more fibroblastic in shape rather than spherical [14]. In order to repair osteoarthritic cartilage it is vital to understand how chondrocytes maintain the balance of growth factors necessary to create a healthy extracellular matrix. Finally, it is critical to understand how chondrocytes interact with the extracellular matrix itself.

2.1.3 Basic Principles of Cellular Signaling

The functions of chondrocytes are stimulated during their attachment to the extracellular matrix or specifically when an extracellular signaling molecule binds to a receptor. These extracellular interactions start a cascade of steps that eventually leads to cellular effects of the cytoskeleton, gene expression, and metabolism. A general outline of a signal cascade starts with an extracellular signal that attaches to a receptor protein within the plasma membrane of the cell [16-18]. Cell surface receptors are proteins located within the plasma membrane. Their basic structure contains an amino terminus, transmembrane domain, and carboxyl tail. The attachment of extracellular signaling molecules to the amino terminus of the receptor results in the release or activation of intracellular signaling molecules by the cytoplasmic side of the receptor [19]. The intracellular signaling molecules then interact with target proteins to further relay its signal. There are multitudes of signaling pathways that can lead to either results in the same or different outcomes [20]. Furthermore, these pathways are integrated with one

another [16]. Additionally, there are a variety of regulatory proteins present in the areas such as the extracellular matrix and cytoplasm of the cell.

2.1.4 Native Effectors on Chondrocyte Signaling

2.1.4.1 Extracellular Matrix

The structural integrity and properties of articular cartilage is partially due to the extracellular matrix. Chondrocytes are responsible to maintain compounds in the ECM, such as type II collagen and aggrecan. Conversely, chondrocytes need the ECM to function. This is mediated by integrin receptors within the cell membrane of chondrocytes that become activated when bound to the ECM [10, 11, 21-23]. Additionally, integrin signaling can affect growth factor and cytokine receptors [22, 24].

Integrins are glycoproteins that contain α and β subunits that have an influence in signal transduction and cell shape [18, 25, 26]. The response of the integrin is controlled by both the extracellular and cytoplasmic domains. However, the β subunits interact with cytoskeletal proteins to activate various signaling cascades (Figure 2.1). Signaling through integrins depends on the formation of focal adhesions, where cytoskeletal and other proteins are concentrated at the surface of the plasma membrane. Aggregation of these focal adhesions activates the FAK and Shc pathways. Intracellular activation of FAK involves its phosphorylation by β subunit of the integrin. This activation allows FAK to attach to the Src homology 2 (SH2) domains of the Src proteins [22]. FAK has been found to affect the JNK, MAPK, p38 and PI3K pathways [22]. The activation of the Shc pathway is initiated by the phosphorylation of the Shc protein when in contact with an integrin attached to the extracellular matrix. This results in the recruitment of

Grb2 and SOS proteins that eventually attach to a Ras protein, responsible for activating the MAPK pathway.

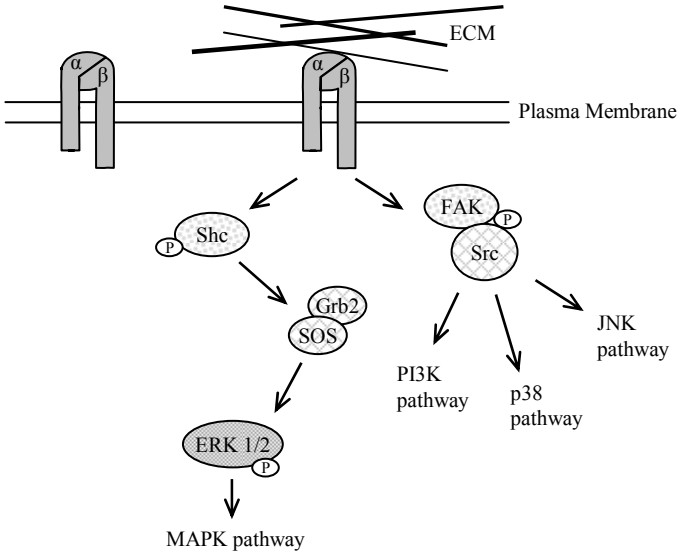

Figure 2.1. Integrin signaling pathway of chondrocytes. Integrins interact with ECM proteins to phosphorylate Shc and/or FAK proteins. These molecules lead to the activation of the MAPK, PI3K, p38, and/or JNK pathways.

The most predominant integrin expressed by chondrocytes is the α5β1, which is known to be a fibronectin receptor [24, 25, 27, 28]. However, α5β1 has also been found to interact with type II collagen [27]. Other integrins that interact with type II collagen are α1β1, α2β1, and α10β1 [24, 28]. β1 integrins have a vital role in the relationship of chondrocytes to the ECM and have been identified in cartilage [11, 23, 28, 29]. Chondrocyte attachment to type II collagen through integrins α1β1, α2β1, and α3β1 has recently been identified and is critical to chondrocyte survival [24, 27, 30]. Others have stated that α1 and β3 integrins are not expressed by chondrocytes and α2 expression is low in the presence of type II collagen [23]. Another well known integrin receptor is CD44, which interacts with hyaluronan and has been found to be highly expressed in cartilage [10, 11]. The interaction of chondrocytes with fibronectin resulted in higher

phosphorylation levels of FAK and ERK 1/2 protein compared to when the cells were in suspension.[24] When chondrocytes are in contact with insulin-like growth factor-1 protein and type II collagen, the production of the Shc, Grb2 and ERK 1/2 proteins increased.[31] However, the presence of these respective proteins was less apparent when chondrocytes were attached to type I collagen surfaces in the presence of IGF-1. These results indicate that there is an interactive merging of integrins and growth factor signaling pathways.

2.1.5 Signaling Molecules of Chondrocytes

An initiator for cellular signaling is an extracellular signaling molecule, allowing cells to communicate amongst each other. There are several different signaling transportation mechanisms: autocrine, paracrine, and endocrine. A cell that releases signaling molecules that bind to receptors from the same cell is known autocrine signaling. When a signal acts as a local mediator to neighboring cells it is referred to as paracrine signaling. Finally, endocrine signaling involves ligands being distributed throughout the body. Extracellular signaling molecules function is mediated by its binding to its receptor within the plasma membrane of the cell. However, the extracellular signaling molecules are inhibited by antagonists, binding proteins that block the signaling protein's ability to bind a cell surface receptor. Most ligands have extracellular antagonists that can inhibit their function. A balance must exist between the signal concentration, antagonist concentration, and their affinities for one another. Additionally, extracellular signaling molecules can become degraded by enzymes as well as immobilized within the ECM.

Chondrocytes synthesize and express various proteins referred to as growth factors, which affect their function. The two main types of growth factors are anabolic and catabolic. Anabolic growth factors enable chondrocytes to produce the necessary proteins to maintain its environment. Catabolic growth factors do the opposite in that they degrade molecules within the extracellular matrix. The interplay between these two types of growth factors is necessary in order to maintain homeostasis for articular cartilage through the initiation of appropriate signaling pathways.

2.1.5.1 Growth Factors

Insulin-like Growth Factor-1

In articular cartilage, insulin-like growth factor-1 (IGF-1) is a dominant growth factor that leads to type II collagen, hyaluronan and aggrecan synthesis [2, 14, 32-35]. Additionally, IGF-2 has also been found to affect the proteoglycan synthesis [36]. Insulin-like growth factor is a protein that has similar homology to insulin [37]. More specifically, IGF-1 is a small soluble protein with a molecular weight of 7.5 kDa [38-40]. Normal versus reparative cartilage show a lower response to IGF [41]. In the extracellular part of chondrocytes, IGF-1 is bound to an antagonist that maintains its stability. There are 6 known IGF binding proteins (IGFBP) in cartilage, which can bind to extracellular matrix proteins [34, 42, 43]. The most predominant is IGFBP-3, which has a high affinity for IGF-1.[39, 40, 43, 44] IGFBP-3 has been found in both normal and osteoarthritic cartilage [36, 45]. However, its degradation is more apparent in cartilage that is damaged. It has been found that IGFBP-3 has a higher affinity for IGF-1 than its receptor, IGF-1R. These binding proteins regulate the availability of the IGF-1. In order for IGF-1 to bind to IGF-1R, the binding protein must undergo proteolytic cleavage [38,

43]. IGF-1R is a heterodimeric protein, containing two α and two β subunits that are attached by disulfide bonds [37, 39, 40].

The binding of IGF-1 to the α subunits activates the β subunits to initiate several intracellular signaling pathways (See Figure 2.2) [39, 40]. The tyrosine kinases of insulin receptor substrates (IRS) can become activated as well as Shc proteins by phosphorylation. Insulin receptor substrates lead to the activation of PI3K and MAPK pathways by binding to Grb2/SOS proteins. When the Ras attaches to a Raf protein this initiates the MEK1/2 and then ERK1/2. Both IRS and Shc lead to the same pathway. Besides the MAPK pathway it can go through the JNK and p38 pathway. Conversely, IGF-1 has been observed not to activate JNK or p38 proteins [46]. For the PI3K pathway, the p85 and p110 subunits of PI3 kinase activate PDK1 and PDK2 to move and phosphorylate an Akt protein located within the membrane. By activation of the PI3K pathway by IGF-1, chondrocyte have been found to express type II collagen and proteoglycans [39, 40]. Additionally, this has shown to inhibit nitric oxide production, which is stimulated through the p38, ERK1/2 and PKC pathways [39, 40]. The inhibition of nitric oxide is implicated in the reduction of apoptosis.

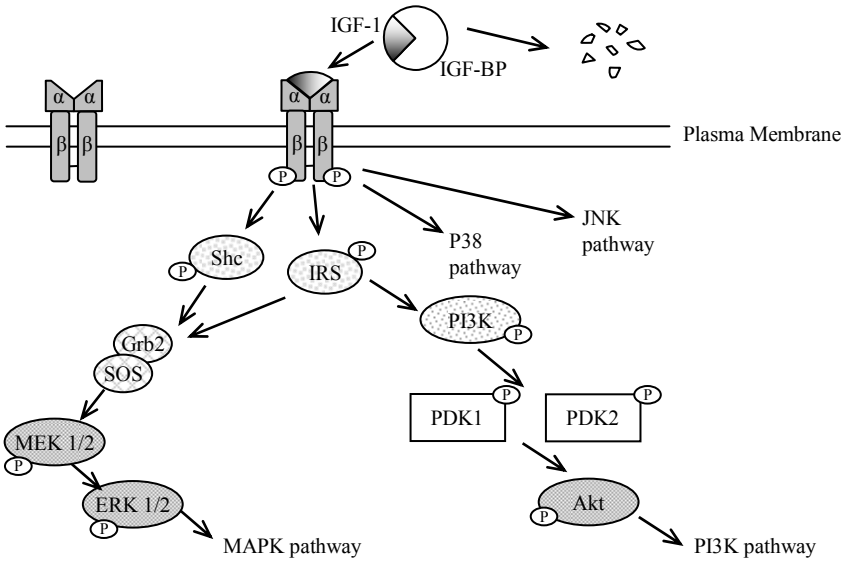

Figure 2.2. Signaling cascade of IGF-1. IGF-1 growth factors activate the β subunits of IGF-1R, which translocates proteins to the integrin to active the MAPK, PI3K, p38, and/or JNK pathway.

Transforming Growth Factor-β Superfamily

There are several ligands within the class of the transforming growth factor-β (TGF-β) superfamily. In chondrocytes, the two major types are TGF-β1 and bone morphogenic proteins (BMPs). Both of these ligands interact with two receptors, type I and type II, which are both required to transduce an intracellular signaling response [47]. When a ligand adheres to the dimeric type II receptor, it causes the formation of a heterotetrameric complex with the dimeric type I receptor. The activation of the type I receptor through phosphorylation of its serine/threonine kinase domains in the intracellular domain initiates the signaling cascade [48]. Since the type II receptor is constantly in an active state, the type I receptor recruits the specific proteins (Figure 2.3).

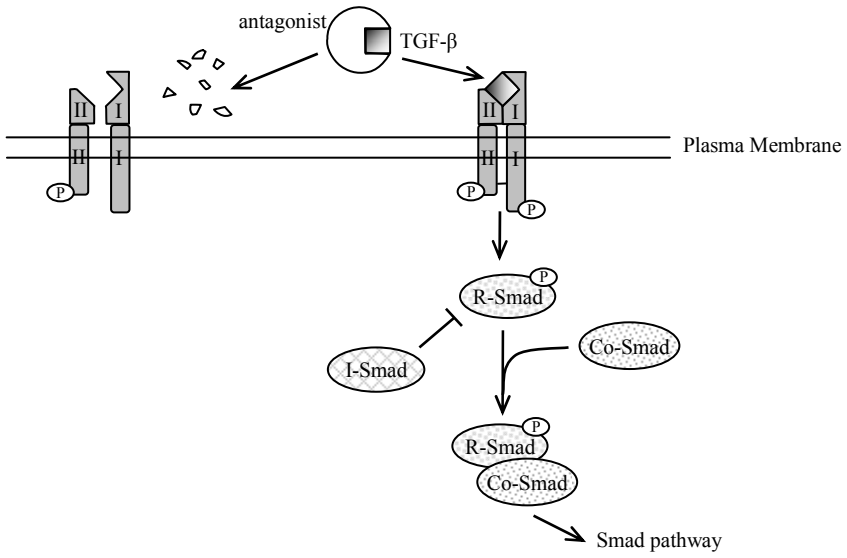

Figure 2.3. Scheme of the TGF-β superfamily activation pathway. Type I and II receptors integrate together after the adherence to TGF-β proteins. This results in the phosphorylation of R-Smads. I-Smads act as intracellular antagonists to regulate the Smad signaling pathway. Co-Smads aid in the translocation of R-Smads into the nucleus, which affects chondrocyte gene expression.

Most commonly in this pathway, the first intracellular proteins involved are Smad proteins. There are three types of Smad proteins, which are referred to as regulator Smads (R-Smads), common Smads (Co-Smads) and inhibitory Smads (I-Smads).[49-52] All Smads except for I-Smads contain two important domains, an amino terminal (MH1) and carboxyl terminal (MH2), which have been found to be inactive when linked. I-Smads have been found not to contain MH1 domains. When R-Smads become phosphorylated by type II receptors, the interaction between MH1 and MH2 domains is terminated. This enables the MH2 domains of R-Smads to interact with Co-Smads, whose role is to aid in transporting this complex to the nucleus and affect gene transcription [47]. I-Smads regulate and inhibit the activation of R-Smads by adhering to type I receptors. In general I-Smads have a higher affinity for type I receptors than R-Smads, which dissociate after time [53, 54]. Another regulation mechanism in the

cytoplasm of chondrocytes is the proteolytic degradation of Smads. There is also competition between the TGF-β and BMP signaling pathway for R-Smads (e.g., Smad-4), as they share a common pathway [53, 54].

Transforming Growth Factor- β1

Transforming growth factor-β1 (TGF-β1) is a protein that is part of the TGF-β superfamily that stimulates ECM synthesis [47, 53-56]. TGF-β1 has been found to affect the production and prevent degradation of proteoglycans in cartilage. More specifically, TGF-β1 increases aggrecan mRNA expression [14, 57]. A higher level of total proteoglycan synthesis was observed in the presence of type II collagen and TGF-β1 [14, 57]. The stability and activation of TGF-β1 is regulated by the extracellular matrix, with a strong affinity for proteoglycan decorin [10, 58].

Three TGF-β isoforms, TGF-β1, TGF-β2 and TGF-β3, are present in cartilage. However, the most prominent form in chondrocytes is TGF-β1, which is a 100 kDa peptide that contains two subunits, active (25 kDa) and inactive (75 kDa) [15, 59-61]. In order for TGF-β1 to bind to its receptor, TGF-βI (ALK5) or TGF-βII (ALK1), TGF-β1 must first remove the inactive peptide [48, 49].

The specific Smad proteins that are part of the TGF-β1 pathway are Smad-2, -3, -4, -6 and -7 [48, 50]. The two R-Smad proteins are Smad-2 and -3. The Co-Smad protein is Smad-4. Finally, Smad-6 and -7 are considered I-Smads, which prevent complex formation of R-Smads to Co-Smads [48, 49]. The amino terminal of Smad-7 has been found to affect the MH2 domain of R-Smads to inhibit TGF-β1 signaling [47]. The TGF-β1 signaling pathway includes Smad, ERK, JNK and p38 kinases as well as the JAK/STAT pathways [47, 48, 53, 54]. In the MAP kinase pathway, ERK prevents the

transport of R-Smads and their Co-Smads into the nucleus. This is true for both TGF-β1 and BMP [54].

It has been shown that tumor necrosis-α, a cytokine, prevents the activation of the TGF-β signaling through Smad-7, which can be produced by NF-κB [62]. Another cytokine, IL-1 has been found to increases the degradation of proteoglycans within articular cartilage. When TGF-β1 was introduced to cartilage, it was found to overwhelm the tissue and prevent the effects of IL-1 [56]. This could be a result of Smad-7, which is responsible for inducing other signaling pathways, such as IL-1 [54]. The expression of aggrecan has been found to occur when Smad-2 is phosphorylated by TGF-β. By expressing Smad-7 at high levels, it has been found to prevent the effects of TGF-β1 on the proteoglycan synthesis [55]. The intracellular signaling proteins Smad-2 and Smad-3 both became phosphorylated when human chondrocytes are stimulated by TGF-β1, type II collagen, or both simultaneously [63]. Thus, indicating the possible influence of the integrin and TGF-β signaling pathways with each other.

Bone Morphogenic Protein-7

Bone morphogenic proteins (BMP), also referred to as osteogenic proteins (OP), are part of the TGF-β superfamily. BMPs are dimeric proteins that are approximately 32-36 kDa. Several BMPs have been found to affect chondrocyte function, including BMP-2, -4, -6 and -7 [12, 51, 64, 65]. However, the most notable effects have been found with BMP-7 [13]. Initially, BMPs are synthesized with an amino terminal region. The removal of this region allows BMPs to become activated. When BMPs bind to type I and type II receptors (e.g., BMPR-IA, BMPR-IB, ACTR-I, BMPRII, ACTRII and ACTR-IIB), the serine/threonine kinases become phosphorylated. Additionally, the interaction

between type I and type II receptors lead to the initiation of R-Smads (Smad-1, -5 or -8) [50, 51, 55]. The Co-Smad (Smad-4) aids in the translocation of the R-Smads to the nucleus allowing for gene transcription to occur.

The BMP signaling pathway can be controlled both in the extracellular and intracellular part of the cell. A few extracellular antagonists for BMP are noggin, chordin, follistan, and DAN [66]. BMP-2, -4 and -7 bind to noggin and chordin with a higher affinity than to BMP receptors [48, 50, 51, 66, 67]. DAN has been found to bind to BMP-2 [50]. The interaction of BMPs to their binding proteins can be broken down by BMP-1, a metalloprotease [51, 66]. Additionally, BMPs can adhere to extracellular matrix components such as collagen and heparin derivatives to prevent receptor activation [11, 66]. Soluble inhibitory intracellular proteins are present in chondrocytes, commonly referred to as Smad-6 and -7. They both reside in the nucleus and travel into the cytoplasm after R-Smad activation. I-Smads adhere to the type I receptor and prevent the receptor interaction with the appropriate R-Smads. There are a few regulatory elements in the BMP Smad signaling pathway. For instance, Smad-6 can form a complex with Smad-1, therefore, preventing Smad-4 from binding.

Several BMPs have been found to affect chondrocytic production of type II collagen, such as BMP-2, -4, -6 and -7 [12]. BMP-2 has been shown to promote the expression of type II collagen, aggrecan and not type X collagen [13, 15]. However, it does cause matrix degradation as well as induce the formation of proteases [13, 68]. BMP-7 was found to maintain type II collagen and produce extracellular matrix components [13, 15, 69-71]. In comparison to basal medium, chondrocytes incubated with BMP-7 showed an increase in proteoglycan synthesis, with 95% being chondroitin

sulfate [71]. Additionally, when chondrocytes were induced with BMP-7 an increase in the expression of the intracellular protein FAK, as well as other focal adhesion proteins, occurred [70]. In the presence of IL-1, BMP-7 allowed chondrocytes to maintain and continue synthesizing proteoglycans [15].

Platelet-Derived Growth Factor

Platelet-derived growth factor (PDGF) is a 30 kDa glycoprotein found at platelet migration sites, such as injured tissue [12]. PDGF is a disulfide-linked heterodimer with four types of isoforms (PDGF-A, -B, -C and –D) [72]. There are two receptors for PDGF (-α, -β), which are both tyrosine kinase enzymes. Individually, the two receptors have specificity for the different PDGF isoforms. PDGF- α and PDGF-β can also bind together, which results in an increase in enzymatic activity compared to when they are alone [72, 73]. The MAPK, PI3K and PKC signaling pathways have been found to become activated by PDGF in various cell lines [72]. PDGF has been shown to be produced locally in cartilage by chondrocytes [12, 15, 73]. PDGF can induce proteoglycan synthesis and aggrecan without inducing chondrocyte proliferation [15, 74, 75]. By inducing chondrocytes with PDGF, an increase in IL-1 receptor gene expression was observed [75]. When PDGF and IL-1 were incubated together, there was noticeably more proteoglycan and aggrecan degradation. This also correlated with an increase in mRNA of proteases, such as metalloproteases. However, the extracellular matrix was maintained with PDGF and IL-1 combined compared to just IL-1 alone.

Fibroblastic Growth Factor

Fibroblast growth factor (FGF) is a polypeptide that is 14-16 kDa in molecular weight that binds to heparin proteoglycans, present in articular cartilage [11, 12]. It is known to be in a basic and acidic form. FGF regulation of chondrocyte function is important to articular cartilage homeostasis by aiding in the synthesis and degradation of proteoglycans and type II collagen [76]. FGF determines its functionality as either an anabolic or catabolic growth factor by its concentration within articular cartilage. The interaction of FGF with chondrocytes and its effect on the signaling pathway is still trying to be understood. It has been found that FGF-18, a specific type of fibroblastic growth factor, attaches to the FGF receptor-3 (FGFR-3). The activation of the FGFR-3 increased the gene expression of α1 integrin, which has been found to adhere to type II collagen. Additionally, when FGF and IL-1 are exogenously added to chondrocytes, the expression of the IL-1 receptor increases, leading to an increase in matrix degradation attributed to IL-1 [77].

Epithelial Growth Factor, Vascular Endothelial Growth Factor, Hepatocyte Growth Factor

Endothelial growth factor (EGF) is a very small protein, approximately 1.6kDa.[12] It has been found to degenerate articular cartilage by breaking down proteoglycans. The expression of type II collagen and aggrecan decreases in the presence of EGF [12, 78]. Some inflammatory responses that occur due to EGF have been a higher expression of cyclooxygenase-2 (COX2) and production of prostaglandin E_2 (PGE_2) [79]. EGF has been found to activate the ERK 1/2 pathway but not effect Sox9, which aids in the transcription of type II collagen and aggrecan [78]. However, a

correlation between EGF and these inflammatory proteins can be seen by the activation of two pathways, primarily the ERK 1/2 and p38 kinase pathway [79].

Vascular endothelial growth factor (VEGF) is 23kDa protein, commonly associated with angiogenic activity [12, 80]. Several different isoforms of VEGF ($VEGF_{121,}$ $VEGF_{165}$ and $VEGR_{189}$) that have been found in normal and osteoarthritic cartilage [80, 81]. These VEGF proteins adhere to two different types of receptors, VEGF-R1 (Flt-1, fms-like tyrosine kinase) and VEGF-RII (KDR, kinase insert domain-containing receptor). Additionally, the co-receptor neutropilin-1 (NRP-1) increases the ability of VEGF to bind to VEGF-R2 [80, 82]. This co-receptor is activated in osteoarthritic cartilage at higher amounts compared to healthy cartilage [80]. VEGF has been found to adhere to heparin and heparin-sulfate proteoglycans. Additionally, the adhesion of VEGF to the ECM can loosen the binding of basic FGF [82]. VEGF receptor gene expression is present in osteoarthritic cartilage with an increase in metalloproteases synthesis, specifically MMP1 and MMP3 [80]. When chondrocytes are induced with IL-1β, VEGF protein synthesis decreases. However, VEGF production increases when chondrocytes are incubated with both IL-1β and TGF-β [83].

Hepatocyte growth factor (HGF) is a heterodimeric glycoprotein with an α and β subunit with molecular weights of 69kDa and 32 kDa respectively [84]. It has been found to bind collagen, chondroitin sulfate and hyaluronic acid. When chondrocytes are introduced to HGF, there is an increase in proteoglycan synthesis compared to basal levels. HGF attaches to a transmembrane receptor, *c-met*, which is a tyrosine kinase. The mRNA for HGF and *c-met* have both been observed in normal and arthritic cartilage. However, HGF protein and *c-met* have are present at higher levels in damaged cartilage

[15, 84]. This correlates to other data, indicating that HGF expression increased in the presence of IL-1 [15].

2.1.5.2 Catabolic Growth Factors/Cytokines

Interleukin-1

Interleukins (ILs) are cytokines present in articular cartilage that have been associated with degenerative cartilage. There are many different forms of interleukins (IL-1, -4, -6, -8, -10, -11,-17 and -18) [12, 46, 85]. IL-1β has been found to strongly associate with damaged cartilage, increasing the expression of metallanoproteases and decreasing the expression of ECM components, such as type II collagen and aggrecan [12, 21, 70, 84, 86-88]. IL-1β is synthesized with two components to maintain it at an inactive state at a molecular weight of 31kDa [46]. An enzyme breaks down the IL-1β protein into a smaller active 17kDa fragment [21, 46].

There are two antagonists that control the extracellular IL-1s (Figure 2.4). The interleukin-1 receptor I (IL-1RI) can attach to IL-1ra to inhibit signal transduction. Additionally, interleukin-1 receptor II (IL-1RII) binds to IL-1β [21, 35]. When IL-1β attaches to IL-1RI, an intracellular protein is recruited and becomes attaches to the receptor. This protein is known as the IL-1 associating protein (IL-1RAcP). This enables an adaptor protein, MyD88, to procure kinases IRAK-1 and -2 to activate further intracellular proteins. IRAK-1 and -2 stimulate the response of the NF-κB inducing kinase (NIK) to activate the IKKαβ complex, which finally induces the NF-κB protein to effect gene transcription. Other signaling pathways that can become activated by IL-1 are the MAPK and PI3K pathway [21, 46, 89]. It has been found that IL-1 activates the expression of metalloproteinases (MMPs) through JNK and p38 kinases [46]. Other

interleukins, such as IL-6, activate the JAK/STAT pathway [89, 90]. IL-6 as well as IL-1 negatively affects the mRNA and protein amounts of Sox9, a protein that has been attributed to enable the gene expression of type II collagen and aggrecan [21, 78, 90].

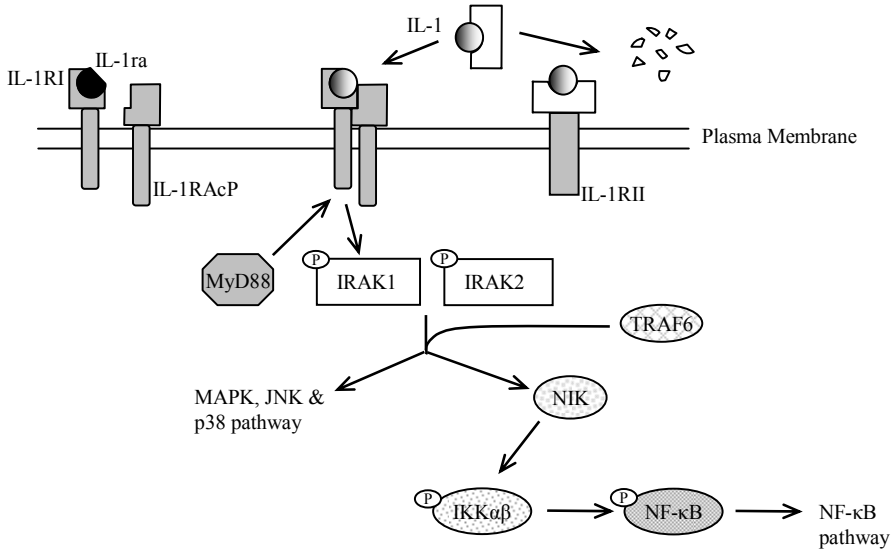

Figure 2.4. The transduction of the IL-1 pathway by chondrocytes. IL-1 can be bound to the IGF-1RII antagonist, which is present within the plasma membrane and in soluble form. Additionally, IL-1ra prevents IL-1 from adhering to its respective receptor, IL-1RI. The activation of IL-1RI results in either the activation of MAPK, JNK, p38, and/or NF-κB pathways.

In order for ILs to have an effect on gene expression by chondrocytes, they adhere to their respective receptors (IL-1R). Low levels of ILs are maintained in healthy cartilage. Additionally, this lessens the extent of MMPs production as well as its gene expression [46]. However, the presence of TGF-β, osteoarthritic cartilage was found to increase the expression of IL-6 [46, 85]. Additionally, IL-1β was found to increase the expression of TGF-β. When chondrocytes are incubated with exogenous IGF-1, there is upregulation of IL-1RII [35].

Other forms of IL have shown to effect chondrocytes function. In the presence of IL-17 and IL-18, chondrocytes induce the expression and synthesis of several MMPs as

well as produce nitric oxide, which causes apoptosis [21, 46, 91]. Therefore, decreasing the normal levels of proteoglycan synthesis. In arthritic cartilage, the mRNA of IL-6 and -8 have been found to be present more often than healthy cartilage [46, 86]. The mRNA of several ILs show a trend of higher expression in damaged versus healthy cartilage, such as IL-6, IL-8 and IL-18 [86]. Chondrocytes expression of IL-18 increases in the presence of IL-1β. When IL-1β and IL-18 are incubated with chondrocytes together, the results indicate that nitric oxide is produced concurrently with a decrease in proteoglycan synthesis [92].

Tumor Necrosis Factor-α

Tumor necrosis factor-α (TNF-α) is another cytokine that acts similarly to ILs on chondrocytes [93]. TNF-α has been found to increase gene expression of MMPs and decrease the expression of extracellular matrix components [12, 78, 93]. TNF-α gene expression and their respective receptors are more present in damaged cartilage compared to normal cartilage [86, 94]. It has an initial molecular weight of 51 kDa and reduces down to 17 kDa [12, 95]. It is synthesized as a membrane bound protein, but after it is cleaved off the membrane by a metalloproteinase known as TACE, it becomes activated and can adhere to its appropriate receptor, TNF-R1 or TNF-R2 [94-96]. This enables the receptors to attach to either two cytoplasmic proteins, TRAF2/5 and FADD, through an adaptor protein, TRADD (TNF-R1 associated death domain protein) [95, 96]. The TRAF protein activates two main signaling pathways, MAPK and NF-κB. The MAPK signaling pathway includes transcriptional factors such as AP1 [96]. It has been recently discovered that chondrocytes activate the MEK pathways with minimal detection of the p38 and JNK pathways [93, 97]. The activation of the NF-κB transcriptional protein is

initiated by the TRAF protein. NF-κB can be further controlled by I-κB proteins through the IKK complex, which is also recruited by TRAF proteins [95, 96]. Through the activation of the NF-κB signaling pathway, TNF-α, similar to IL-1β, affects type II collagen expression [78, 93].

Chondrocytes incubated with exogenous TNF-α resulted in the expression of IL-6 [85]. The synthesis of IGFBPs by chondrocytes was shown to be greater in the presence of TNF-α, which could limit the availability of IGF-1 [98]. Other studies have shown that chondrocytes induced with EGF and TNF-α affects the mRNA of type II collagen and aggrecan more significantly compared to their individual effects [78, 93].

2.1.6 Tissue Engineering Approaches to Regulate Signaling

The interactions of environmental cues and chondrocytes have been proven to be important in determining cell function. In the field of tissue engineering, it is vital to fully understand these underlying principles to create an appropriate biomaterial scaffold that can integrate and eventually heal the tissue. Therefore, many researchers have looked into biomaterials. Both natural and synthetic polymers have been utilized to aid in chondrocyte encapsulation. Natural polymers are typically polysaccharides or polypeptide chains isolated from natural plants or organisms. While synthetic polymers are fabricated and their properties can be altered more readily compared to natural polymers. These polymers can be shaped into various three dimensional forms, such as meshes, foams and gels. However, a common form that mimics the articular cartilage environment is a hydrogel. The primary reason for interest in hydrogels as artifical matrices for chondrocytes is that they are water-laden polymer networks that have the ability to retain up to 99% water volume [99-101]. This attribute enables the

encapsulation of chondrocytes as well as proteins within the bulk of the network. Hydrogels have been shown to maintain the spherical morphology and gene expression of chondrocytes [102].

Alginate is common natural polymer that has been used to encapsulate chondrocytes. A unique property of alginate is that there is limited cellular adhesion due to the lack of cellular recognition proteins. It has been found that chondrocytes encapsulated in alginate are able to express their phenotypic type II collagen expression [103-105]. Adult human chondrocytes were found to express aggrecan, metalloproteinases-3 and -8 for as long as eight months after their encapsulation in alginate beads [106]. The expression of BMP-2 was also apparent for chondrocytes in alginate [105]. A recent study has shown that when chondrocytes in alginate were incubated with exogenous IGF-1, there was an activation of both the PI3K and MAPK pathway, as demonstrated by phosphorylation of the Akt and ERK proteins respectively [107]. Inhibitors of Akt promoted a decrease in proteoglycan synthesis at a greater extent than compared to MEK inhibitors. Thus, indicating the importance in the PI3K pathway with production of extracellular matrix components. The effects of catabolic growth factor, IL-1β activated ERK, p38 and JNK proteins, but not Akt proteins [107].

Arginine-glycine-aspartic acid (RGD) sequences, which are commonly found in the ECM, have been covalently bound to alginate, forming a natural and synthetic hybrid. These constructs have allowed chondrocytes to express type II collagen at a far greater extent than when cultured in unmodified alginate [104]. Alternatively, cyclic RGD incubated with chondrocytes inside alginate decreased proteoglycan synthesis [23]. This work indicates that chondrocyte adhesion is critical to extracellular matrix production.

Alginate gels that were embedded with fibrin gels allowed chondrocytic production of type II collagen, and proteoglycans, such as aggrecan [108, 109]. Alginate and type II collagen constructs promoted an increase in chondroitin-6 sulfate production by chondrocyte [110] When stimulated with TGF-β1, an increase in keratin sulfate synthesis by chondrocytes was observed but also a decrease in the expression of chondroitin-6-sulfate was noted [57, 110]. The expression of type II collagen of chondrocytes within alginate beads was negatively effected by IL-1 while TGF-β1 and BMP-2 individually showed an enhancement [13, 105, 106]. BMP-2 also showed an greater aggrecan expression of chondrocytes in alginate [105]. When cultured in alginate, BMP-7 was found to effect the synthesis of type II collagen and proteoglycans greater than with just serum [111].

In terms of integrin expression, chondrocytes encapsulated in type II collagen and alginate were found to express α5β1 [23]. When these chondrocytes were incubated with an antibody that attached to β1 integrins with exogenous TGF-β1 there was a significant decrease in proteoglycan synthesis [23]. However, there was no effect when β1 integrins were blocked without TGF-β1. This indicates that there is a possible interaction of TGF-β1 to integrin signaling activation. Further studies also show the effects of integrin signaling on chondrocytes. When fibronectin beads are in contact with chondrocytes, the activation of the α5β1 integrin occurs [112]. This resulted in the phosphorylation of focal adhesion kinases, indicating the role of integrin signaling. A higher level of proteoglycan synthesis is observed when FGF and IGF-1 are incubated with chondrocytes and fibronectin beads, further suggesting that integrin activation can be enhanced or aided by growth factors.

Hyaluronic acid is a component in the extracellular matrix and therefore has been of interest for tissue engineers to encapsulate chondrocytes. For instance, TGF-β mRNA expression increased when chondrocytes adhered to hyaluronic acid through the CD44 integrin [10]. A modification of hyaluronic acid has been made with benzyl alcohol. In these constructs, chondrocytes expression of type II collagen and Sox9 increased while maintaining their low level of type I collagen expression and high level of aggrecan [113]. Hyaluronic acid has also been incorporated with other types of polymers, including alginate. Chondrocytes are able to produce type II collagen and proteoglycans in both alginate beads and sponges that contain hyaluronic acid. Investigations additionally indicated that the ECM protein levels were stabilized in the alginate beads versus alginate sponge structures [114].

Synthetic scaffolds have also been researched in determining the effect of chondrocyte signaling. On poly(glycolic acid) meshes, it was found that chondrocytes produce type II collagen [8]. Further studies have been done with chondrocytes on a poly(glycolic acid) scaffold with incorporation of various growth factors [33]. IGF-1 increased the GAG fraction compared to constructs with low protein supplemented media. TGF-β resulted in high type II collagen expression. IL-4 prevented a decrease in GAG compared to other growth factors and PDGF was found to decrease GAG concentration. Chondrocytes were encapsulated in photopolymerized poly(ethylene oxide) hydrogels with TGF-β1 and IGF-1 growth factors within poly(lactic-glycolic) acid microspheres [115]. There was an increase in the glycosaminoglycans concentrations with IGF-1 individually and with a combination of IGF-1 and TGF-β1. Poly(ethylene glycol) has also been co-polymerized with various other synthetic polymers. A

poly(propylene fumarate-co-ethylene glycol) was shown to maintain the viability of chondrocytes encapsulated within this construct [116]. Proteoglycan synthesis occurred in these constructs, but was found to be lower when compared to alginate and agarose hydrogels by producing 25% of type II collagen. Recently, different armed-poly(ethylene glycol) polymers have been altered with metallanoprotease sensitive peptides [117]. This polymeric construct encapsulated chondrocytes and showed that the mRNA expression for type II collagen and aggrecan was highest for the poly(ethylene glycol) polymers that contained the MMP sensitive peptides versus without. Additionally, in these scaffolds, the expression of MMP-13 was the lowest compared to the scaffolds without MMP sensitive peptides.

The effect of biomaterials on chondrocyte function is vital for creating a proper scaffolding environment to recreate articular cartilage. It is important to investigate the effect of biomaterial properties on controlling molecular signaling of chondrocytes and therefore chondrocyte function. We propose that fully understanding the interactions of chondrocytes amongst the extracellular matrix proteins and the cells to one another will enhance our ability to engineer a viable construct for articular cartilage.

2.1.7 Summary

Chondrocytes depend on their environment to aid in their expression of appropriate proteins. It has been found that the interaction of integrin receptors with chondrocytes effects the production of extracellular molecules such as type II collagen and aggrecan. Additionally, the presence of growth factors such as IGF-1, TGF-β1 and BMP-7 induce various signaling pathways that also aid in transducing phenotypic expressions by chondrocytes. Natural and synthetic polymers have been used to act as a

scaffold for chondrocytes. The production of extracellular matrix proteins by chondrocytes has been studied. As tissue engineers, it is advantageous to explore the possibility of how altering biomaterial properties affect the signaling cascades by activation of receptors and transduction through the cytoplasm. This vital information will be able to aid in the future of engineering an appropriate biomaterial that can incorporate chondrocytes to act as a scaffold for articular cartilage.

2.2 Polymeric Scaffolds for Tissue Engineering Applications*

2.2.1 Introduction

The incorporation of polymeric scaffolds in tissue regeneration occurred in the early 1980's, and it continues to play a vital role in tissue engineering [118-120]. The function of a degradable scaffold is to act as a temporary support matrix for transplanted or host cells so as to restore, maintain or improve tissue. Scaffolds may be created from various types of materials, including polymers. There are two main classes of polymers, based upon their source: natural or synthetic. Polymeric scaffolds may be used to support a variety of cells for numerous tissues within the body. The design of a polymeric scaffold plays a significant role in proper cell growth. Therefore, several important properties must be considered: fabrication, structure, biocompatibility, biodegradability and mechanical strength. This review will discuss natural and synthetic polymers, as well as the properties that scaffolds exhibit.

2.2.2 Natural Polymers for Scaffold Fabrication

There are two major classes of natural polymers used as scaffolds: polypeptides and polysaccharides (Table 2.2, Figure 2.5). Natural polymers are typically biocompatible and enzymatically biodegradable. The main advantage for using natural polymers is that they contain bio-functional molecules that aid the attachment, proliferation, and differentiation of cells. However, disadvantages of natural polymers due exist. Depending upon the application, the previously mentioned enzymatic

---

***** This chapter was published as: Yoon DM and Fisher JP. Polymeric Scaffolds for Tissue Engineering Applications. CRC's Biomedical Engineering Handbook: Tissue Engineering and Artificial Organs. 2006; 37-1 - 37-18.

degradation may inhibit function. Further, the rate of this degradation may not be easily controlled. Since the enzymatic activity varies between hosts, so will the degradation rate. Therefore it may be difficult to determine the lifespan of natural polymers in vivo. Additionally, natural polymers are often weak in terms of mechanical strength but crosslinking these polymers have shown to enhance their structural stability.

2.2.2.1 Polysaccharides

Agarose

Agarose is a polysaccharide polymer extracted from algae (Table 2.2, Figure 2.5). Its molecular structure contains an alternating copolymer linkage of 1,4-linked 3,6 anhydro-α-l-galactose and 1,3-linked β-d-galactose [121]. Agarose is water-soluble due to the presence of hydroxyl groups. Two agarose chains interact with each other through hydrogen bonding to form a double helix. At low temperatures the agarose chains form a thermally reversible gel. Thus, at high temperatures agarose gels may be made water soluble. Many of the properties of agarose gels, particularly strength and permeability, can be adjusted by altering the concentration of agarose [121]. For example, low concentrations of agarose lead to a highly porous entangled structure with limited mechanical strength. Agarose in its native state is enzymatically degradable by agarases.

For tissue culture systems, agarose hydrogels are widely investigated because they permit growth of cells and tissues in a three-dimensional suspension [122]. Agarose gels have been found to maintain chondrocytes, the predominant cell type in cartilage, in culture for 2-6 weeks [123]. Furthermore, agarose hydrogels embedded with chondrocytes allow the expression of type II collagen and proteoglycans [122, 124]. These results show promise for using agarose gels in cartilage repair. Additionally,

agarose gels have been investigated as a matrix for nerve regeneration [125, 126]. Dorsal root ganglia (DRG), a neural cell, has been encapsulated in agarose hydrogels. The influence of increasing porosity and incorporating charged biopolymers (e.g., chitosan) produced an increased in neurite extension of DRG isolated from chicks [126].

Alginate

Alginate is a naturally derived water-soluble polysaccharide obtained from algae (Table 2.2, Figure 2.5) [121]. It is a polyanion composed of two repeating monomer units: β-d-mannuronate and α-l-guluronate [127, 128]. Alginate is readily degraded at the β(1-4) linkage site, located in between the monomer units, by alginate lyases [127]. The physical and mechanical properties of alginate are dependent on the length and proportion of the guluronate block within the chain. Due to alginate's polyelectrolytic nature, it readily forms into an ionotropic crosslinked hydrogel when exposed to divalent ions, the most common being calcium ions [129, 130]. Furthermore, alginate gels may be solubilized when these cations are removed or sequestered. This ease in gel reversibility allows alginate to be especially useful for studies requiring the retrieval of encapsulated cells. Alginate does not contain cellular recognition proteins, limiting cell attachment to the natural polymer. By crosslinking alginate with poly(ethylene glycol)-diamine the mechanical properties of alginate can be controlled and even improved [121].

A variety of different cells have been found to maintain their morphology in alginate scaffolds [127, 131-134]. The adhesion of fibroblasts in alginate sponges was found not to be affected by the porosity of the scaffold [131]. Chondrocytes embedded in alginate proliferated and expressed type II collagen [135]. Hepatocytes, the functional cell in liver, were also found to grow in alginate scaffolds. When hepatocytes were

seeded in 3-dimensional porous alginate, albumin was secreted, indicating proper cell function [136]. Other types of cells studied in alginate include cardiomyocytes, rat marrow cells and Schwann cells [127, 134, 137].

Hyaluronic acid

Hyaluronic acid (hyaluronan, HA) is a naturally occurring polysaccharide with a β(1-3) linkage of two sugar units: d-glucuronate and N-acetyl-d-glucosamine (Table 2.2, Figure 2.5). Hyaluronic acid is an abundant glycosaminoglycan within the extracellular matrix of tissues that promotes early inflammation critical for wound healing [138]. Furthermore, hyaluronic acid is non-immunogenic and non-adhesive, making it an attractive option for biomedical applications. In dilute concentrations hyaluronic acid has a random coil structure which becomes entangled as its concentration increases [139]. Some disadvantages of hyaluronic acid are that it is highly water soluble and it degrades rapidly by enzymes, such as hyaluronidase. However, when fabricated into a hydrogel, hyaluronic acid is often more stable [121, 125, 138].

Currently, an ester derivative of hyaluronic acid has been used as a tissue engineering scaffold [125, 140, 141]. Adipose precursor cells proliferated and differentiated in HA sponges [140, 141]. Additionally, HA has been used for osteochondral repair by incorporating mesenchymal progenitor cells, which differentiate into osteoblasts and chondrocytes [125]. Furthermore, the interaction of chondrocytes embedded in HA has resulted in the expression of collagen type II, forming a tissue similar to native cartilage [140].

Chitosan

Chitosan is a partially deacetylated derivative of chitin, found in the exoskeleton of crustaceans and insects (Table 2.2, Figure 2.5). It is a linear polysaccharide composed of β(1-4) linked d-glucosamine with randomly dispersed N-acteyl-d-glycosamine groups [121, 139, 142, 143]. Less than 40% of chitosan is comprised of the N-acteyl-d-glycosamino group, which makes its molecular structure similar to glycosaminoglycans [121, 125]. Chitosan is easily degraded by enzymes such as chitosanase and lysozyme. Chitosan is catonic with semi-crystalline properties of a high charge density. These attributes allow chitosan to be insoluble above pH 7 and fully soluble below pH 5. At high pH solutions, chitosan can be gelled into strong fibers [143]. Furthermore, hydrogels can also be formed by either ionic bonding or covalent cross-linking, using crosslinking agents such as glutaraldehyde [121].

Chitosan is a well defined matrix and as a porous scaffold, hepatocytes were found to maintain a rounded morphology when cultured within chitosan scaffolds [144]. Results showed an increase in albumin secretion as well as urea synthesis, vital metabolic activities of liver cells [144]. Additionally, crosslinking chitosan gels with glutaraldehyde showed increased urea formation by hepatocytes [145]. Furthermore, chitosan has shown promise as an orthopaedic scaffold. When a sponge form of chitosan was seeded with rat osteoblasts, alkaline phosphatase production was detected, as well as bone spicules, indicating initial bone formation [146]. Also, chitosan scaffolds were found to support chondrocyte attachment and expression of extracellular matrix proteins [147].

2.2.2.2 Polypeptides

Collagen

Collagen is a major component of structural mammalian tissues (Table 2.2, Figure 2.5). Currently, 19 different types of collagen have been found, with the most abundant being type I collagen [148]. Collagen is composed of three polypeptide chains that intertwine with one another to form a triple helix. The polypeptide chains have a repeating sequence of glycine-X-Y, where X and Y are most often found to be proline and hydroxyproline. The chains are held together through hydrogen bonding of the peptide bond in glycine and an adjacent peptide carbonyl group [149]. The presence of adhesion domains allows collagen to display an attractive surface for cell attachment [148]. Some drawbacks in collagen are its high variability due to the numerous forms. Collagen is enzymatically biodegradable and has a tendency to degrade quickly, limiting its mechanical properties. Crosslinking collagen with glutaraldehyde decreases its degradation rate [150].

Collagen naturally promotes healing wounds by promoting blood coagulation [148]. These attributes allow collagen to be used as a scaffold for cells within the epithelium, such as fibroblasts and keratinocytes [151-153]. Type II collagen is suitable for attaching chondrocytes and aiding in their proliferation and differentiation [154]. Additionally, rat hepatocytes attached onto collagen-chitosan scaffolds secreted albumin, which confirms cell function [155]. Furthermore, corneal keratocytes cultured on collagen sponges synthesized proteoglycans, indicating corneal extracellular matrix formation [156].

Gelatin

Gelatin is a collagen derivative acquired by denaturing the triple-helix structure of collagen into single-strand molecules (Table 2.2, Figure 2.5). It is water-soluble, and entangles easily to form into a gel through changes in temperature [121, 130]. Gelatin is broken down enzymatically by various collagenases. The primary form of a gelatin scaffold is a hydrogel. Stabilization of gelatin hydrogels occurs through chemical crosslinking with agents such as glutaraldehyde [139].

Gelatin has been used to support cells for orthopaedic applications. Rat marrow stromal osteoblasts encapsulated in gelatin microparticles retained their phenotype [157]. Also, porous gelatin scaffolds supported human adipose derived stem cell attachment and differentiation into a variety of cell lineages. These constructs expressed a chondrogenic phenotype, indicated by the expression of hydroxyproline and glycosaminoglycans, both of which are present in the extracellular matrix of cartilage [158]. Furthermore, non-orthopaedic cell types , such as respiratory epithelial cells and cardiocyocytes, have been shown to attach and form rounded morphologies in gelatin scaffolds [134, 159].

Silk

Silks are fibers that have a protein polymer basis (Table 2.2, Figure 2.5) [160]. There are two main sources of silks: spiders and silkworms. The primary structure of silks is a repetitive sequence of proteins that are glycine-rich. The secondary structure of silks is a β-sheet, which allows silks to exhibit enormous mechanical strength and is the primary reason for its strong interest as a scaffold. Most types of silks undergo slow proteolytic degradation by proteases, such as chymotrypsin [160]. A drawback for using silks is the potential formation of a granuloma as well as an allergic response. There has

been a positive attachment and growth response of fibroblasts on fibroin silks. And recently, osteoblasts seeded on silks have displayed bone growth characteristics [161, 162].

2.2.3 Synthetic Polymers for Scaffold Fabrication

Polymers that are chemically synthesized offer several notable advantages over natural-origin polymers. A major advantage of synthetic polymers is that they can be tailored to suit specific functions and thus exhibit controllable properties. Furthermore, since many synthetic polymers undergo hydrolytic degradation, a scaffold's degradation rate should not vary significantly between hosts. The most common synthetic polymers are polyesters. Other types include polyanhydrides, polycarbonates and polyphosphazenes (Table 3, Figure 6). A significant disadvantage for using synthetic polymers is that some degrade into unfavorable products, often acids. At high concentrations of these degradation products, local acidity may increase, resulting in adverse responses such as inflammation or fibrous encapsulation [125, 163, 164].

2.2.3.1 Polyesters

Poly(glycolic) acid

Poly(glycolic) acid (PGA) is a linear aliphatic polyester in the family of poly(α-hydroxy esters) (Table 2.3, Figure 2.6). It is formed by ring-opening polymerization of cyclic diesters of glycolide [163]. Due to the crystallinity of glycolide, PGA is a highly crystalline polymer that has a high melting point (185-225 ºC) and low solubility in organic solvents [164, 165]. Further, PGA is hydrophilic and undergoes bulk degradation, often leading to a sudden loss in mechanical strength. PGA degrades hydrolytically into

glycolic acid, which is metabolized in the body. An unfortunate attribute of glycolic acid is that at high concentrations it lowers the pH of the surrounding tissue, causing inflammation and possible tissue damage [163].

Poly(glycolic) acid polymers has been investigated as a scaffold to support various types of cell growth. Bovine chondrocytes seeded on PGA scaffolds in vitro expressed sulfated glycosaminoglycans 25% more than native cartilage [166]. In vivo results using a mouse model were comparable to these in vitro results. Other studies seeded myofibroblasts and endothelial cells on a PGA fiber matrix. These cells persisted and expressed elastic filaments and collagen, demonstrating the potential use of PGA scaffolds for heart valve engineering [167]. Hepatocytes have also attached to PGA and initiated albumin synthesis [168]. Some investigations have coated PGA with other poly(α-hydroxy esters). Results with these scaffolds have shown that smooth muscle and endothelial cell growth may be supported [169].

Poly(l-lactic) acid

Poly(l-lactic) acid (PLLA) is one of two isomeric forms of poly(lactic acid): d(-) and d,l(-). (Table 2.3, Figure 2.6) Similar to PGA, PLLA is classified as a linear poly(α-hydroxy acid) that is formed by ring-opening polymerization of l-lactide [170]. PLLA is structurally similar to PGA, with the addition of a pendant methyl group. This group increases the hydrophobicity and lowers the melting temperature to 170-180 ºC for PLLA [165]. Additionally, the methyl group hinders the ester bond cleavage of PLLA, and thus decreasing the degradation rate [163]. PLLA typically undergoes bulk, hydrolytic ester-linkage degradation, decomposing into lactic acid. The body is thought to excrete lactic acid in the form of water and carbon dioxide via the respiratory system [164, 170]. The

hydrophobic nature of PLLA allows for protein absorption and cell adhesion making them suitable as scaffolds.

In recent investigations, results have shown that the hydrophobic surface of PLLA has resulted in decreased adhesion of cells compared to other types of polymers, such as PGA [171]. However, PLLA has been found to support various cell types. Nerve stem cells seeded in PLLA fibers differentiated and expressed positive cues for neurite growth for potential regeneration of neurons [172]. Furthermore, human bladder smooth muscle cells seeded onto PLLA scaffolds also exhibited normal metabolic function and cell growth [133]. There has been similar work done with chondrocytes. The tissue engineered cartilage showed collagen, glycosaminoglycan, and elastin expression, vital for extracellular matrix formation [173].

*Poly(*D,L*-lactic acid-co-glycolic acid)*

Poly(glycolic acid) and poly(lactic acid) can be copolymerized to form poly(D,L-lactic acid-co-glycolic acid) (PLGA) (Table 2.3, Figure 2.6). This copolymer is amorphous, which decreases the degradation rate and mechanical strength of PLGA compared to PLLA. PLGA typically undergoes bulk degradation by ester hydrolysis. The degradation rate of PLGA can be controlled by adjusting the ratio of PLLA/PGA. However, it is important to note that know that the copolymer composition is not linearly related to the mechanical and degradation properties of PLGA. For example, a 50:50% ratio of PGA and PLLA typically degrades faster than either homopolymer [165, 174].

PLGA has been extensively researched as a tissue engineering scaffold and shown to support the growth of a variety of cell types. For instance, PLGA can facilitate human foreskin fibroblasts to regenerate an extracellular matrix [125]. Similar studies has been

conducted with chondrocytes and osteoblastic cells [171, 175]. Osteoblastic cells seeded on PLGA scaffolds expressed collagen, fibronectin, laminin, and a variety of other extracellular matrix proteins, indicating proper cell function. Furthermore, PLGA promoted smooth muscle cell growth as well as the production of collagen and elastin [176]. Similar works showed enhancement of axon regeneration by murine neural cells seeded on PLGA scaffolds [177]. Additionally, an epithelial layer has been formed on PGLA by seeded enteroctyes derived from intestinal epithelial cells [178].

Poly(ε-caprolactone)

Poly(ε-caprolactone) (PCL) is a aliphatic polyester with semi-crystalline properties (Table 2.3, Figure 2.6). PCL has repeating unit of one ester group and five methylene groups. It is highly water soluble with a melting temperature of 58-63 ºC [139, 165]. PCL is formed through ring-opening polymerization, forming a degradable ester linkage. The degradation of PCL occurs by bulk or surface hydrolysis of these ester linkages, resulting in a byproduct of caproic acid. PCL degrades at a slow rate with results showing that it can persist in vivo for up to two years [165]. To increase the degradation rate, PCL has been copolymerized with collagen, poly(glycolic acid), poly(lactic acid), and polyethylene oxide [179-181]. The ease with which PCL can be copolymerized with a variety of polymers has made it an attractive component of polymeric scaffolds.

PCL has been investigated as a stabilizing polymer on PGA scaffolds to aid in the formation of spherical aggregates by human biliary epithelial cells (hBEC). These hBECs proliferated on the synthetic scaffold and expressed phenotypic proteins, indicating cell stability [180]. Further studies of PCL as a homopolymer have demonstrated to support

human osteoblast and dermal fibroblast cell viability [182, 183]. The results with osteoblasts on porous PCL has shown a production of alkaline phosphatase, a marker of bone mineralization [182]. Also, dermal fibroblasts on mechanically stretched PCL films proliferated and maintained their rounded morphology [183].

Poly(propylene fumarate)

Poly(propylene fumarate) (PPF) is a linear polyester with a repeating unit containing two ester groups and one unsaturated carbon-carbon double bond (Table 2.3, Figure 2.6). The hydrolysis of the ester bonds in PPF, forms fumaric acid and propylene glycol as the two primary degradation products. Covalent cross-linking of PPF through its double bond allows cured PPF to possess significant compressive and tensile strength. Furthermore, this crosslinking aids in the formation of a synthetic scaffold in situ [184, 185]. Crosslinked PPF is a potential orthopaedic, especially bone, engineering material due to the strength that it exhibits [184]. Additional research has also been conducted with PPF copolymerized with PEG (PPF-co-PEG). This hydrophilic copolymer has been shown to support endothelial cell attachment and proliferation [186, 187].

Polyorthoester

A family of surface eroding polyorthoesters (POE) has been synthesized and studied for tissue engineering applications (Table 2.3, Figure 2.6). One particular form of POE has been considered as a scaffold. This type of POE is created by reacting ketene acetals with diols [188]. The hydrophobic nature of POE's surface allows this polymer to undergo primarily surface degradation [125, 189]. By incorporating short acid groups, such as glycolic or lactic acid, the degradation rate of the copolymer can be controlled

[189]. Furthermore, the hydrolysis of the orthoester linkages in POE is mostly sensitive to acids and is stable in bases [139, 174].

The surface eroding characteristics of POE has led to the research of this polymer for bone reconstruction [125, 190]. Surface degradation allows a scaffold to sustain mechanical support for the surrounding tissue since the bulk of the material remains structurally intact. In other studies, hepatocytes were grafted onto polyorthoesters and adhered to the surface of the synthetic scaffold [191].

2.2.3.2 Other Synthetic Polymers

Polyanhydride

Polyanhydrides are a class of hydrophobic polymers containing anhydride bonds, which are highly water reactive (Table 2.3, Figure 2.6) [192]. Polyanhydrides are also crystalline polymers, with a melting temperature of approximately 100 ºC [193]. Aliphatic polyanhydrides are synthesized by a dehydration reaction between diacids. The instability of the anhydride bond allows polyanhydrides to degrade within a period of weeks. The degradation rate is predictable for polyanhydrides and can be altered through changes in the hydrophobicity of the diacid building blocks [193]. Polyanhydrides are generally thought to degrade following a surface degradation mechanism.

Similar to polyorthoesters, polyanhydrides has been investigated primarily for orthopaedic applications. However, the modest Young's Modulus for entangled polyanhydride networks has limited their application in weight bearing environments [164]. This limitation resulted in further studies involving the formation of crosslinked polyanhydrides networks with incorporated imides [170, 194]. Scaffolds formed from these networks possess significant mechanical properties, such as compressive strength

(30-60 MPa), which are in the intermediate range of cortical and trabecular human bone (5-150 MPa) [164, 193-195].

Polyphosphazene

Polyphosphazenes are a class of polymers formed from an inorganic backbone containing nitrogen and phosphorous atoms (Table 2.3, Figure 2.6). Polyphosphazene is hydrophobic and typically undergoes hydrolytic surface degradation into phosphate and ammonium salt byproducts. There are a variety of polyphosphazenes that may be synthesized, due to the numerous types of hydrolytically labile substituents that can be can be added to the phosphorous atoms [196]. These viable substituents allow the properties of polyphosphazenes to be extremely controllable. Nevertheless, most polyphosphazenes display a slow degradation rate in vivo [196].

A number of different polyphosphazenes has been synthesized for use as tissue engineering scaffolds. Due to its high strength and surface degradation properties, it has been particularly investigated as an orthopaedic biomaterial [197]. Osteoblast cells that support skeletal tissue formation has been seeded and proliferated on a three-dimensional polyphosphazene scaffold [198]. Additionally, poly(organo)phosphazenes has been studied as scaffolds for synthetic nerve grafts in peripheral nerve regeneration [199].

Polycarbonate

Tyrosine-derived polycarbonate (P(DTR carbonate)) is an amorphous polycarbonate widely studied for biomedical applications (Table 2.3, Figure 2.6). The linear chain of P(DTR carbonate) contains a pendant R group, allowing it to be easily modified [200]. Further, P(DTR carbonate) has three bonds susceptible to hydrolytic

degradation: amide, carbonate, and ester [170, 200]. The carbonate and ester bonds readily degrade, with the former typically having a faster degradation rate. Nevertheless, the overall degradation time for P(DTR carbonate) can be months to years [201]. The ester bond degrades into carboxylic acid and alcohol, while the carbonate bond releases two alcohols and carbon dioxide [200]. The amide has been found to be relatively stable in vitro [200]. Overall, P(DTR carbonate) undergoes bulk degradation and its mechanical properties are determined by the pendant group [170, 200].

The slow degradation rate of polycarbonates has led to its investigation in orthopaedic tissue engineering applications. Additionally, P(DTR carbonate) elicits a response for bone ingrowth at the bone-polymer implant interface, supporting the use of P(DTR carbonate) as a bone scaffold.[201] Recent studies has shown that osteoblast cells do attach to the surface of P(DTR carbonate). Results indicate that these osteoblasts maintained their phenotype and rounded cell morphology[202].

Poly(ethylene glycol)/Poly(ethylene oxide)

Poly(ethylene glycol) (PEG) is generally a linear-chained polymer consisting of an ethylene oxide repeating unit (-O-CH2-CH2)n (Table 2.3, Figure 2.6). Poly(ethylene oxide) (PEO) has the same backbone as PEG, but a longer chain length and thus a higher molecular weight [101, 203]. PEG is hydrophilic and synthesized by an anionic/cationic polymerization [121, 125]. The ability of PEG to act as a swelling polymer has primarily led to its function as a hydrogel, and in some instances an injectable hydrogel. Unfortunately, the linear chain form of PEG leads to rapid diffusion and low mechanical stability [125]. PEG networks may be created by attaching functional groups to the ends of the PEG chain and then initiating covalent crosslinking.[101, 125, 149, 204-206] PEG is

naturally non-degradable. However, PEG may be made degradable by copolymerization with hydrolytically or enzymatically degradable polymers [207].

The ease with which PEG may be modified, whether with crosslinkable groups for network formation or degradable groups for resorbable applications, has probably led to the widespread interest in PEG for tissue engineering or other biomedical applications. For example, PEG has been copolymerized with PLGA as well as alginate to form hydrogels. Results have shown that DNA content of chondrocytes on copolymerized PLGA-PEG increases as the percentage of degradable components becomes higher [208]. Similarly, islets of Langerhans in alginate-PEG hydrogels retained their viability and expressed function through insulin excretion [209].

Polyurethane

Recent investigations have developed polyurethane polymers as scaffold materials. Polyurethane is an elastomeric polymer that is typically non-degradable (Table 2.3, Figure 2.6). Positive attributes, such as flexible mechanical strength and biocompatibility, has led to the synthesis of degradable polyurethanes with non-toxic diisocyanate derivatives [164, 210-212]. Studies have shown that polyurethane scaffolds support cell attachment with chondrocytes, bone marrow stromal cells, and cardiomyocytes [212-214].

2.2.4 Scaffold Design Properties

2.2.4.1 Fabrication

There are two main considerations in the assembly of a polymeric tissue engineering scaffold. First is the curing method, or the method by which the polymer is

assembled into a bulk material. Second is the fabrication strategy. The chemical nature of the polymer often determines both the curing method and fabrication strategy. There are two main curing methods: polymer entanglement and polymer cross-linking. Entanglement usually involves intertwining long, linear polymer chains to form a loosely bound polymer network. An advantage of this type of method is that it is simple, allowing the polymer to be molded into a bulk material using heat, pressure or both. However, a disadvantage of this process is that the bulk material sometimes lacks significant mechanical strength. The second curing method is cross-linking, which involves the formation of covalent or ionic bonds between individual polymer chains. Typically either a radical or ion is needed to promote crosslinking along with an initiator, such as heat, light, chemical accelerant, or time. The advantages of crosslinked polymers are that they often have significant mechanical properties. Furthermore, crosslinked polymers may be injected into a tissue defect and cured in situ. However, one major disadvantage is the possible cytotoxicity issues with crosslinking systems. The multiple components used by crosslinking polymers as well as the necessary chemical reaction may lead to the use of cytotoxic components or the formation of cytotoxic reaction byproducts.

There are two basic strategies of polymeric scaffold fabrication: prefabrication and in situ. Prefabrication structures are cured before implantation. This strategy is often preferred since it is formed outside the body, allowing the removal of cytotoxic and non-biocompatible components prior to implantation. However, the notable disadvantage of prefabricated scaffolds is that it may not properly fit in a tissue defect site, causing gaps between the engineered graft and the host tissue. These void spaces may lead to

undesirable results, including fibrous tissue formation. Therefore, the deficiencies of prefabricated scaffolds have led to investigations towards in situ fabrication of a scaffold, which involves curing of a polymeric matrix within the tissue defect itself. The deformability of an in situ fabricated matrix creates an interface between the scaffold and the surrounding tissue, facilitating tissue integration [215]. Furthermore, the implantation of an in situ fabricated scaffold may require as little as a narrow path for injection of the liquid scaffold, allowing minimally invasive surgery techniques to be utilized. A disadvantage of in situ fabrication of scaffolds is that the chemical or thermal means of curing the polymer can significantly affect the host tissue as well as any biological component of the engineered graft.

2.2.4.2 Micro-structure

Tissue regeneration through cell implantation in scaffolds is dependent on the micro-structure of the scaffold. Since most cells are anchorage dependent, the scaffold should possess properties that aid cell growth and facilitate attachment of a large cell population [163, 216]. To this end, a large scaffold surface area is typically favorable. Furthermore, highly porous scaffolds allow for an abundant number of cells to infiltrate the scaffold's void space. Similarly, the continuity of the scaffold's pores is important for proper transport of nutrients and cell migration. It is also generally advantageous for scaffolds to possess a large surface area to volume ratio. This ratio promotes the use of small diameter pores that are larger than the diameter of a cell. However, high porosities compromise the mechanical integrity of the polymeric scaffold. Clearly, balancing a scaffold's surface area, void space, and mechanical integrity is a necessary challenge that must be overcome in the construction of viable tissue engineering scaffolds.

Additionally, a polymer's effectiveness as a scaffolding material is dependent on its interaction with transplanted or host cells. Thus the polymer's surface properties should facilitate their attachment, proliferation, and (possible) differentiation. A strong cell adhesion favors the proliferation of cells, while a rounded morphology promotes their differentiation [163]. The hydrophilic nature of some polymers promotes a highly wettable surface and allows cells to be encapsulated by capillary action [217]. Furthermore, cellular attachment and function on polymeric scaffolds may be enhanced by providing a biomimetic surface through the incorporation of proteins and ligands.

2.2.4.3 Macro-structure

A scaffold can be formed into a number of different macro-structures including, fiber meshes, hydrogels, and foams. Fiber meshes are formed by weaving or knitting individual polymeric fibers into a three-dimensional structure and are attractive for tissue engineering as they provide a large surface area for cell attachment.[165] Furthermore, a fiber mesh scaffold structure mimics the properties of the extracellular matrix, allowing the diffusion of nutrients to cells and waste products from cells. A disadvantage to this form is the lack of structural stability. However, fiber bonding, which involves bonding at fiber cross points, has been introduced to create a more stable structure [163, 165, 218].

Hydrophilic polymers are often formed into hydrogels by physical polymer entanglements, secondary forces, or chemical crosslinking [101, 130]. The significant property of hydrogels is their ability to absorb a tremendous amount of water, up to a thousand times their own dry weight [130]. This aqueous environment, ideal for cell encapsulation and drug loading, has encouraged many investigations into hydrogels for biomedical applications. Hydrogels are generally easy to inject or mold, and therefore are

often incorporated into strategies involving minimally invasive surgical techniques [149]. Some drawbacks to hydrogels are that they lack strong mechanical properties and they are difficult to sterilize [130, 149].

Foam and sponge scaffolds provide a macro-structural template for the cells to form into a three-dimensional tissue structure. There are several different processing techniques for porous constructs, including phase separation, emulsion freeze drying, gas foaming, and solvent casting/particulate leaching [163, 219-221]. A recent technology that has become of interest in tissue engineering is rapid prototyping or solid freeform fabrication. These techniques are quite exciting since they allow for the precise construction of scaffold architecture, often based upon a computer aided design model[222]. The most appropriate scaffold macro-structure is dependent on the type of the polymer utilized and the application (tissue) of interest.

2.2.4.4 Biocompatibility

One of the most essential properties of an engineered construct is its biocompatibility, or ability to not elicit a significant or prolonged inflammatory response. It is important to know that any injury will elicit some inflammatory response, and this is certainly true with the implantation of a polymeric scaffold. However, this response should be limited and not prolonged.

When a polymeric scaffold is implanted in a tissue, there is typically a three phase tissue response [223-225]. Phase I incorporates both acute and chronic inflammation, which occurs in a short period of time (1-2 weeks). Phase II involves the granulation of tissue, a foreign body reaction and fibrosis. The rate of phase II is primarily dependent on the degradation rate of the polymeric scaffold. Finally, the fastest step, phase III is when

the bulk of the scaffold is lost. These phases are directly influenced by the properties of the polymeric scaffold. Therefore, it is important to evaluate a variety of scaffold properties including synthesis components, fabrication, micro-structure, and macro-structure. It is a general thought that as the complexity of a scaffold system increases, the more likely it will result in a significant response by the body [190].

2.2.4.5 Biodegradability

Most polymeric scaffolds are designed to provide temporary support and, therefore to be biodegradable. Therefore, the degraded products of the scaffold must have a safe route for removal from the host. The rate of degradation is often affected by the properties of the polymeric scaffold including synthesis components, fabrication, micro-structure, and macro-structure. Most investigations intend for the scaffold degradation rate to closely follow the rate of tissue repair [139, 163]. However, this intention may be difficult to implement. An alternative approach is to design the scaffold's degradation rate so that it is quicker than the rate of degradation product removal, in an effort to minimize negative host responses.

There are two types of degradation: surface and bulk [226]. Surface degradation of a scaffold is characterized by a gradual decrease in the dimensions of the scaffold with no change in its mechanical attributes. At a critical point during surface degradation, both size and mechanical properties of the scaffold decrease rapidly. Bulk degradation is characterized by loss of material throughout the scaffold's volume during degradation. Thus, mechanical strength decreases during bulk degradation and is dependent on the degradation rate. Since bulk degradation maintains an intact surface, it may facilitate cell adhesion to a greater extent than surface eroding scaffolds. Natural polymers mainly

undergo surface degradation, since enzymes are generally too large to penetrate into the bulk of the scaffold. However, synthetic polymers can degrade by surface, bulk, or both, depending on its composition.

2.2.4.6 Mechanical Strength

Since many tissues undergo mechanical stresses and strains, the mechanical properties of a scaffold should be considered. This is especially true for the engineering of weight bearing orthopaedic tissues. In these instances, the scaffold must be able to provide support to the forces applied to both it and the surrounding tissues. Furthermore, the mechanical properties of the polymeric scaffold should be retained until the regenerated tissue can assume its structural role [6]. In cases where mechanical forces are thought to be required for cell growth and phenotype expression, a scaffold which displays surface eroding properties may be preferred. Alternatively, hydrophobic polymers tend to resist water absorption and thus sustain their strength longer than hydrophilic polymers.

2.2.5 Summary

Tissue engineering has emerged as a growing field for restoring, repairing, and regenerating tissue. Polymeric scaffolds especially have a profound impact on the possibilities of tissue engineering by providing structure for the attachment, proliferation, and differentiation of transplanted or host cells. These constructs have led to exciting and novel clinical options for the repair of tissues, including but not limited to skin, bone, cartilage, kidney, liver, nerve, and smooth muscle. To this end, scaffold properties must be carefully considered for the intended application. Most importantly, the polymeric

scaffold must allow invading cells to express proper functionality of the tissue being formed. Thus, tissue engineering research is continuously trying to enhance polymeric scaffold properties to form tissue that closely resembles the native tissue.

Table 2.2. Properties of degradable natural homopolymers that have been utilized in the fabrication of tissue engineering scaffolds.

	Natural Polymer	Curing Method	Primary Degradation Method	Primary Degradation Products
A	Agarose	entanglement	enzymatic agarases	oligosaccharides
B	Alginate	crosslinking	alginate lyases	mannuronic acid and guluronic acid
C	Hyaluronic Acid	entanglement	enzymatic hyaluronidase	β(1-4) linked glucuronic acid and glucosamine
D	Chitosan	crosslinking	enzymatic chitosanase	glucosamines
E	Collagen	crosslinking	enzymatic collagenase or lysozyme	various peptides depending on sequence
F	Gelatin	entanglement	enzymatic collagenases	various peptides depending on sequence
G	Silk	entanglement	proteolytic proteases	various peptides depending on sequence

Table 2.3. Properties of degradable synthetic homopolymers that have been utilized in the fabrication of tissue engineering scaffolds.

	Synthetic Polymer	Curing Method	Primary Degradation Method	Primary Degradation Products
A	Poly(glycolic acid)	entanglement	ester hydrolysis	glycolic acid
B	Poly(L-lactic acid)	entanglement	ester hydrolysis	lactic acid
C	Poly(D,L-lactic acid-co-glycolic acid)	entanglement	ester hydrolysis	lactic acid and glycolic acid
D	Poly(caprolactone)	entanglement	ester hydrolysis	caproic acid
E	Poly(propylene fumarate)	crosslinking	ester hydrolysis	fumaric acid and propylene glycol
F	Polyorthoester	entanglement	ester hydrolysis	various acids depending upon R group
G	Polyanhydride	entanglement	anhydride hydrolysis	various acids depending upon R group
H	Polyphosphazene	entanglement	hydrolysis	phosphate and ammonia
I	Polycarbonate (tyrosine derived)	entanglement	ester and carbonate hydrolysis	alkyl alcohol and desaminoyrosyl-tyrosine
J	Poly(ethylene glycol) /Poly(ethylene oxide)	entanglement	non-degradable	not applicable
K	Polyurethane	crosslinking	ester, urethane, or urea hydrolysis	diisocyanate and diols

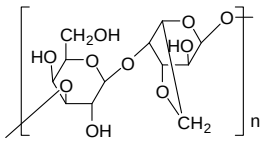

(A) Agarose

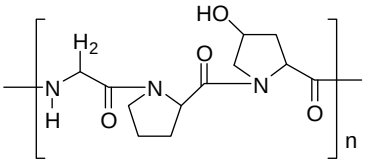

(E) Collagen*

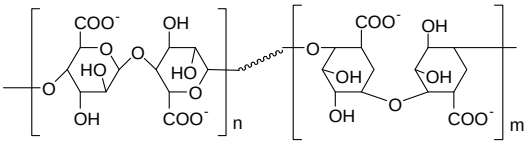

(B) Alginate

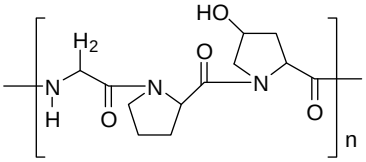

(F) Gelatin*

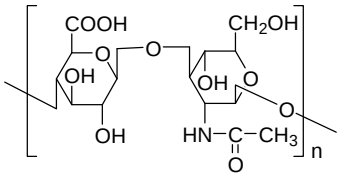

(C) Hyaluronic acid

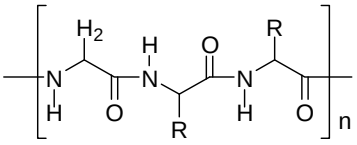

(G) Silk**

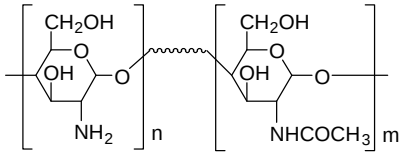

(D) Chitosan

Figure 2.5. Repeating structural unit of degradable natural homopolymers under investigation as scaffold materials for tissue engineering applications. (*Collagen and gelatin have variable sequences, but are predominately glycine, proline, and hydroxyproline. **Silks have a glycine rich sequence, with glycine repeating every second or third amino acid residue. The variable residues are primarily alanine or serine.)

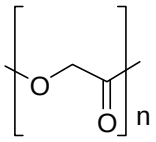

(A) Poly(glycolic acid)

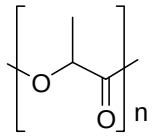

(B) Poly(L-lactic acid)

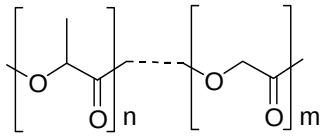

(C) Poly(D,L-lactic acid-co-glycolic acid)

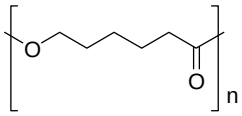

(D) Poly(caprolactone)

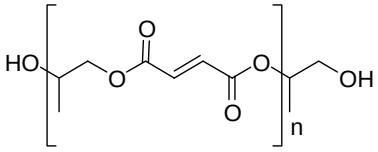

(E) Poly(propylene fumarate)

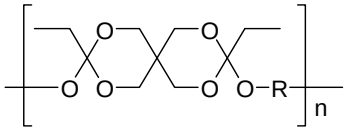

(F) Polyorthoester

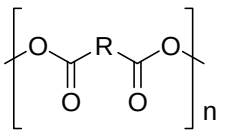

(G) Polyanhydride

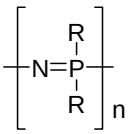

(H) Polyphosphazene

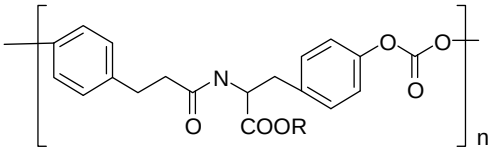

(I) Polycarbonate(tyrosine derived)

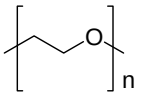

(J) Poly(ethylene glycol)/Poly(ethylene oxide)

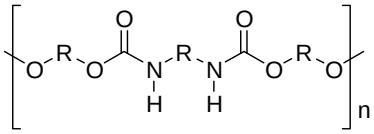

(K) Polyurethane

Figure 2.6. Repeating structural unit of degradable synthetic homopolymers under investigation as scaffold materials for tissue engineering applications.

3 Effect of Construct Properties on Encapsulated Chondrocyte Expression of Insulin-like Growth Factor-1*

3.1 Introduction

Many biodegradable materials have been developed and investigated for use in reconstructing damaged articular cartilage [3, 6, 103, 116, 227]. Previous works indicate that hydrogels may be a preferred biomaterial for chondrocytes as they allow retention of the cells' spherical morphology, which has been further correlated to stable phenotypic function [132, 228]. Alginate is a common natural biomaterial that has been used extensively to encapsulate chondrocytes [103, 116, 229, 230]. A hydrogel is formed by crosslinking the glucoronate chains of alginate with one another by divalent ions, such as calcium. An important property of this polymer is that it does not contain cell adhesive groups along its backbone, which allows for the investigation of cell function in the absence of matrix influences [231].

It is clear that external signals are critical for chondrocytes to maintain their phenotype [2, 33, 232, 233]. Many cartilage engineering strategies are based upon the delivery of exogenous signals to an encapsulated cell population [234, 235]. The type, concentration, and delivery profile of the exogenous signal is engineered to maintain phenotype, most importantly the synthesis of type II collagen. We propose a novel view of engineered tissues, where biomaterials are utilized to encourage endogenous expression of signaling proteins. Therefore, we hypothesize that an environment that facilitates signaling among an encapsulated cell population is critical to the successful development of engineered tissues.

---

* This chapter was published as: Yoon DM, Hawkins, EC, Francke-Carroll, S, and Fisher JP. Effect of Construct Properties on Encapsulated Chondrocyte Expression of Insulin-like Growth Factor-1. Biomaterials. 2007; 28: 299-306.

In order to examine this hypothesis, we have begun investigating insulin-like growth factor-1 (IGF-1) signaling of chondrocytes encapsulated in alginate hydrogels. IGF-1 is a protein with a molecular weight of 7.5 kDa, which has a similar homology to insulin [37, 38, 40]. In cartilage, IGF-1 is generally viewed as an anabolic growth factor of chondrocytes, which has been shown to increase cartilage matrix synthesis [236, 237]. IGF-1 signaling, as well as most protein signaling, can be broadly characterized as involving multiple steps including expression, synthesis, secretion, transport, antagonist binding, and receptor binding [16]. This study focused on the endogenous expression of IGF-1 by chondrocytes. By varying the encapsulating alginate concentration, the water content of the alginate hydrogel was altered to affect the diffusional resistances of protein signals among neighboring chondrocytes. Additionally, the paracrine signaling distance between chondrocytes was modified by changing the density of chondrocytes encapsulated in each alginate hydrogel bead. We investigated the effects of these fabrication parameters, cell density and alginate concentration, on chondrocyte IGF-1 expression and resulting phenotypic type II collagen expression over 8 days, using quantitative reverse-transcriptase polymerase chain reaction (qRT-PCR). The objectives for this work were to determine the (1) effect of cell density on chondrocyte IGF-1 expression, (2) effect of alginate concentration on chondrocyte IGF-1 expression and (3) effect of IGF-1 expression on type II collagen expression by chondrocytes.

3.2 Materials and Methods

3.2.1 Cartilage Extraction and Chondrocyte Isolation

Fresh cartilage was harvested from the metatarsal phalangeal joint of calves (15-18 wk old), washed three times in Dulbecco's modified eagle medium: nutrient mixture

F-12 ham (DMEM/F12) media (Gibco, Carlsbad, CA) supplemented with 50 μg/mL ascorbic-2-phosphate (Sigma-Aldrich, St. Louis, MO), 1 mg/mL bovine serum albumin (Sigma-Aldrich), 1.2 mg/mL sodium bicarbonate (Sigma-Aldrich), 0.1% penicillin/streptomycin (Gibco), and 0.1% sodium pyruvate (Gibco) (supplemented DMEM). Cartilage was digested in 0.2% *collagenase P* (Roche, Indianapolis, IN) overnight at 37°C at 5% CO_2. Chondrocytes were filtered through a 70 μm nylon mesh and washed three times in the supplemented DMEM/F12 media to remove residual undigested cartilage. The final chondrocyte solution was placed in supplemented DMEM/F12 media with 10% fetal bovine serum (FBS, Gibco). Cell counts and viability were assessed by visualization on a hemacytometer using a phase contrast microscope. Primary chondrocytes were incubated for approximately 2 hrs in supplemented DMEM/F12 media with 10% FBS before being encapsulated into alginate beads.

3.2.2 Chondrocyte Encapsulation in Alginate and Culture

Alginate solutions (0.8%, 1.2%, and 2.0% w/v) were prepared by mixing alginic acid sodium salt from brown algae (Sigma-Aldrich), 0.15 M NaCl, and 0.025 M HEPES (Sigma-Aldrich) in deionized water (pH 7.4). This solution was heated on a hot plate to dissolve the alginate and then stored for a day before being sterile filtered. Primary chondrocytes without preculture (0 d) were encapsulated at two different densities (25,000 and 100,000 cells/bead). The alginate and chondrocytes were passed through a 22 gauge needle and injected into a continuously stirred 100 mM $CaCl_2$ solution (Sigma-Aldrich). Alginate beads, approximately 3 mm in diameter, formed instantaneously and were incubated for 15 min in the $CaCl_2$ solution. The alginate beads were rinsed once with supplemented DMEM/F12 media and then placed into a 6-well plate, with each well

containing approximately 500,000 total chondrocytes (20 or 5 beads). Chondrocytes encapsulated in the alginate beads were cultured in supplemented DMEM/F12 media and 10% FBS at 37°C and 5% CO_2. The media was changed every 2-3 days. Chondrocytes were isolated from the alginate beads for analysis at day 1, 4, and 8, by the addition of 3 mL of 0.1 M ethyldiaminetetraacetic acid (Sigma-Aldrich) for 30 min at 37°C, which disrupted the bead by Ca^{2+} chelation. A cell pellet was formed by centrifugation at 1000x*g* for 8 min. The chondrocyte pellet was resuspended in phosphate buffer saline (PBS) and used for subsequent assays.

3.2.3 Alginate Water Content

The water weights of alginate beads were determined by investigating their swollen weight (Ws) and dry weight (Wd). Ten alginate beads of 0.8%, 1.2%, and 2.0% w/v concentrations without cells were incubated in supplemented DMEM/F12 media with 10% FBS at 37°C. The media was changed every 2-3 days. At various time points, 1, 4, and 8 d, the alginate beads were weighed (Ws). Then the alginate beads were placed into an oven at 100°C for approximately two weeks and weighed again (Wd). The water content percentage was calculated using the formula: (Ws-Wd)/Ws x 100%. Mean water contents and associated standard deviations (n = 3) are reported.

3.2.4 Cell Viability

Trypan blue stain 0.4% (Gibco) was used to distinguish viable cells from non-viable cells. Viable cells appeared round and clear. Non-viable cells were asymmetrical and absorbed the dye, therefore appearing blue. Cell viability percentage was determined

by the following equation: (alive cells)/(alive cells + dead cells) x 100. Mean viabilities and associated standard deviations (n = 3) are reported.

3.2.5 Histological Preparation

Samples were collected and fixed in 4% paraformaldehyde (Sigma-Aldrich) and 0.1 M sodium cacodylate (Sigma-Aldrich) buffer containing 10 mM $CaCl_2$ at pH 7.4 and 4^{o}C. The beads were washed with 0.1 M sodium cacodylate buffer and 10 mM $CaCl_2$ at pH 7.4 at room temperature for 24 hrs. The beads were placed in histological cassettes and dehydrated for histological processing by passing through an ascending ethanol line (40-100% for 20 min each) with two final xylene washes. The samples were embedded in paraffin (Paraplast X-tra, Fisher Scientific, Pittsburgh, PA) and cut into 4 μm thickness sections, which were then placed onto glass slides (Superfrost, Fisher Scientific). Sections were oven dried at 62^{o}C for 2 hrs, deparaffinized in xylene (three times each for 3 min), rehydrated in ethanol (100% and 95% for 1 min), and then stained with Hematoxylin and Eosin (H&E, Richard-Allan Scientific, Kalamazoo, MI) on an automated stainer (Richard Allan Microm HMS 760X).

3.2.6 Chondrocyte Distribution Analysis

The number of chondrocytes for each cell density case (*e.g.*, 25,000 and 100,000 cells/bead) in 1.2% w/v alginate beads was determined by counting the cells with microscopic examination of histological sections. Alginate beads with encapsulated chondrocytes were fixed, embedded, sectioned, and stained with H&E. Images were taken for each histological section at a radius of 0, 0.75, and 1.50 mm. The total number

of cells was counted at these locations. Mean cells per area and associated standard deviations (n = 3) are reported.

3.2.7 RNA Isolation

Total RNA was isolated from chondrocytes using an RNeasy Mini Kit (QIAGEN, Valencia, CA). Chondrocytes were isolated as described above. The chondrocyte pellet was suspended in a lysis buffer with β-mercaptoethanol. The suspension was homogenized by both vortexing and using a syringe and needle. Ethanol was mixed into this solution and added to a spin column. Centrifugation adsorbed the RNA to the silica gel membrane within the spin column, which underwent several washes with buffer and DNA digestion by adding in a DNase solution (QIAGEN). Total RNA was eluted into 30 μL of RNase free water (QIAGEN).

3.2.8 Quantitative Reverse Transcriptase Polymerase Chain Reaction (qRT-PCR)

Isolated mRNA was reverse transcribed into cDNA using a cDNA Archive Kit (Applied Biosystems, Foster City, CA). Quantitative RT-PCR was performed by combining the cDNA solution with a Universal Master Mix (Applied Biosystems), as well as oligonucleotide primers and Taqman probes (Applied Biosystems) that were created for the genes of interest (IGF-1 and type II collagen) and the endogenous gene control (glyceraldehyde 3 phosphate dehydrogenase, GAPDH). The primer and probe sequences for IGF-1, type II collagen and GAPDH are detailed in Table 3.1. By using Taqman probes, the specific amplicon for the gene of interest was detected. The reaction was conducted on an ABI Prism 7000 sequence detector (Applied Biosystems) using thermal conditions of 2 min at 50^{o}C, 30 min at 60^{o}C, 5 min at 95^{o}C, and 40 cycles of 20 s

at 94°C, and 1 min at 62°C. Each sample was studied in triplicate for each mRNA of interest. The gene expression for IGF-1 and type II collagen were analyzed for all of the groups in the study using a relative standard curve method, and were both normalized to GAPDH. The calibrator for each gene expression sample set data was selected to be the 2.0% w/v alginate bead group with a 25,000 chondrocyte density population per bead for each gene of interest. This calibrator was chosen because the fold change values were the lowest, compared to all other groups. Therefore, the fold change amongst the samples was visually observable in the qRT-PCR data graphs. Mean fold changes and associated standard deviations (n = 3) are reported.

3.2.9 Western Blotting

Total protein concentration was extracted from the isolated cell pellet by using M-Per Mammalian Protein Extraction Reagent (Pierce, Rockford, IL) and Halt Protease Inhibitor Cocktail (Pierce). All protein samples were stored in a -80°C freezer until their analysis. The protein solutions were dot blotted onto a nitrocellulose membrane and conjugated to the primary and secondary antibody solution as in a western blot. Supplemented media was used as a negative control to validate that signals obtained from the sample blots were only from protein produced by chondrocytes. Antibodies were used to study type II collagen and IGF-1 proteins. The primary antibodies are: anti-type II collagen (sheep polyclonal antibody, ab300, Abcam, Cambridge, MA) and anti-hIGF-1 (goat IgG antibody, AF-291-NA, R&D Systems, Minneapolis, MN). The secondary antibodies are all horse radish peroxidase (HRP) conjugated: sheep polyclonal antibody (ab6795, Abcam) and goat IgG antibody (ab6885, Abcam). All antibodies were diluted 1000 fold in tris buffer-saline with non-fat milk powder. Protein blots were developed

using a SuperSignal West Pico Chemiluminescent Substrate (Pierce). The blots were scanned with a BioRad ChemiDoc XRS image analyzer. The same blots were used to detect type II collagen and IGF-1 respectively, which was achieved by using Restore Western Blot Stripping Buffer (Pierce).

3.2.10 Statistical Analysis

All experiments were conducted in triplicate. Data from all studies were analyzed using one-way analysis of variance (ANOVA) and Tukey's multiple-comparison test were used to determine statistical significance with a 95% confidence interval ($\alpha = 0.05$). The means and standard deviations are reported in each figure.

3.3 Results

3.3.1 Physical Characterization of Encapsulated Chondrocytes in Alginate Beads

In order to demonstrate the effects of alginate concentration on the physical properties of the model beads, the water content of the beads was examined using concentrations of 0.8%, 1.2%, and 2.0% w/v alginate. These concentrations were chosen as they spanned the entire range in which alginate beads could be reproducibly fabricated. The results demonstrate that water content was greater than 95% for all conditions examined (Figure 3.1). The water content was greatest, over 97%, in the 0.8% w/v alginate beads. There was no significant change in water content for 0.8% w/v alginate over the course of the 8 d study ($p = 0.59$). The lowest water content, less than 96%, was found in the 2.0% w/v alginate beads. All three alginate concentrations were significantly different from one another at day 1 and 4 ($p < 0.01$). On day 8, the water content was

determined to be similar amongst the 0.8% and 1.2% w/v alginate concentration beads, while both were significantly higher than 2.0% w/v alginate beads ($p < 0.01$).

Primary bovine articular chondrocytes were then encapsulated in the three alginate bead classes and cell viability was investigated. A slight trend of decreased cell viability was observed during the 8 d study, however viability was found to be greater than 65% for all alginate concentrations and at all time points (Figure 3.2). The microscopic images taken at day 1 (Figure 3.3a and b) show chondrocytes at both cell densities encapsulated homogeneously throughout a 2.0% w/v alginate bead. Furthermore, the average distance between the cells was estimated for the two chondrocyte densities. Assuming a chondrocyte diameter of 15 μm [238, 239] and an alginate bead diameter of 3 mm (See Figure 3.3a and b), the average effective distance for paracrine signaling was calculated to be approximately 87.6 μm (25,000 cells/bead) and 49.6 μm (100,000 cells/bead). See Appendix A for calculations of cell-to-cell distance.

Histological analysis was utilized to examine chondrocyte morphology and distribution throughout the alginate beads. Figure 3.4 depicts a thin layer section of the chondrocytes within 1.2% w/v alginate beads with cell densities of 25,000 cells/bead (Figure 3.4a) and 100,000 cells/bead (Figure 3.4b). Chondrocyte nuclei were visible as dark violet circles. The surrounding alginate also stains a light violet color due to the alginate ionic charge. Cell distribution may be qualitatively described by measuring the number of cells per area at a radius of 0, 0.75, and 1.50 mm out from the center of the alginate bead (Figure 3.5). For both the 25,000 and 100,000 cell density cases, there was no statistical difference of the average number of cells per area at all three locations

examined ($p = 0.04$ and $p = 0.05$, respectively). When comparing the 25,000 and 100,000 cell densities, the average number of cells per area was determined to be statistically different at each radius examined ($p < 0.01$), as expected.

3.3.2 IGF-1 mRNA Expression

Over the course of 8 d, IGF-1 mRNA expression was detected for chondrocytes encapsulated in all alginate concentrations. For the 25,000 density case, there was an increasing trend of IGF-1 mRNA expression in all alginate concentrations (Figure 3.6). During the 8 d study, encapsulated chondrocytes exhibited approximately a 3 fold increase in IGF-1 expression for the 0.8% w/v alginate beads, a 10 fold increase for the 1.2% w/v alginate beads, and a 35 fold increase for the 2.0% w/v alginate beads. At day 1, the IGF-1 fold change values for all of the alginate concentrations were similar ($p = 0.08$). At day 8, there was no statistical difference between the 0.8% and 1.2% w/v alginate concentration case ($p = 0.02$) and both were greater than the 1.2% w/v alginate case ($p < 0.01$).

Overall, the encapsulation of 100,000 chondrocytes per alginate bead demonstrated significantly higher IGF-1 mRNA expression when compared to the lower cell density case (Figure 3.7). At this higher cell density, chondrocytes showed an increased level of IGF-1 mRNA expression for all alginate cases and at all time points, except for the 0.8% w/v alginate group at day 1.

For the 100,000 density case, the 0.8% w/v alginate group showed similar fold change levels for IGF-1 at all time points ($p = 0.05$). Alternatively, the 1.2% and 2.0% alginate beads showed increased IGF-1 expression from day 1 to 8. However, in both of these groups, IGF-1 expression peaked at day 4 and subsequently fell at day 8. At each

time point, the 2.0% w/v alginate group's IGF-1 fold change levels are greater than that for the 0.8% w/v alginate group ($p < 0.01$).

3.3.3 Type II Collagen mRNA Expression

Type II collagen mRNA expression was detected for chondrocytes encapsulated in all alginate concentrations and time points. For the 25,000 chondrocyte density case (Figure 3.8), cells encapsulated in 0.8% w/v alginate beads demonstrated a trend of decreasing type II collagen mRNA expression over the course of 8 d. Chondrocytes encapsulated in 1.2% w/v alginate demonstrated similar type II collagen expression levels at all time points examined ($p = 0.10$). Type II collagen fold change levels for the 2.0% w/v alginate case were greatest at day 4 but similar between day 1 and 8 ($p < 0.01$).

Overall, and similar to the IGF-1 study, the encapsulation of 100,000 chondrocytes per alginate bead demonstrated higher type II collagen mRNA expression when compared to the lower cell density case (Figure 15). Specifically, chondrocytes encapsulated at a 100,000 cells/bead density had a greater type II collagen mRNA expression for 1.2% and 2.0% alginate concentrations compared to the lower cell density case ($p < 0.05$).

Considering the results of the 100,000 chondrocyte density cases alone, the type II collagen mRNA expression levels for 0.8% and 2.0% w/v alginate groups did not significantly change over the course of the 8 d study ($p = 0.22$ and $p = 0.14$, respectively). However, the chondrocytes encapsulated in 1.2% w/v alginate showed mRNA expression levels to be greatest at day 8 compared to day 1 and 4, which were similar in value ($p < 0.01$). There was no significant difference between the any of the alginate cases at day 8 ($p = 0.08$).

3.3.4 IGF-1 and Type II Collagen Protein Expression

The intracellular proteins of chondrocytes in all of the sample groups were extracted for detection of IGF-1 and type II collagen. Results indicate that both proteins were being synthesized by chondrocytes from every sample group during the 8 d study. Figure 3.10a shows the IGF-1 protein dot blot for chondrocytes in all of the alginate bead cases. The production of type II collagen was supported by the dot blot pictured in Figure 3.10b. These results showed that protein production occurred, but no correlation was observed with mRNA expression levels by chondrocytes. This is expected as the dot blot method is not quantitative.

3.4 Discussion

In order to create an engineered articular cartilage construct based upon transplanted chondrocytes, it is essential to develop the proper environmental conditions for chondrocytes to retain their phenotype. Currently, investigators propose cartilage engineering strategies that ensure a stable chondrocyte phenotype by delivering exogenous signals to a transplanted cell population [234, 240]. We aimed to investigate whether construct properties may be altered to enhance endogenous signal expression, in order to ensure a stable chondrocyte population. In particular, this work investigates the effect of construct properties on chondrocyte expression of IGF-1 within an alginate hydrogel. The two properties, cell density and alginate density, were chosen to be varied simultaneously since each has a limited working range. Cell density is bounded at a lower limit by a reasonable cell population for analysis and at a higher limit by the ability to encapsulate isolated (non-contacting) chondrocytes. Alginate density, in contrast, is

limited at both the lower and higher limit by concentrations that can produce beads under standard conditions. Nevertheless, by varying cell density, the cell-to-cell distance was altered, which therefore influenced paracrine signaling distance. Furthermore, by varying alginate density, the water content or soluble protein transport resistance was changed. Using these parameters, the following three objectives were addressed in this study: (1) effect of cell density on IGF-1 expression by chondrocytes in alginate beads, (2) effect of alginate concentration on IGF-1 expression by chondrocytes and (3) effect of IGF-1 expression on type II collagen expression by encapsulated chondrocytes.

To this end, chondrocytes were encapsulated homogenously within the alginate hydrogel beads, with the homogenous distribution of chondrocytes demonstrated by histological examination of cells per area (Figure 3.5). For both cell density cases, the average number of cells per area was similar at each of the three radii examined, indicating that the chondrocytes were distributed homogenously. Furthermore, a significant difference in cell density was observed between the 25,000 and 100,000 cells/bead, as expected.

The results of this work demonstrate that cell density plays a significant role in augmenting IGF-1 expression. Over the 8 d study, a generally increasing trend of IGF-1 expression by chondrocytes was found for both density cases and all of the alginate concentrations. However, the overall expression of IGF-1 was dramatically greater for the 100,000 versus 25,000 cell density case, with an order of magnitude difference demonstrated by chondrocytes in these two cases (Figures 3.6 and 3.7). This result indicates that a difference in the paracrine signaling distance between chondrocytes impacted the expression of IGF-1, with smaller cell-to-cell distances associated with

increased levels of IGF-1 mRNA expression. We propose that increased cell density enhances chondrocyte competition for IGF-1, thereby inducing the endogenous expression of IGF-1.

Secondly, the results indicate that IGF-1 expression by chondrocytes is strongly augmented by alginate hydrogel concentrations, but only at a high cell density (Figure 3.7). Increasing alginate concentration to 2.0% w/v is associated with a slight, but significant decrease in water content, indicating an increase in diffusional resistances of soluble molecules. The effect of alginate concentration is not seen at the 25,000 cell density level. However, at the 100,000 cell density level IGF-1 mRNA expression is significantly altered by alginate concentration. These results indicate that changing construct properties, particularly by increasing both cell density and matrix concentration, may be utilized to enhance IGF-1 mRNA expression.

Finally, we examined the effect of IGF-1 expression on chondrocyte phenotype, as measured by type II collagen expression (Figures 3.8 and 3.9). Although understanding the influence of construct parameters on molecular signaling is significant, the resulting affect upon cell phenotype is critical. In all cases, type II collagen expression was observed, demonstrating phenotypic function of the chondrocytes. Similar to IGF-1 mRNA expression, chondrocytes encapsulated at a density of 100,000 cells/bead expressed type II collagen mRNA at a significantly higher level than at a density of 25,000 cells/bead, demonstrating the major influence of cell density on cell function. Also similar to the IGF-1 results, there was no observable trend for type II collagen expression at the low density case, while at the high density case type II collagen mRNA expression generally increased with alginate concentration. Thus these

results indicate that alterations in cell density and polymer concentration do alter encapsulated chondrocyte IGF-1 expression and, furthermore, chondrocyte function, as demonstrated by type II collagen expression.

3.5 Conclusion

The optimal construct for chondrocyte transplantation is of great interest in the biomaterials community. While most approaches for studying chondrocytes in these engineered environments focus on exogenous protein delivery, we present a novel approach in understanding chondrocytes within a biomaterial by focusing on the endogenous signaling. The results of this work demonstrate that both cell density and alginate concentration altered IGF-1 mRNA expression by chondrocytes encapsulated within alginate beads. Furthermore, IGF-1 mRNA expression trends were shown to follow those observed for type II collagen expression, a key phenotypic marker of chondrocytes.

Table 3.1. Primer and Probe Sequences for Quantitative RT-PCR.

Protein	Segment	Sequence
Insulin-Like Growth Factor-1 (IGF-1)	Forward Primer	CCCAGACAGGAATCGTGGAT
	Reverse Primer	ACATCTCCAGCCTCCTCAGATC
	Probe	CTGCTTCCGGAGCTG
Type II Collagen	Forward Primer	CGGGCTGAGGGCAACA
	Reverse Primer	CGTGCAGCCATCCTTCAGA
	Probe	CAGGTTCACATATACCG
GAPDH	Forward Primer	TGCCGCCTGGAGAAACC
	Reverse Primer	CGCCTGCTTCACCACCTT
	Probe	CCAAGTATGATGAGATCAA

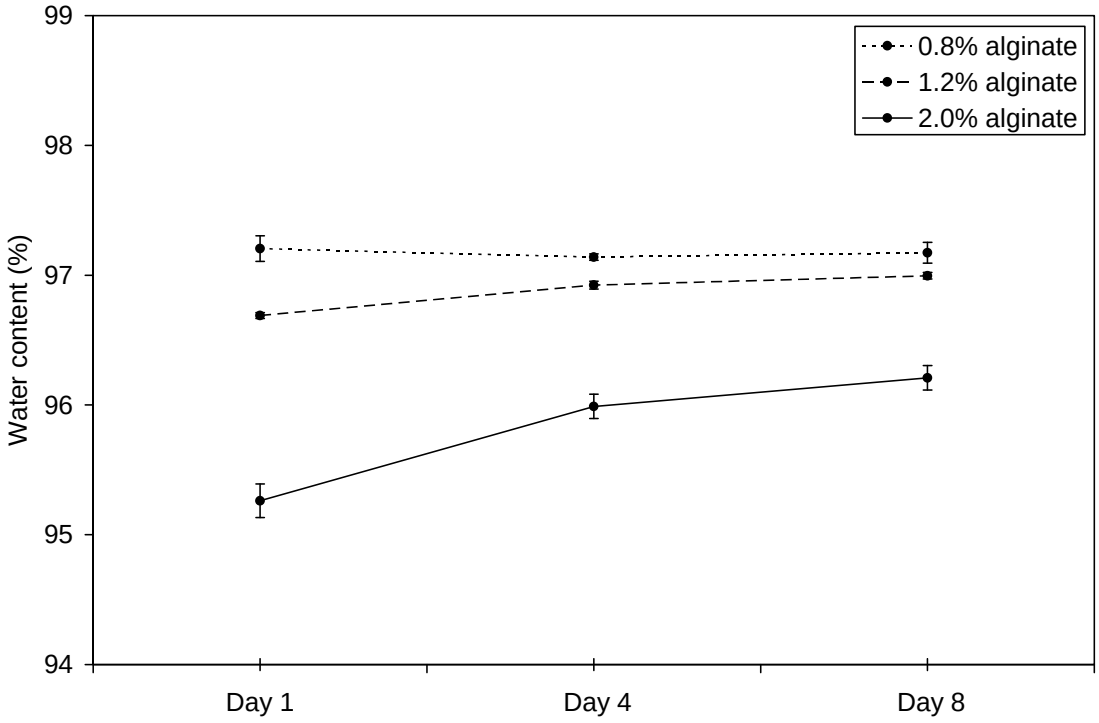

Figure 3.1. Percentage of water content in 0.8%, 1.2%, and 2.0% w/v alginate bead concentrations. The means and standard deviations are reported (n = 3).

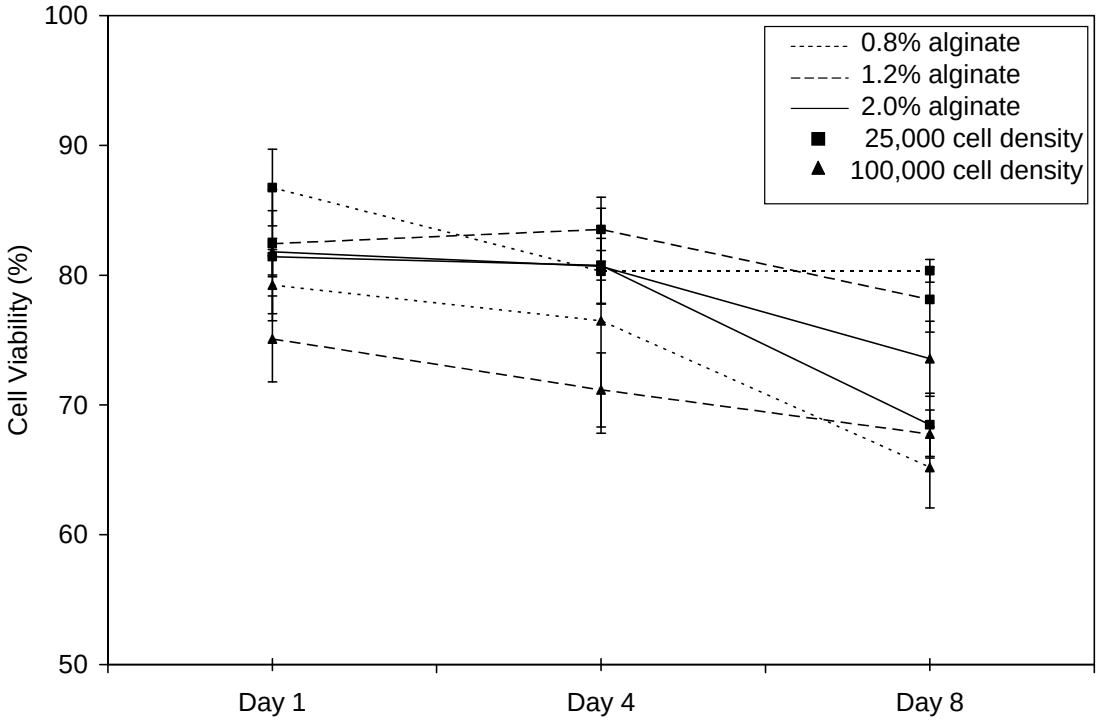

Figure 3.2. Percentage of chondrocyte viability when encapsulated in 0.8%, 1.2%, and 2.0% w/v alginate bead concentrations for 25,000 and 100,000 cell density over the 8 d study. The means and standard deviations are reported (n = 3).

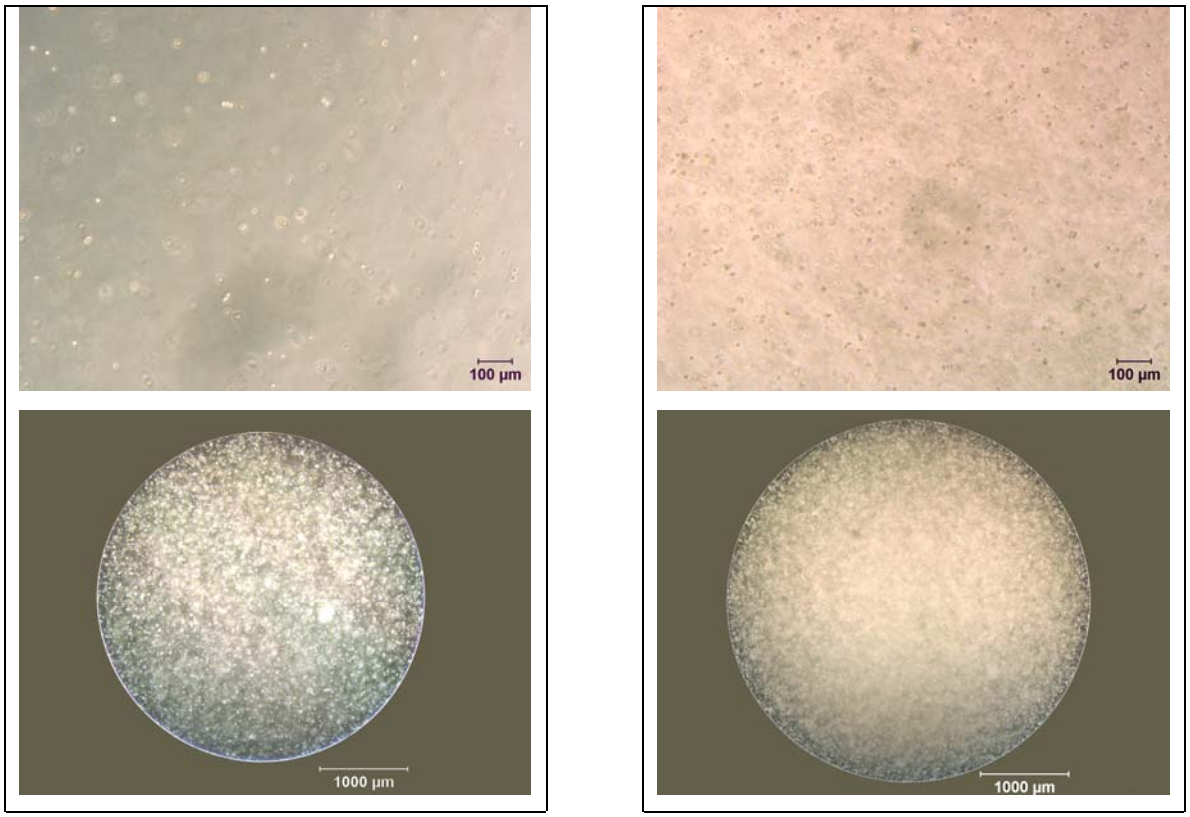

Figure 3.3. Microscopy images of 2.0% w/v alginate beads with (a) 25,000 chondrocytes/bead and (b) 100,000 chondroctyes/bead at day 1 in two different magnifications. The scale bars are located in the bottom right hand corner of each image.

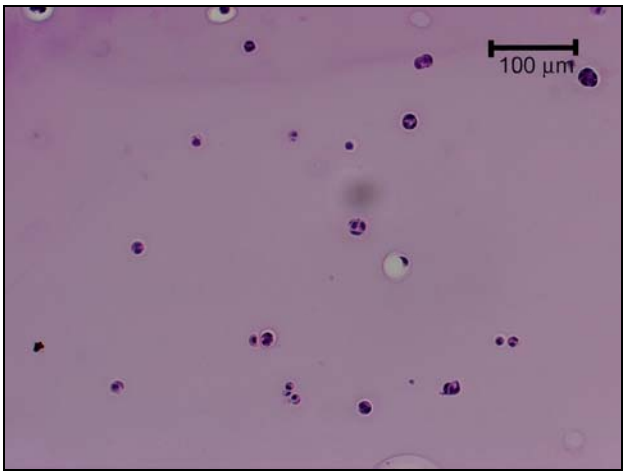

(a)

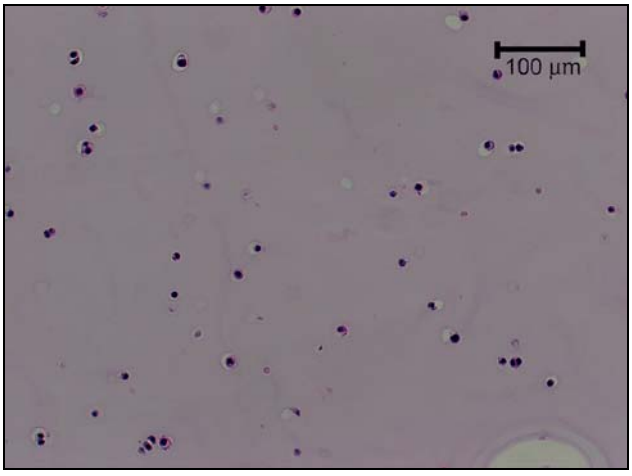

(b)

Figure 3.4. Hematoxylin and eosin stained sections of 1.2% w/v alginate bead with (a) 25,000 and (b) 100,000 chondrocyte density encapsulated after 8 and 4 d of culture, respectively. The alginate matrix stained with a light violet hue, while the chondrocytes stained darker purple. The scale bars are located in the top right hand corner of each image.

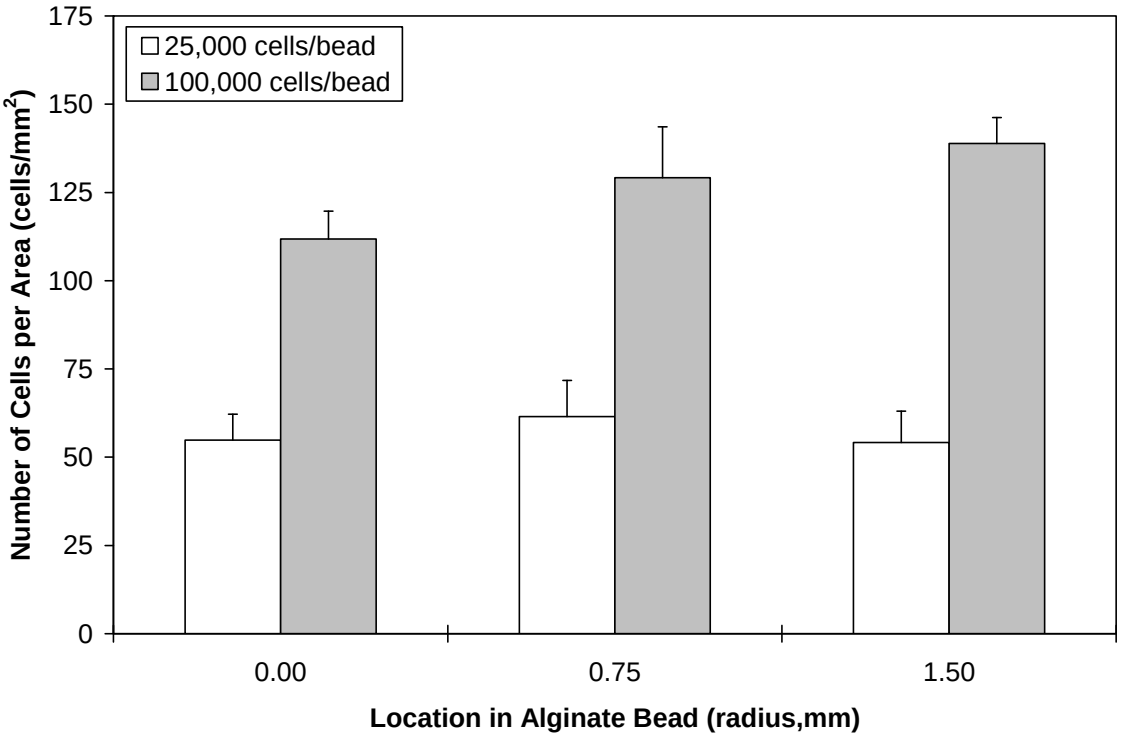

Figure 3.5. Average number of cells per area determined from hematoxylin and eosin stained 1.2% w/v alginate beads at 25,000 and 100,000 chondrocyte densities. Both cell densities investigated are associated with a homogenous cell distribution throughout the alginate bead. The means and standard deviations are reported (n = 3).

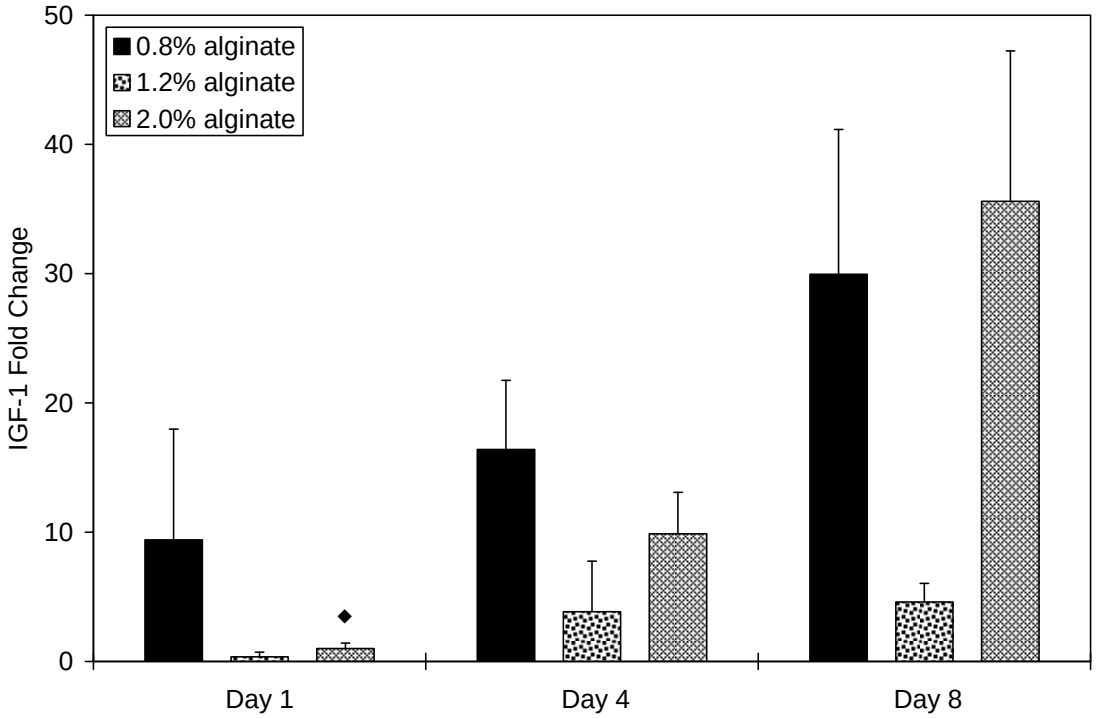

Figure 3.6. IGF-1 mRNA expression for 0.8%, 1.2%, and 2.0% w/v alginate hydrogels with an initial chondrocyte density of 25,000 cells per bead over 8 d. An increase in IGF-1 mRNA expression by encapsulated chondrocytes occurs for all alginate concentrations from day 1 to 8. The calibrator for all the samples tested for IGF-1 expression is indicated by (◆). The means and standard deviations are reported (n = 3).

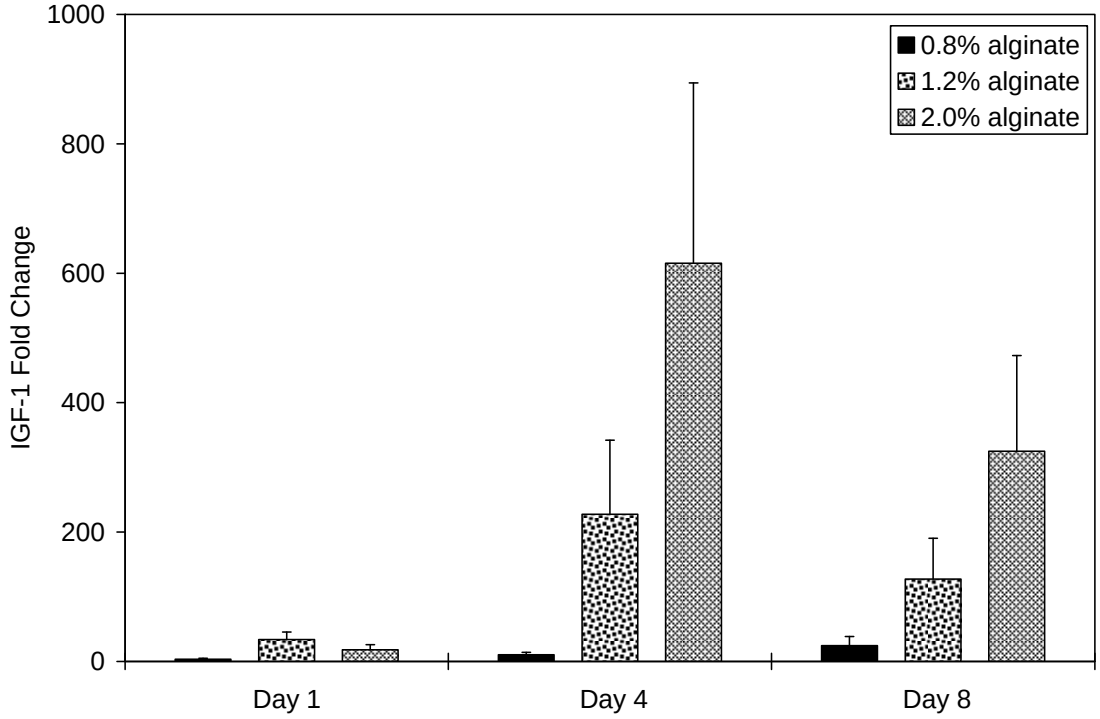

Figure 3.7. IGF-1 mRNA expression for 0.8%, 1.2%, and 2.0% w/v alginate hydrogels with an initial chondrocyte density of 100,000 cells per bead over 8 d. In general, chondrocytes encapsulated in all alginate bead concentrations increased their mRNA expression of IGF-1 over 8 d. The means and standard deviations are reported (n = 3).

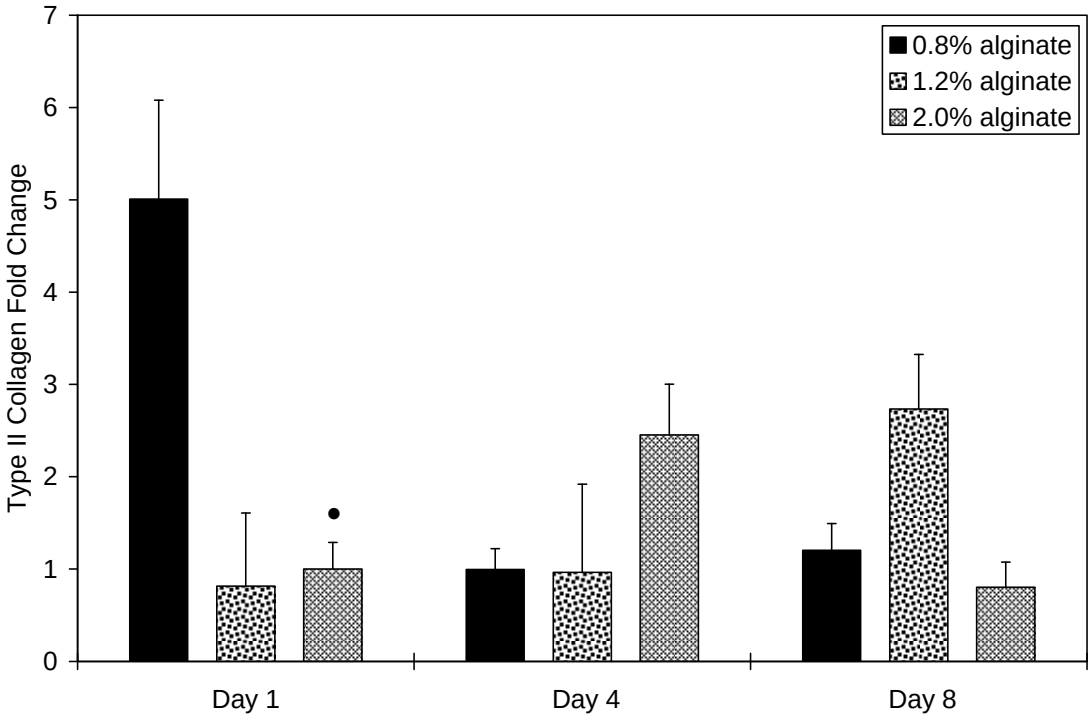

Figure 3.8. Type II collagen mRNA expression for 0.8%, 1.2%, and 2.0% w/v alginate hydrogels with an initial chondrocyte density of 25,000 cells per bead over 8 d. Chondrocytes sustain their mRNA expression of type II collagen in various alginate bead concentrations. The calibrator for all the samples tested for type II collagen expression is indicated by (●). The means and standard deviations are reported (n = 3).

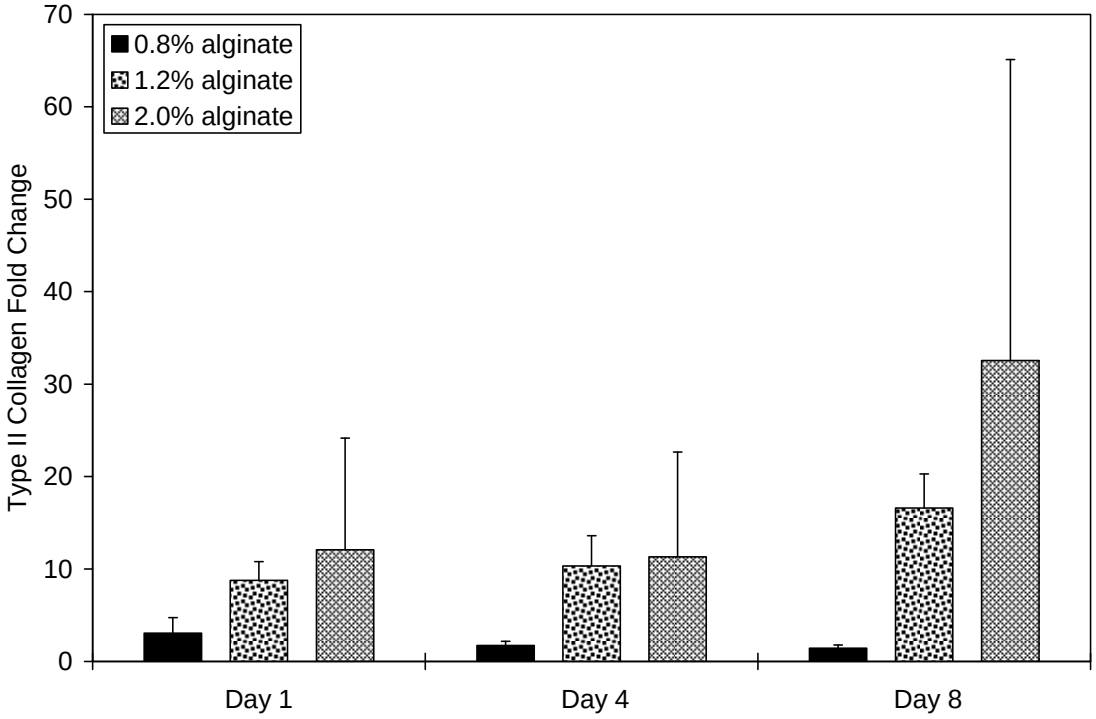

Figure 3.9. Type II collagen mRNA expression for 0.8%, 1.2%, and 2.0% w/v alginate hydrogels with an initial chondrocyte density of 100,000 cells per bead over 8 d. Phenotypic type II collagen mRNA expression of encapsulated chondrocytes within all alginate bead concentrations is observed. The means and standard deviations are reported (n = 3).

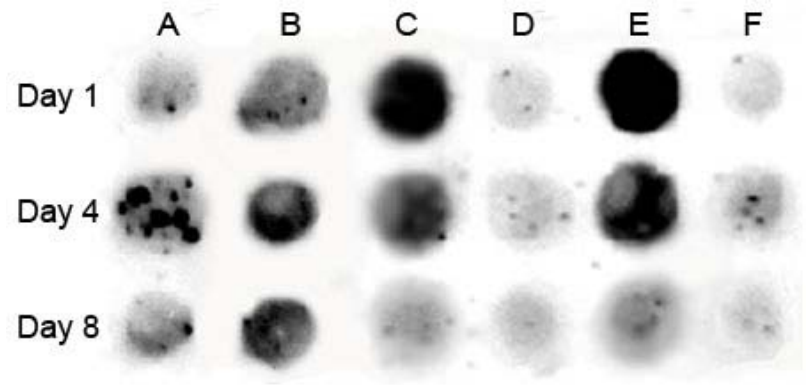

(a)

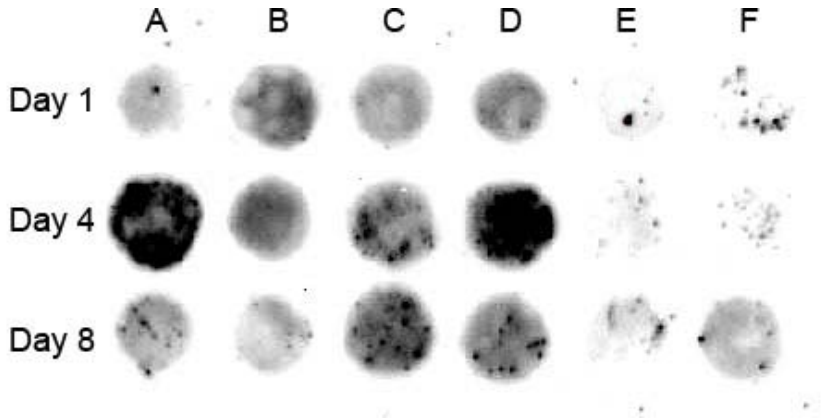

(b)

Figure 3.10. Dot blots of intracellular protein samples from a density of 25,000 (A, C and E) and 100,000 (B, D and F) chondrocytes/bead as well as all alginate concentrations, 0.8% w/v (A and B), 1.2% w/v (C and D), and 2.0% w/v (E and F). These samples are taken from day 1, 4, and 8 time points, where **(a)** indicates IGF-1 protein amounts and **(b)** shows type II collagen levels.

4 Effects of Exogenous IGF-1 Delivery on the Early Expression of IGF-1 Signaling Molecules by Alginate Embedded Chondrocytes*

4.1 Introduction

A fundamental role of chondrocytes is to synthesize the extracellular matrix proteins and biomolecules within articular cartilage. However, when this matrix is disrupted, chondrocytes are often unable to reestablish healthy cartilage tissue. As a result, both researchers and clinicians are investigating ways to engineer functional cartilage tissue. While an understanding of both chemical and mechanical mechanisms are important to achieve this objective, here we focused on molecular factors. In particular, our goal was to determine how growth factor stimulation of chondrocytes embedded in an alginate hydrogel affects chondrocyte upstream signaling and therefore phenotypic function.

A multitude of intercellular signaling proteins have been identified within articular cartilage. For example, insulin-like growth factor-1 (IGF-1) is a major anabolic growth factor of articular cartilage that has been found to enhance chondrocyte proliferation as well as the synthesis of vital extracellular matrix proteins, including type II collagen.[2, 236, 237] IGF-1 is a small, 7.5 kDa protein with a half life of 10 minutes when it is in free form.[241] However, the stability of free IGF-1 can be enhanced by binding to insulin-like growth factor binding proteins (IGFBPs).[40, 242] There are several binding proteins with a predominant one being IGFBP-3 in serum.[40, 43, 243-246] Proteolytic enzymes in the synovial fluid as well as those released by chondrocytes

---

***** This chapter was published as: Yoon DM and Fisher JP. Effects of Exogenous IGF-1 Delivery on the Early Expression of IGF-1 Signaling Molecules by Alginate Embedded Chondrocytes. Tissue Engineering Part A. 2008; 14(7): 1263-1273.

can break down the IGFBPs, therefore allowing IGF-1 to bind to the insulin-like growth factor-1 receptor (IGF-1R), a tyrosine kinase membrane receptor.[38, 43] The activation of IGF-1R results in a cascade of several intracellular pathways of chondrocytes, typically leading to matrix expression.[40, 107, 247]

Previous works have shown that glycosaminoglycans, proteoglycans, and type II collagen protein synthesis as well as mRNA expression occurs in cartilage extracts, chondrocytes in monolayer, and chondrocytes in alginate when incubated with exogenous IGF-1.[230, 236, 237, 248] A standard concentration range of 0-100 ng/mL has been used in most experiments with varying culture times of up to 6 days.[230, 236, 237, 248, 249] Results have shown that exogenous IGF-1 delivery to chondrocytes in monolayer, resulted in an increase of aggrecan, type II collagen, and IGF-1 mRNA levels after 72 hours.[248] Similarly, other investigations focused on how culturing conditions for 10 days affected chondrocytes that were reseeded in monolayer and introduced to 50 ng/mL IGF-1. The results here showed that pre-cultured chondrocytes in alginate experienced higher total RNA levels of IGF-1, IGF-1R and IGFBP-2 as well as phenotypic mRNA expression than cultures in monolayer.[249] These studies indicate the importance of understanding IGF-1 signaling of chondrocytes. However, they focus on the short term effects (hours to days) of exogenous IGF-1 upon chondrocytes in monolayer.

Our objective here is to examine the effects of signal delivery on a system which is relevant to many tissue engineering strategies, therefore involving culture of articular chondrocytes for at least one week and within a 3D scaffold. To the best of our knowledge, this is the first reported study that thoroughly investigates endogenous expression of IGF-1 signaling molecules by chondrocytes embedded in a 3D scaffold.

Alginate was chosen as the biomaterial because it allows chondrocytes to maintain their spherical morphology.[106, 116, 250] Additionally, alginate contains no amine groups or cellular recognition proteins that factor into charge mediated adhesion.[251, 252] Thus, the mostly benign properties of alginate allow one to focus particularly upon the delivery of IGF-1 on the chondrocytes. We have previously shown that endogenous IGF-1 expression was enhanced in a 2.0% w/v alginate concentration with a density of 100,000 chondrocytes per bead.[253] Utilizing these previous results, we examined how exogenous IGF-1 affects expression of upstream IGF-1 signaling molecules. Our specific objectives are to investigate the effects of exogenous IGF-1 delivery upon (1) endogenous IGF-1, IGF-1R and IGFBP-3 expression as well as (2) chondrocyte phenotype, as demonstrated by type II collagen and type I collagen expression.

4.2 Materials and Methods

4.2.1 Cartilage Extraction and Chondrocyte Isolation

Slices of cartilage were removed from the metatarsal phanlangeal joint of calves (15-18 weeks old) and then washed in Dulbecco's Modified Eagle Medium/Nutrient Mixture F-12 Ham (DMEM/F12) media (Gibco, Carlsbad, CA), which contained the following additives: 50 μg/mL ascorbic-2-phosphate (Sigma-Aldrich, St. Louis, MO), 1 mg/mL bovine serum albumin (Sigma-Aldrich), 1.2 mg/mL sodium bicarbonate (Sigma-Aldrich), 0.1% penicillin/streptomycin (Gibco) and 0.1% sodium pyruvate (Gibco). Chondrocytes were isolated by digesting the cartilage in 0.2% *collagenase P* (Roche, Basel, Switzerland) overnight at 37 ^{o}C and then filtered through a 40 μm nylon mesh to remove any undigested tissue. Primary chondrocytes without pre-culture were utilized for this study.

4.2.2 Chondrocyte Encapsulation in Alginate and Culture

Chondrocyte culture techniques follow closely from previously published work.[253] Briefly, 2.0% w/v alginate solution was prepared by mixing and heating alginic acid sodium salt from brown algae (Sigma-Aldrich), 0.15M sodium chloride and 0.025M HEPES (Sigma-Aldrich) into deionized water (pH 7.4) and then sterile filtered. The alginate solution was mixed with chondrocytes and injected through a 0.22 gauge syringe into a continuously stirred 100mM calcium chloride (Sigma-Aldrich) to create a density of 100,000 cells per bead. The beads were incubated in the calcium chloride solution and DMEM/F12 for 15 minutes each. Afterwards, 5 beads were transferred into each well of a 6-well plate and cultured in DMEM/F12 media and 10% fetal bovine serum (supplemented DMEM/F12 media) at 37^{o}C (day 0) for 2 days. This was done to stabilize the chondrocytes within the hydrogel.[132, 254] The media was changed on day 3 with supplemented DMEM/F12 media and human insulin-like growth factor-1 (IGF-1; R&D Systems, Minneapolis, MN). Human IGF-1 was used because it has a similar homology to bovine IGF-1.[255] The following IGF-1 concentrations were studied: 0, 10, 50, and 100 ng/mL. In this paper, 0 ng/mL IGF-1 case will be labeled as the control group, while the 10, 50, and 100 ng/mL IGF-1 cases will be referred to as the experimental groups. The media and IGF-1 were changed daily. Chondrocytes were isolated from five alginate beads for analysis at day 1, 4, and 8 by the addition of 3 mL of 0.1M ethylenediaminetetraacetic acid (EDTA) for 30 min at 37^{o}C. A cell pellet was formed by centrifugation and then resuspended in PBS and split for RNA and DNA isolation. Four alginate beads with embedded chondrocytes were also lyophilized with a

Labconco Freeze Dry System/Lyph Lock 4.5 (Labconco, Kansas City, MO) and then weighed to determine the dry weight.

4.2.3 RNA Isolation

Total RNA was isolated from chondrocytes using the RNeasy Plus Mini Kit (Qiagen, Valencia, CA). Total RNA was eluted into RNase free water and detected using a NanoDrop ND-1000 Spectrophotometer (NanoDrop Technologies, Wilmington, DE). The RNA concentrations at 1, 4, and 8 d for all groups were approximately 50 ng/uL, 200 ng/uL, and 450 ng/uL respectively.

4.2.4 DNA Isolation and Quantification

Total DNA was isolated from chondrocytes using a DNeasy Blood and Tissue Kit (Qiagen). Total DNA was eluted in 400 uL of Buffer AE. This DNA solution was incubated with PicoGreen to determine the amount of double stranded DNA (dsDNA) by using a Quant-iT PicoGreen dsDNA Assay kit (Invitrogen, Carlsbad, CA). The samples were excited at 480nm and evaluated at an emission of 520nm using a fluorescence microplate reader (Molecular Devices SpectraMax M5, Sunnyvale, CA). A standard curve was prepared from a known concentration of DNA provided in the kit and this curve was used to quantify nanograms of DNA per bead.

4.2.5 Histology

All samples were collected and fixed in 4% paraformaldehyde / 0.1M sodium cacodylate buffer containing 10mM $CaCl_2$ (pH 7.4) for 24 hours at 4^{o}C. The beads were washed with 0.1M sodium cacodylate buffer with 10mM $CaCl_2$ (pH 7.4) for 24 hours at

room temperature. Afterwards, the beads were dehydrated in a series of ethanol concentrations (40-100%) with a final xylene wash. The samples were embedded in Paraplast X-tra paraffin (Fisher Scientific, Pittsburgh, PA) and cut into 4μm thickness sections, which were placed onto charged microscope slides and kept at 4°C until staining.

4.2.6 Histochemical Staining

Sections were oven dried for 2 hours at 60°C, deparaffinized in Citrisolv Hybrid (Fisher Scientific) two times for 3 minutes, rehydrated in 100% and 95% ethanol for 1 minute each, and rinsed in distilled water. Sections were stained with Safranin-O (0.1%; Poly Scientific, Bay Shore, NY) and counter stained with Fast Green (0.001%, Fisher Scientific, Pittsburgh, PA).

4.2.7 Immunohistochemistry

Sections were dried at 60°C for 1 hour, deparaffinized in Citrisolv Hybrid two times for 5 minutes, rehydrated in a descending line of ethanol (100%, 95%, and 70% for 3 minutes each), rinsed in tap water, and then rinsed in deionized water. The sections were then incubated with PEROXI*DAZED1* (Biocare, Concord, CA), an endogenous peroxidase blocker, and Background*SNIPER1* (Biocare), a blocking reagent. The sections were then stained with antibodies that detect the presence of type II collagen and IGF-1 proteins. The primary antibodies are: anti-type II collagen (rabbit polyclonal antibody, ab300, Abcam, Cambridge, MA) and anti-hIGF-1 (goat IgG antibody, AF-291-NA, R&D Systems). Each antibody was diluted at 1:200. A HISTOSTAIN®-SP kit (Zymed, San Francisco, CA) was used to reveal the presence of type II collagen by using

a horseradish peroxidase (HRP)-strepavidin-biotin system. This complex formation was detected by a 3,3'-diaminobenzidine tetrahydrochloride (DAB) chromogen. For IGF-1, a HRP conjugated secondary antibody (goat IgG antibody, ab6885, Abcam) was used at a dilution of 500 times and detected by a histochemical substrate (Liquid DAB Substrate Kit, Zymed). All samples were counterstained with hematoxylin, dehydrated in 95% and 100% ethanol twice for 1 minute each, cleared in Citrisolv Hybrid twice for 1 minute, and coverslipped using Permount (Fisher Scientific). To show non-specific staining, samples were not incubated with the primary antibody and then incubated with the secondary antibody for each protein (negative staining control).

4.2.8 Quantitative Reverse Transcriptase-Polymerase Chain Reaction (qRT-PCR)

The total isolated mRNA for all groups at all time points was reverse transcribed using a cDNA Archive Kit, which can convert up to 10 μg of RNA to cDNA (Applied Biosystems, Foster City, CA). Quantitative RT-PCR was performed by combining the cDNA with a Universal Master Mix (Applied Biosystems), as well as oligonucleotide primers and probes (Applied Biosystems) that were created for the genes of interest (IGF-1, IGF-1R, IGFBP-3, type I collagen and type II collagen) and the endogenous gene control (glyceraldehyde 3 phosphate dehydrogenase, GAPDH). The same primer and probes for IGF-1, type II collagen and GAPDH were used from previous work. The sequences for the forward primers for IGF-1R, IGFBP-3, and type I collagen are: 5' TGCATGGTGGCCGAAGA 3', 5' CGCCTGCGCCCTTACC 3', and 5' AGAACCCAGCTCGCACATG 3'. The reverse primer sequences for IGF-1R, IGFBP-3, and type I collagen are: 5' TGTCTCTCGTCATCCCAAAATCT 3', 5'

TTCTTCCGACTCACTGCCATT 3', and 5' CAGTAGTAACCACTGCTCCATTCTG 3'. The probe sequences for IGF-1R, IGFBP-3, and type I collagen are: 5' TTCACAGTCAAAATC 3', 5' CTACCGTCCGCGTCAG 3' and 5' AGACTTGAGACTCAGCC 3'. The reaction was conducted on an ABI Prism 7000 sequence detector (Applied Biosystems), using thermal conditions of 2 min at 50^{o}C, 30 min at 60^{o}C, 5 min at 95^{o}C, and 40 cycles of 20 s at 94^{o}C and 1 min at 62^{o}C. The expression for each gene was analyzed for all the groups in the study using a relative standard curve method, which were normalized to GAPDH. The calibration for the data obtained for each gene expression sample set was analyzed to the control sample (0 ng/mL IGF-1 group). This calibrator was chosen to represent the gene expressions data appropriately.

4.2.9 Statistical Analysis

Two separate and independent experiments were performed. The trends obtained in both experiments were similar. However, the data presented here is derived from a single experiment since the primary cell populations are variable. Data from all studies were analyzed using ANOVA and Tukey's multiple-comparison test. The means and standard deviations are reported; samples were analyzed in triplicate (n = 3).

4.3 Results

4.3.1 Physical Characterization of Embedded Chondrocytes

The water content of alginate (~96-97%) did not change significantly during the 8 day study for all the groups. However, upon calculating the dry weight of each alginate bead, there was an increasing trend for all the groups (Figure 4.1). While the dry weight

was similar for all groups at day 1 and 4, there was a significant difference between the control group versus the experimental groups at day 8 ($p < 0.01$).

The change in physical appearance of the alginate bead over the course of the study can be visually seen in the Safranin-O/Fast Green stained images (Figure 4.2). Chondrocyte nuclei are observed as a gray hue, while the alginate turned into a bright orange color and matrix proteins were colored a lighter orange hue. At day 1 of the experiment, chondrocytes were homogenously embedded within the alginate bead for all conditions, which has also been seen in previous work. Figure 4.2a depicts a typical section of chondrocytes in an alginate bead at day 1 of the experiment. When this image is compared to the pictures of all the groups at day 8 (Figure 4.2b, c, d, and e), clustering is observed at the outer border of the bead and distributed uniformly throughout the periphery. This clustering affect seems to be more predominate in the groups that received exogenous IGF-1 (Figure 4.2c, d, and e). To investigate the effect of IGF-1 on chondrocyte proliferation, DNA levels were measured in each bead. Over the 8 days, there was an increasing trend of DNA for all groups (Figure 4.3). However, at each time point all the groups had similar amounts of DNA.

4.3.2 mRNA Expression of Endogenous IGF-1 Signaling Molecules

IGF-1 mRNA expression occurred in all the sample groups during the study (Figure 4.4). For the control, an increasing trend of IGF-1 expression occurred over the 8 days (3.5 fold increase), but the 10 and 50 ng/mL IGF-1 samples maintained a similar level of IGF-1 expression. At day 1, the 100 ng/mL group had a significantly higher level of IGF-1 expression compared to the rest of the samples ($p < 0.01$). By day 4, the 100 ng/mL IGF-1 group showed its lowest mRNA expression ($p < 0.01$), with an increase

by day 8. Towards the end of the study, the level of IGF-1 expression for the control group was significantly higher compared to the experimental groups ($p < 0.01$), which all showed similar expression levels.

During the 8 days, chondrocytes in all sample groups showed a decreasing trend of IGF-1R expression (Figure 4.5). Similar to IGF-1 expression, at day 1 the 100 ng/mL IGF-1 case had the highest level of IGF-1R expression compared to the other groups ($p < 0.01$). By day 4, the 0 and 100 ng/mL IGF-1 group had similar levels of expression that were lower than the 10 and 50 ng/mL IGF-1 samples ($p < 0.01$). However, by day 8 the control group had the lowest IGF-1 expression level compared to all the experimental cases ($p < 0.01$) with a 10 fold decrease from day 1.

The expression of IGFBP-3 showed a decreasing trend for all groups over the course of 8 days (Figure 4.6). The 100 ng/mL IGF-1 induced group expressed IGFBP-3 at a higher level compared to the other cases at day 1 ($p < 0.01$), which also was seen for both the IGF-1 and IGF-1R expression. However, by day 4 the IGFBP-3 expression levels were not significantly different amongst all the groups ($p < 0.01$). At day 8, the 0 and 10 ng/mL IGF-1 groups had similar levels of expression to each other. These groups express higher levels of IGFBP-3 expression compared to the 50 and 100 ng/mL IGF-1 groups ($p < 0.01$).

4.3.3 mRNA Expression of Phenotypic Matrix Proteins

Type II collagen expression occurred for all samples during the 8 day study (Figure 4.7). Almost all of the groups had similar levels of type II collagen expression at day 1. By day 4, type II collagen expression was lowest for the 0 and 100 ng/mL IGF-1 samples and highest for the 10 and 50 ng/mL IGF-1 groups ($p < 0.01$). However, by day

8 the control samples experienced the lowest level of type II collagen expression with an 11 fold decrease from day 1 compared to the experimental groups.

All samples showed an increasing trend of type I collagen expression (Figure 4.8). At day 1, the 100 ng/mL IGF-1 group had the highest type I collagen expression level ($p < 0.01$) compared to the other samples. By day 4, the control group had a greater expression of type I collagen ($p < 0.01$). The control group continued to experience an increase in type I collagen expression, with a 214 fold increase from day 1 to 8 and with the highest level of type I collagen occurring at day 8 compared to the experimental cases ($p < 0.01$).

4.3.4 IGF-1 and Type II Collagen Protein Expression

The synthesis of IGF-1 and type II collagen proteins by chondrocytes encapsulated in alginate hydrogels with and without IGF-1 delivery was determined by immunohistochemistry for each protein. Results indicate that all proteins were being synthesized over the course of 8 day study with the highest staining intensity occurring at day 8. For the IGF-1 proteins, staining occurred closely around the chondrocytes for all groups at day 1 as seen in the representative image in Figure 4.9a. In Figures 4.9b-d, IGF-1 can be seen in a larger area for all the sample groups at day 8, which all had similar staining intensities. Additionally, similar staining characteristics can be seen for type II collagen over the course of the study (Figure 4.10). For type II collagen staining at day 1, the area of staining was concentrated around the chondrocytes (Figure 4.10a) and by day 8, the intensity and area increased for all the groups (Figure 4.10b-d).

4.4 Discussion

The maintenance of chondrocyte phenotype within a three dimensional hydrogel has been well established. Previous studies indicate that endogenous expression of IGF-1 occurs in chondrocytes embedded in alginate hydrogels, but there is little information for expression of IGF-1 signaling molecules. To the best of our knowledge, this is the first reported study that investigates how exogenous delivery of IGF-1 to chondrocytes, still embedded in alginate, affects endogenous expression of IGF-1 signaling molecules. By varying IGF-1 delivery we were able to address the following two major objectives: (1) effect of exogenous IGF-1 on endogenous IGF-1 signaling molecules and (2) effect of exogenous IGF-1 on chondrocyte phenotypic expression.

The physical characteristics of the construct were visibly altered during the 8 day study. Safranin-O/Fast Green stained images indicate clusters are protruding out of the bead (Figure 4.2). These clusters appear to consist of chondrocytes and matrix proteins, including proteoglycans, glycosaminoglycans and type II collagen (Figure 4.10). Previous studies have indicated that the clusters may consist of pericellular matrices.[230, 234, 256] These matrices appear to be more prevalent as the IGF-1 delivery concentration increases. Cluster formation indicates that the number of chondrocytes, the amount of matrix proteins, or both increased during the 8 day study. An increase in DNA content did occur for all groups from day 1 to day 8 (Figure 4.3). However, as similar DNA levels at each time point were observed for most groups, the results indicate that IGF-1 has a limited effect on chondrocyte proliferation. Additionally, sample dry weight increased significantly by day 8 (Figure 4.1). Thus it appears that the increase in cluster formation is largely due to matrix formation. Finally, while matrix formation is very

apparent for all groups by day 8, there appears to be less matrix proteins in the control group (Figures 4.2 and 4.10).

The spatial dependence of cluster formation, with fewer clusters in the bead's interior and more clusters along the bead's periphery, also indicates that IGF-1 transport may play a role in this system. The diffusion coefficient for molecules with molecular weights similar to IGF-1 in hydrogels has an order of magnitude of approximately 10^{-6} cm^2/s, and thus can diffuse through the matrix.[257-259] However, the concentration of clusters around the periphery of the bead indicates that exogenous signal consumption may be the critical parameter, where chondrocytes at the periphery consume exogenous IGF-1 so that interior chondrocytes see a lower concentration of the signaling molecule. Indeed, previous work has found that adipose derived stem cells entrapped in alginate can alter diffusion coefficients of dextran (3 kDa) by up to two-fold when culturing with chondrogenic media.[259] However, a more complete study of transport effects is necessary in order to fully understand this phenomenon in our experiment.

For chondrocytes embedded in alginate, it is evident exogenous IGF-1 delivery affects endogenous IGF-1 expression during a period of 8 days. Without exogenous IGF-1 delivery, IGF-1 expression levels increased throughout the study (Figure 4.4). This result was expected, as chondrocytes attempt to overcome the lack of the IGF-1 signal by increasing their endogenous expression of the signal. (Please note that the use of fetal bovine serum in the culture media likely provides some basal level of IGF-1 to all groups.) However, in the presence of excess exogenous IGF-1, regardless of concentration, chondrocytes had dramatically lower IGF-1 mRNA expression (Figure 4.4). When focusing upon induced IGF-1 groups, it was interesting to observe that only

the 100 ng/mL group had expression level fluctuations from day 1 to day 8 of the study. This response may indicate that high levels of IGF-1 delivery induce a time lag for reaching equilibrium expression levels. These qRT-PCR measurement of IGF-1 mRNA levels is qualitatively supported by immunohistochemistry observation of IGF-1 protein levels as demonstrated by Figure 4.9, where the control groups is associated with high levels of IGF-1 staining. Therefore, we conclude that the delivery of high concentrations of IGF-1 proteins will induce chondrocytes to decrease their endogenous expression of IGF-1.

The overall trend observed in IGF-1 expression is largely reflected by the IGF-1R expression. At day 1 and 4, differences in IGF-1R expression are observed between the experimental and control groups (Figure 4.5). The fluctuations seen at day 1 and day 4, possibly reflects a sluggish response in gene expression patterns by embedded chondrocytes. This slow response may be concentration dependent, where the delivery of high concentrations of IGF-1 are associated with longer times for chondrocyte gene expression patterns to change and perhaps to also reach equilibrium. However, by observing IGF-1R expression up to day 8, the results indicate that in the presence of excess IGF-1, chondrocytes express higher levels of IGF-1R. This could allow for an increase in the amount of available IGF-1R or, alternatively, a greater turnover rate of IGF-1R so as to potentially bind more available IGF-1.

While distinctive differences in IGF-1 and IGF-1R expression were observed between experimental and control groups by day 8, IGFBP-3 expression did not appear to be largely influenced by IGF-1 delivery (Figure 4.6). Over the course of the study a decrease in IGFBP-3 expression for all the groups was observed. This is interesting

because cartilage explants that are exposed to 100 ng/mL IGF-1 have been found to show an increase in IGFBP-3.[245, 246] However, the consistently low IGFBP-3 expression seen in this study indicates that exogenous IGF-1 has a limited impact on IGFBP-3 expression for alginate embedded chondrocytes. Therefore, since (1) IGF-1 delivery downregulates IGF-1 expression while upregulating IGF-1R expression and (2) IGF-1 delivery does not significantly alter IGFBP-3 expression, we hypothesize that IGF-1 signaling is mostly regulated by IGF-1R expression.

The impact of exogenous IGF-1 delivery is not limited to the expression of IGF-1 signaling molecules, but also has profound effects upon chondrocyte phenotype. Type II collagen mRNA expression (Figure 4.7) is strikingly similar to IGF-1R mRNA expression (Figure 4.5). Furthermore, the expression of type I collagen (Figure 4.8), a marker of chondrocyte dedifferentiation, is almost entirely in opposition to type II collagen and IGF-1R expression. These patterns generally support the hypothesis that IGF-1R is a key factor in regulating IGF-1 signaling. Though in our studies expression levels up to day 8 were our primary focus, we propose that the upregulation of type II collagen expression and low type I collagen expression in response to IGF-1 delivery should continue beyond 8 days, as demonstrated in previous studies.[260, 261]

The results presented here confirm the significant role of IGF-1 in chondrocyte function that has been previously demonstrated. However, here we characterize the effects of IGF-1 delivery to a 3D system relevant to many tissue engineering strategies under development. Interestingly, the results also show that exogenous IGF-1 impacts the endogenous expression of IGF-1 and IGF-1R, but not IGFBP-3. One would suspect that an excess of IGF-1 would trigger the chondrocytes to over express IGFBP-3 because

this would then stabilize the IGF-1. Since IGFBP-3 expression did not change, but IGF-1 and IGF-1R expression did become altered, we hypothesize that the uptake of exogenous IGF-1 is controlled mainly by IGF-1R expression, within the range of exogenous IGF-1 delivery and time length studied.

As many tissue engineering strategies suggest a longer period of *in vitro* culture before implantation, it is important to consider time points beyond 8 days. Since the mRNA expression between the control group and experimental cases for IGF-1, IGF-1R, type II collagen and type I collagen were significantly different at day 8, we speculate that the expression patterns observed here will continue at longer time points, but future studies are certainly required for confirmation. Though, in this particular study we did not observe beyond 8 days, the results indicate that within the 8 days there are notable differences in endogenous expression levels of IGF-1 signaling molecules as well as phenotypic expression between the control versus experimental groups. Therefore, from these observations, we propose that developing engineered tissues relies on critically inspecting endogenous expression of signaling molecules by cells embedded within a scaffold that are delivered with exogenous signals.

4.5 Conclusions

Here we observe for the first time, the expression of IGF-1 signaling molecules by chondrocytes embedded in an alginate hydrogel matrix. The results indicate that IGF-1 and IGF-1R expression, as well as proper chondrocyte phenotypic function, are greatly affected by IGF-1 delivery, although IGFBP-3 expression is largely unaffected by IGF-1 delivery. Therefore, the results indicate that hydrogel embedded chondrocytes, exposed to exogenous IGF-1, control IGF-1 signaling not by IGFBP-3 expression, but largely

through IGF-1R expression. Furthermore these findings demonstrate the profound effect of growth factor delivery upon endogenous signaling in an engineered tissue.

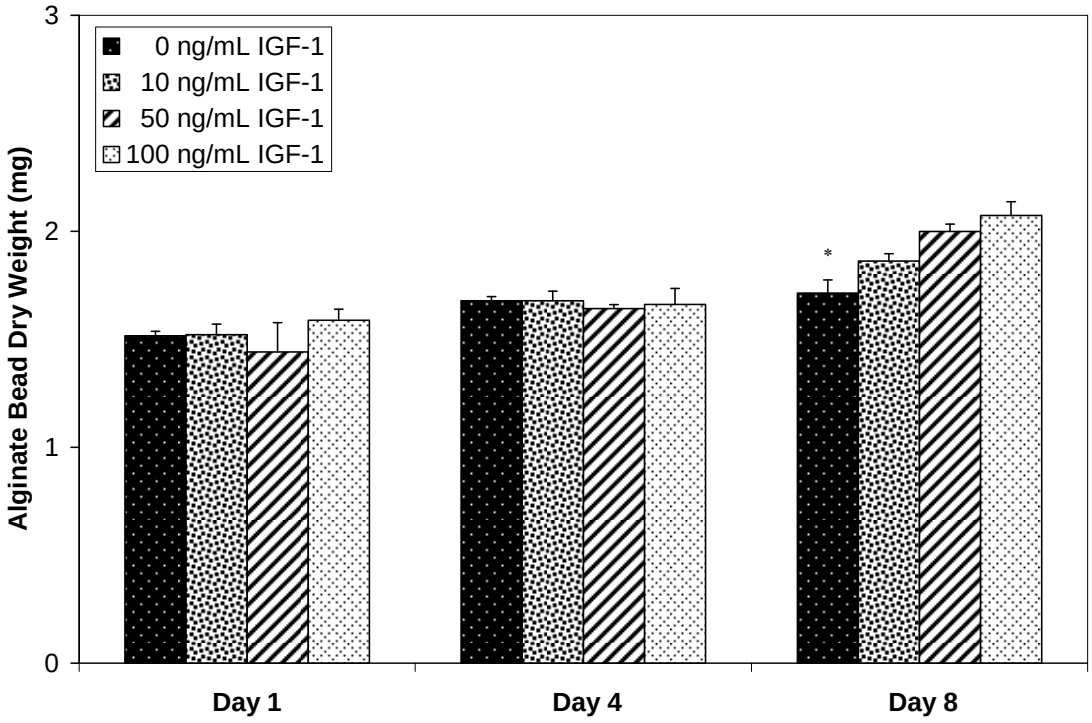

Figure 4.1. The dry weight of alginate beads for the 0, 10, 50, and 100 ng/mL IGF-1 groups. The means and standard deviations are reported ($n = 3$, $*$ indicates $p < 0.01$).

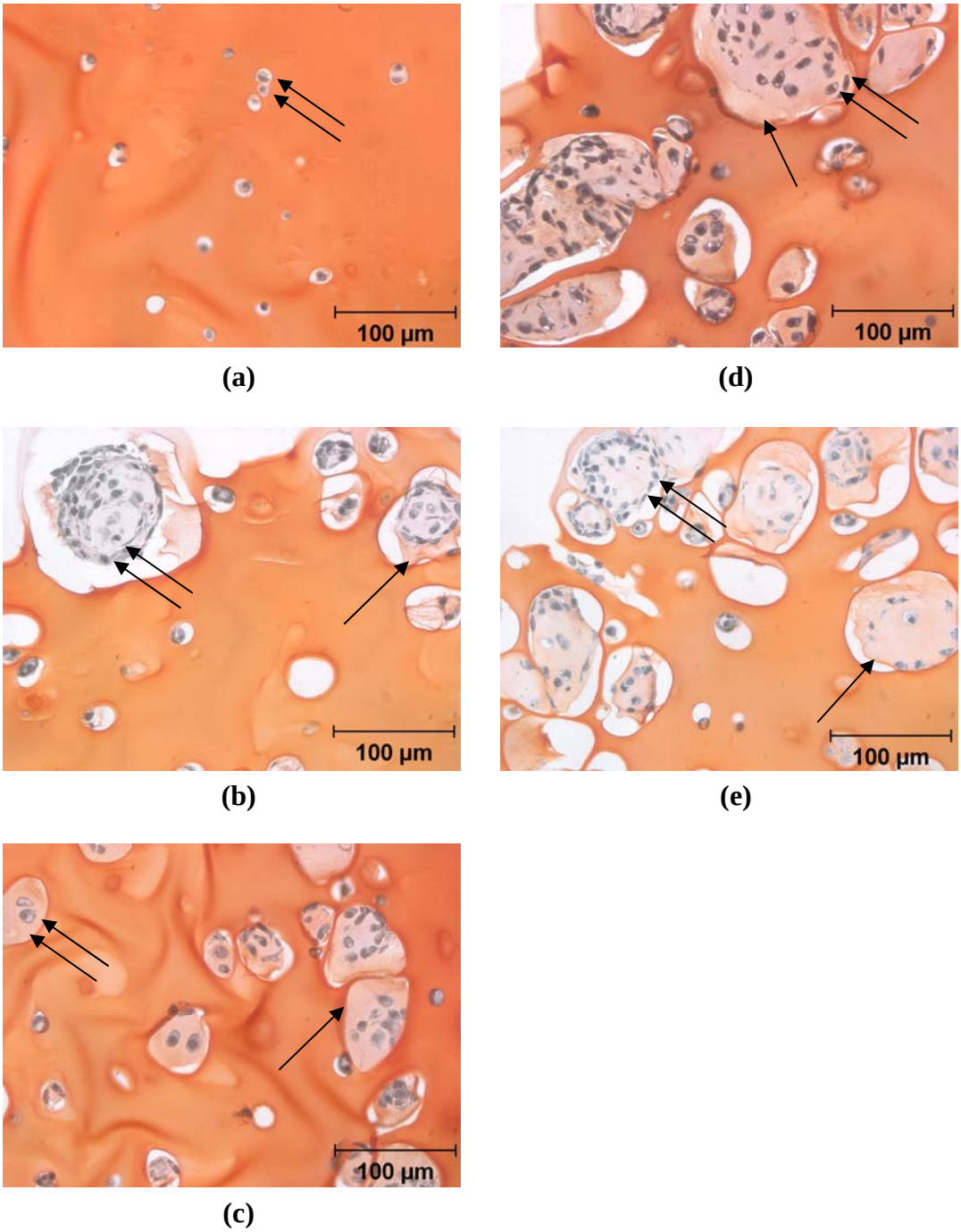

Figure 4.2. Safranin-O/Fast Green stained sections at **(a)** day 1 for 50 ng/mL IGF-1 group, **(b)** day 8 for 0 ng/mL IGF-1 group, **(c)** day 8 for 10 ng/mL IGF-1 group, **(d)** day 8 for 50 ng/mL IGF-1 group, and **(e)** day 8 for 100 ng/mL IGF-1 group. Alginate beads are a bright orange color, while the matrix proteins are shown with an arrow (light orange hue), and chondrocytes are shown with double arrows (gray hue). Scale bars are located on the bottom right corner of each image.

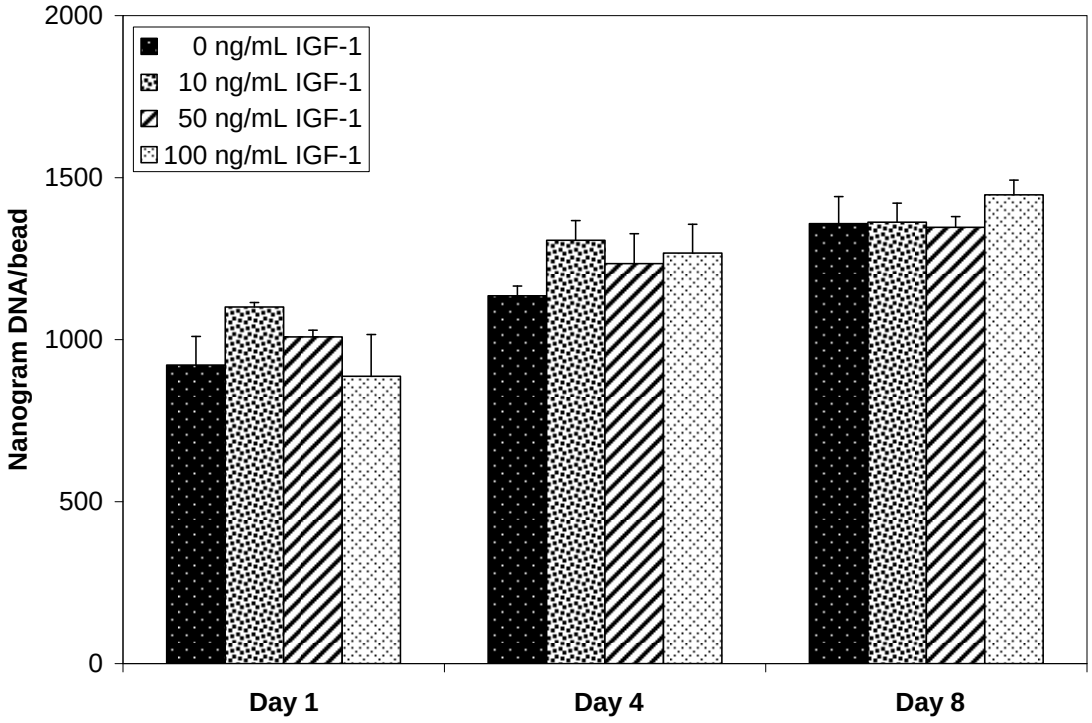

Figure 4.3. DNA content per bead for all sample groups over the course of 8 days. There is an increasing trend of DNA for all groups during the length of the study. However, no differences in DNA levels were seen between all the groups at each time point. The means and standard deviations are reported ($n = 3$).

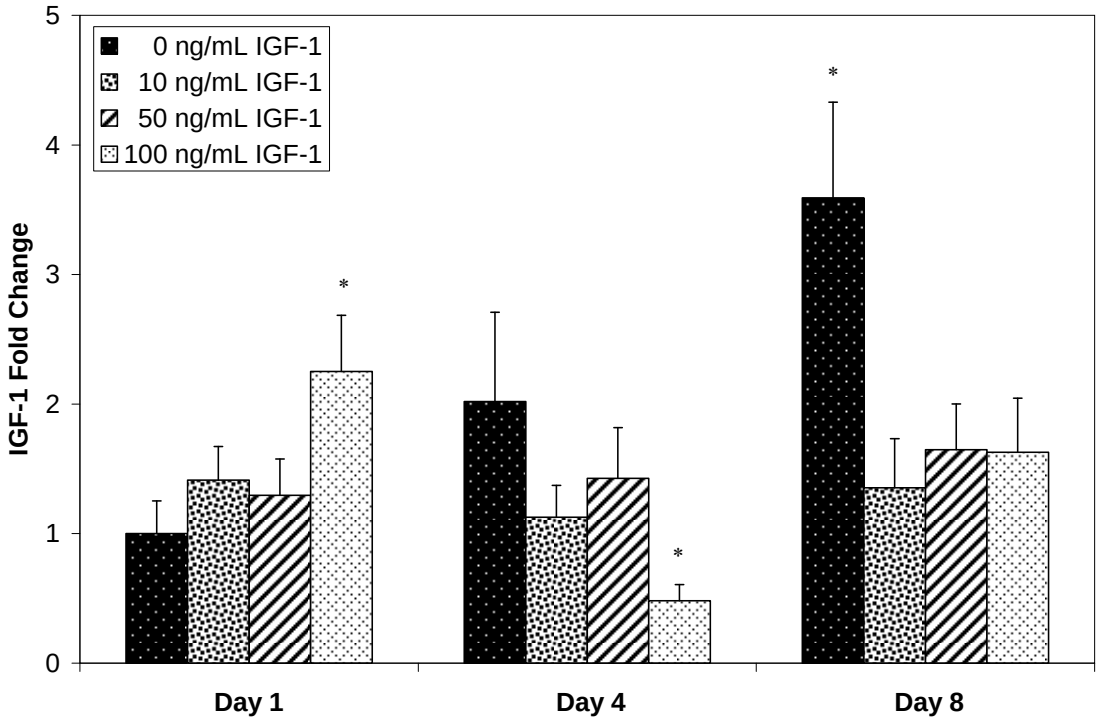

Figure 4.4. IGF-1 mRNA expression for all sample groups over 8 days. Results indicate that at day 8, IGF-1 induced samples had lower levels of gene expression compared to the control group. The means and standard deviations are reported (n = 3, $*$ indicates $p <$ 0.01).

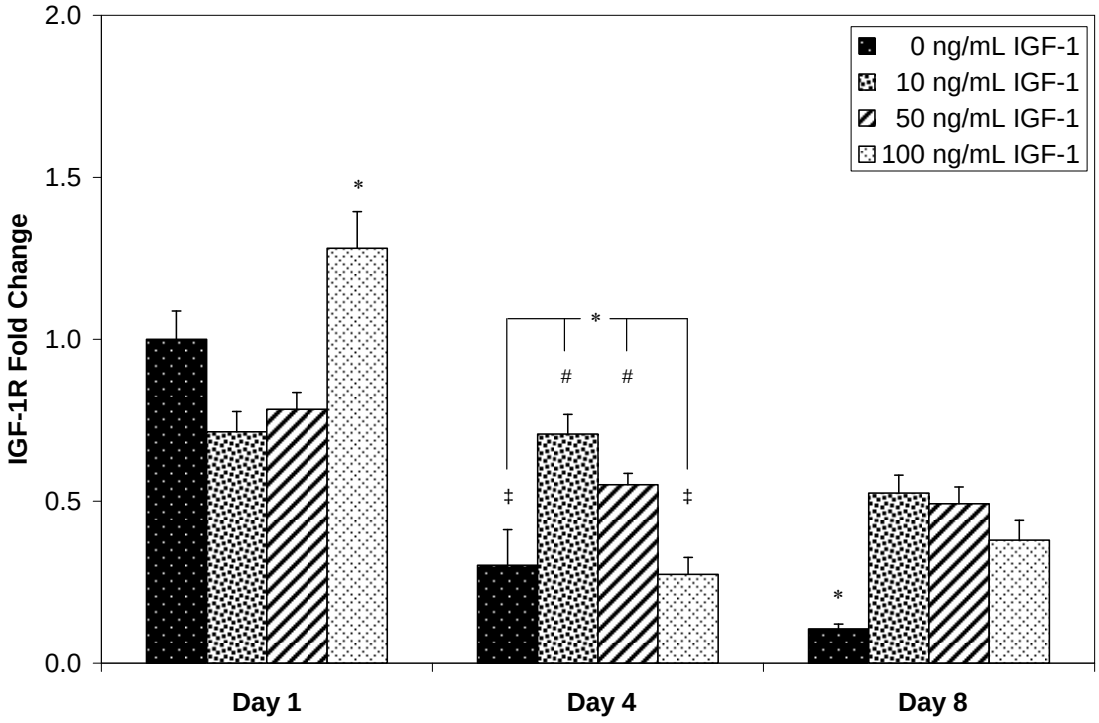

Figure 4.5. IGF-1R mRNA expression for all sample groups over 8 days. An increased level of expression occurred in the experiment groups versus the control group at day 8. The means and standard deviations are reported ($n = 3$, ∗ indicates $p < 0.01$). The labels ‡ and # indicate no statistical differences among the group**.**

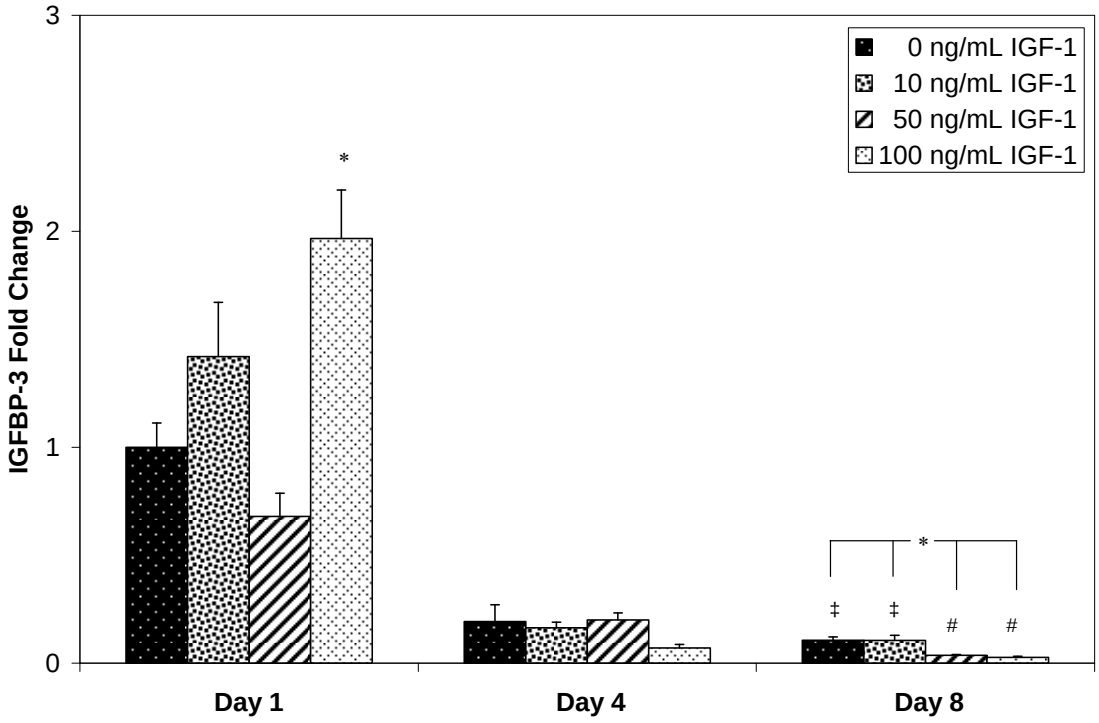

Figure 4.6. IGFBP-3 mRNA expression for all sample groups over 8 days. A decrease in IGFBP-3 expression occurred for all groups by 8 days. The means and standard deviations are reported (n = 3, ∗ indicates $p < 0.01$). The labels ‡ and # indicate no statistical differences among the group.

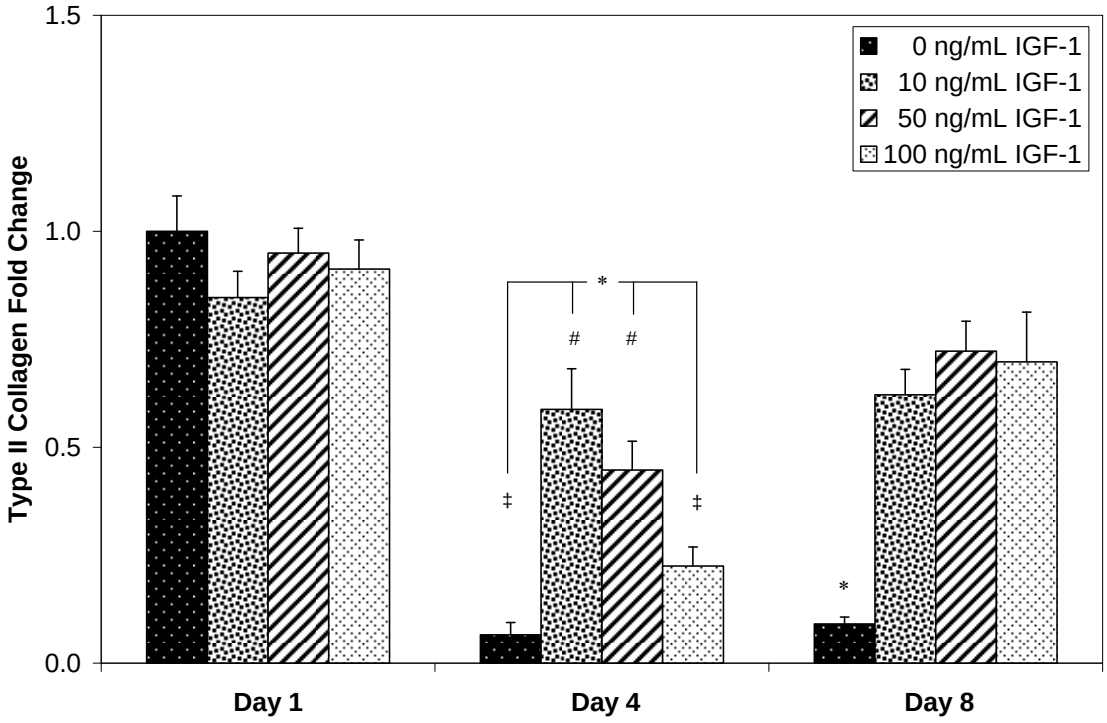

Figure 4.7. Type II collagen mRNA expression for all sample groups over 8 days. Chondrocytes sustained their expression for the experimental groups by day 8, while a decrease in expression occurred for the control group. The means and standard deviations are reported (n = 3, ∗ indicates $p < 0.01$). The labels ‡ and # indicate no statistical differences among the group.

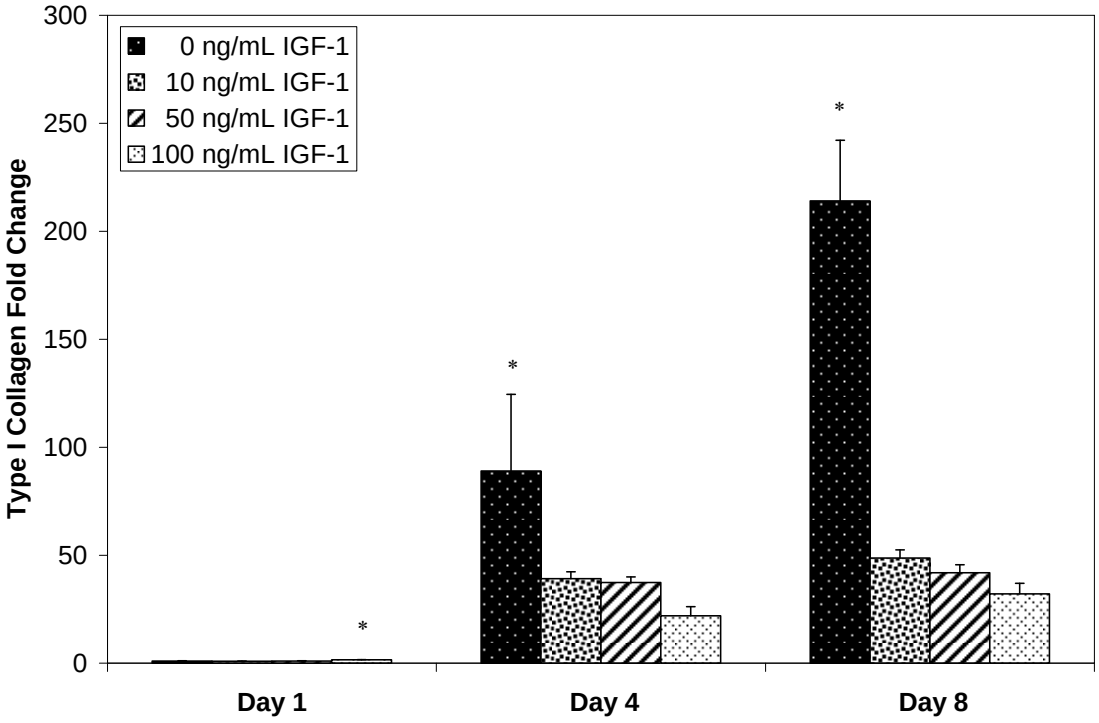

Figure 4.8. Type I collagen mRNA expression for all sample groups over 8 days. A higher level of expression occurred in the control group versus the experimental groups by the day 8 time point. The means and standard deviations are reported (n = 3, ∗ indicates $p < 0.01$).

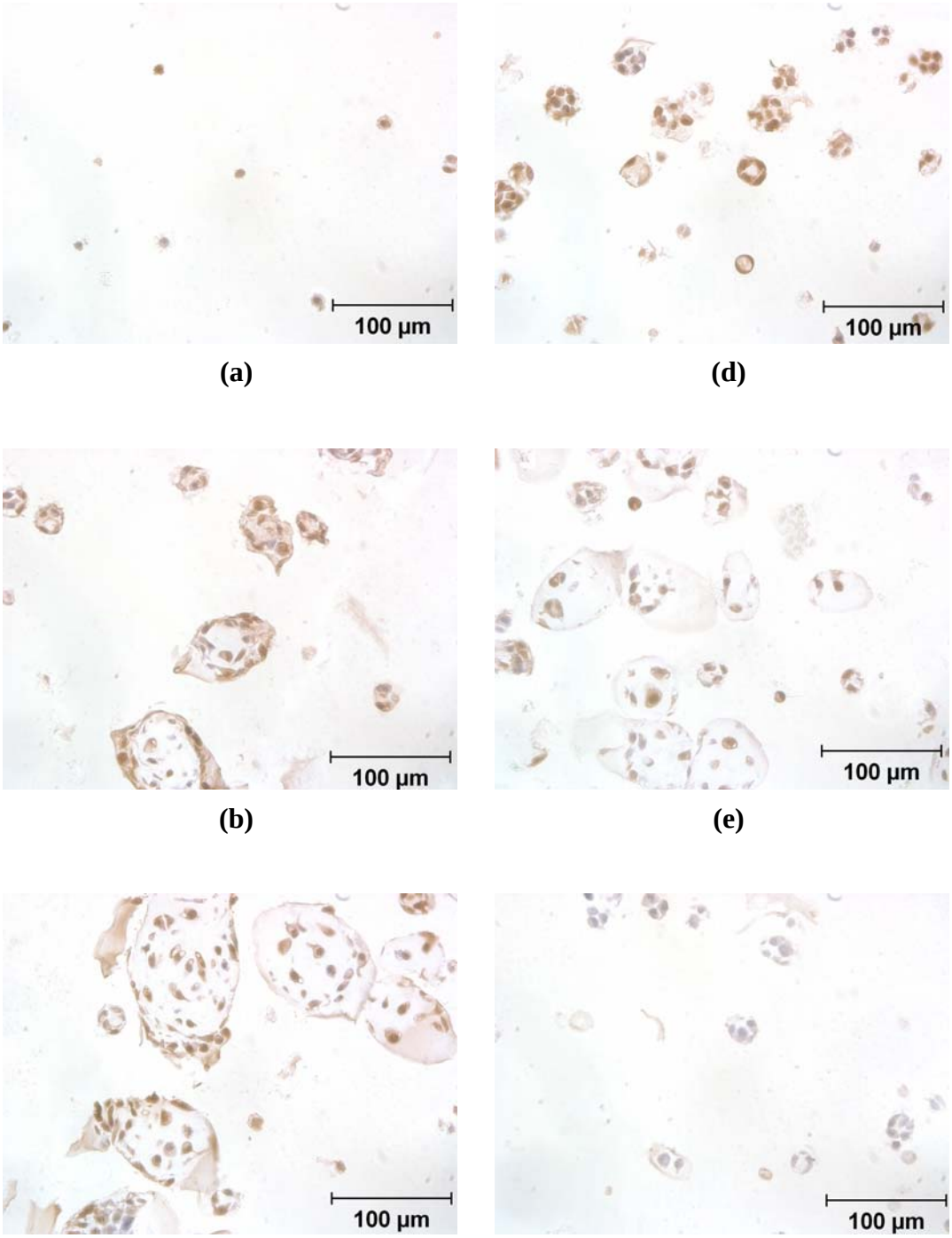

Figure 4.9. IGF-1 immunohistochemistry staining at **(a)** day 1 for 100 ng/mL IGF-1 group, **(b)** day 8 for 0 ng/mL IGF-1 group, **(c)** day 8 for 10 ng/mL IGF-1 group, **(d)** day 8 for 50 ng/mL IGF-1 group, **(e)** day 8 for 100 ng/mL IGF-1 group, and **(f)** a negative staining control. The clusters stained with greater intensity at day 8 compared to the single cells at day 1. Scale bars are located on the bottom right corner of each image.

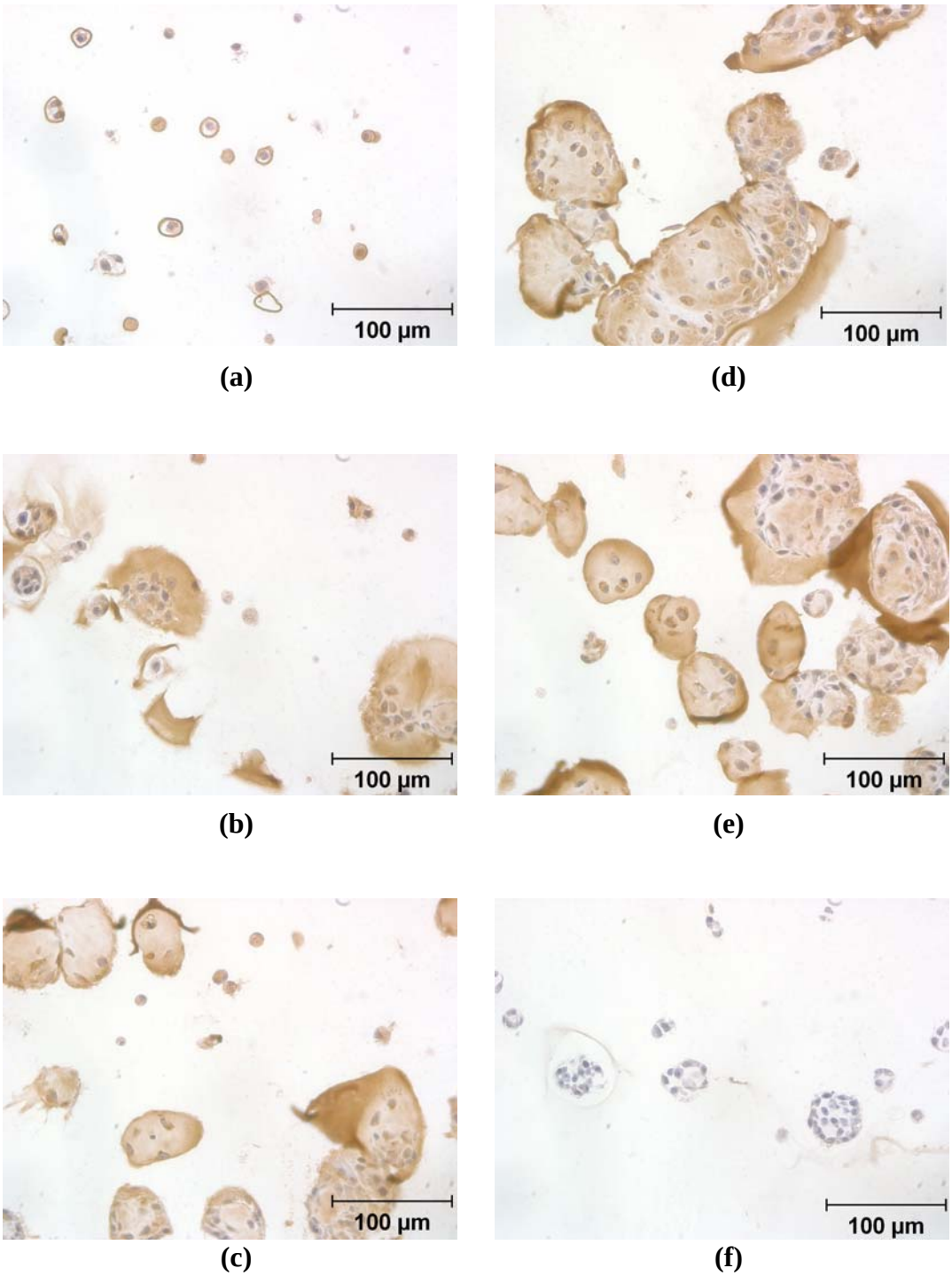

Figure 4.10. Type II collagen immunohistochemistry staining for **(a)** day 1 for 100 ng/mL IGF-1 group, **(b)** day 8 for 0 ng/mL IGF-1 group, **(c)** day 8 for 10 ng/mL IGF-1 group, **(d)** day 8 for 50 ng/mL IGF-1 group, **(e)** day 8 for 100 ng/mL IGF-1 group, and **(f)** a negative staining control. The presence of type II collagen seems to be greater at day 8 for the groups that received exogenous IGF-1. Scale bars are located on the bottom right corner of each image.

5 Hyaluronic Acid Interferes with IGF-1 Signaling Among Alginate Embedded Chondrocytes

5.1 Introduction

In order to maintain healthy cartilage, a balance between the chondrocytes and their environment is required. However it is difficult to investigate all the interactions occurring in cartilage simultaneously. Therefore, most tissue engineers examine a few variables at a time to truly understand the intricate details. Growth factors for example have shown their importance in tissue regeneration [11, 15, 247, 262, 263]. As previously mentioned, insulin-like growth factor-1 (IGF-1) is an essential anabolic growth factor that promotes matrix production as well as chondrocyte proliferation in cartilage explants [2, 236, 237, 264, 265].

Alterations in construct design, such as seeding density, scaffold porosity, scaffold composition, and mechanical stimulation are just a few variables that have been found to impact chondrocyte function [253, 266-271]. Our previous studies investigated the change in expression of IGF-1 signaling molecules by embedded chondrocytes when the construct environment is altered, such as cell density, alginate hydrogel concentration, and exogenous IGF-1 delivery. We found that at a high cell density and alginate concentration, type II collagen and IGF-1 expression were both enhanced [253]. Delivery of exogenous IGF-1 led to chondrocyte expression of IGF-1 to decrease, IGF-1R to increase, and IGFBP-3 to become unchanged [272]. It was interesting to see that varying the IGF-1 concentration (0 - 100 ng/mL) did not impact differences in expression of the upstream IGF-1 signaling molecules.

Here, we have investigated how endogenous IGF-1 expression changed when chondrocytes are introduced to hyaluronic acid (hyaluronan, HA), which is a large molecular weight glycosaminoglycan that is readily found in cartilage. Its molecular weight in the articular cartilage region can range from approximately 500,000 to 7,000,000 [273-275]. The major role of HA is to act as a base for aggrecan molecules, ultimately forming into proteoglycans with a highly negative charge, allowing cartilage to have viscoelastic properties when under biomechanical pressures [275]. Chondrocytes interact with HA by the receptor CD44 to maintain an organized extracellular matrix, which is necessary for cartilage homeostasis [276, 277].

There has been investigation of chondrocyte function in the presence of hyaluronic acid with varying results. Embedded chondrocytes in alginate/HA hydrogels or polylactate and polyglucuronic (PLGA)/HA scaffolds had an increase in proliferation, glycosaminoglycan, and hydroxyproline content compared to just alginate or PLGA alone [278, 279]. However, when hyaluronic acid was added to chondrocytes encapsulated in either alginate or a collagen gel with PLGA acid mesh, chondrocytes proliferation did not fluctuate [280, 281]. For chondrocytes in alginate/HA hydrogels with the presence of dynamic mechanical stimulation it showed the hyaluronic acid increased type I collagen expression [280]. In other studies, hyaluronic acid hydrogels with mechanical loading showed enhancement of type II collagen expression while maintaining low levels of type I collagen expression [282]. Additionally, chondrocytes in collagen/PLGA meshes had a decrease in expression of aggrecan and type II collagen as the hyaluronic acid concentration increased (0, 10, and 100 mg/L) [281]. To our knowledge, there have been few investigations of how IGF-1 signaling molecules are

directly affected by chondrocytes that interact with hyaluronic acid in a 3-D system. Therefore, the objectives of this work are to examine the (1) expression of IGF-1 signaling molecules by chondrocytes in the presence of hyaluronic acid and IGF-1, and (2) to determine if exogenous IGF-1 and hyaluronic acid enhances phenotypic matrix expression.

5.2 Materials and Methods

5.2.1 Materials

The Dulbecco's Modified Eagle Medium: Nutrient Mixture F-12 Ham (DMEM/F12) media (with and without phenol red), penicillin/streptomycin, sodium pyruvate, Quant-iT PicoGreen dsDNA Assay kit, HISTOSTAIN®-SP Kit and Liquid DAB Substrate Kit were obtained from Invitrogen (Carlsbad, CA). The ascorbic-2-phosphate, bovine serum albumin, sodium bicarbonate, alginic acid sodium salt from brown algae, hyaluronic acid sodium salt from *Streptococcus equi* (53747) and HEPES were purchased from Sigma-Aldrich (St. Louis, MO). *Collagenase P* was purchased from Roche (Basel, Switzerland). The human insulin-like growth factor-1 (hIGF-1), anti-hIGF-1 (goat IgG, AF-291-NA), and IGF-1 Elisa Kit were obtained from R&D Systems (Minneapolis, MN). The anti-CD44 (rat monoclonal, ab19622), anti-type II collagen (rabbit polyclonal, ab300), anti-type I collagen (mouse monoclonal, ab6308), and HRP conjugated goat secondary antibody (IgG, ab6885) were purchased from Abcam (Cambridge, MA). The RNeasy Plus Mini Kit and DNeasy Blood and Tissue Kit were obtained from Qiagen (Valencia, CA). The Citrisolv Hybrid, Paraplast X-tra paraffin, Fast Green stain, and Permount were purchased from Fisher Scientific (Pittsburgh, PA). The Safranin-O was obtained from Poly Scientific (Bay Shore, NY). The cDNA Archive

Kit, Universal Master Mix, oligonucleotide primers, and Taqman probes used for RT-PCR were purchased from Applied Biosystems (Foster City, CA). The 12 mm diameter polyester membrane transwell inserts with 3 μm pore size were obtained from Corning Incorporation (Corning, NY).

5.2.2 Methods

5.2.2.1 Cartilage Extraction and Chondrocyte Isolation

Cartilage was removed from the metatarsal phanlangeal joint of calves (20-22 weeks old). The slices were washed in DMEM/F12 media, which contained the following additives: 50 μg/mL ascorbic-2-phosphate, 1 mg/mL bovine serum albumin, 1.2 mg/mL sodium bicarbonate, 0.1% penicillin/streptomycin, and 0.1% sodium pyruvate. The cartilage was incubated overnight in 0.2% *collagenase P* at 37^{o}C and then filtered through a 40 μm nylon mesh to isolate primary chondrocytes.

5.2.2.2 Chondrocyte Encapsulation and Culture

Alginate was chosen to be the base polymer at a 2.0% w/v concentration for this study. Four different amounts of hyaluronic acid were added to alginate to have the following concentrations: 0, 0.05, 0.50, and 5.00 mg/mL. The hydrogel solution was prepared by mixing and heating alginic acid, hyaluronic acid, 0.15 M sodium chloride, and 0.025 M HEPES into deionized water (pH 7.4). The final solution was sterilized through a 0.22 μm syringe filter and then mixed with chondrocytes to obtain a cell density of 100,000 cells/bead. This solution was injected through an 18 gauge syringe into a 100 mM calcium chloride solution for 15 minutes and then rinsed in DMEM/F12 for 15 minutes. Afterwards, 5 beads were transferred into each well of a 6-well plate and cultured in DMEM/F12 media with 10% FBS at 37^{o}C (day 0) for 2 days. The media was

changed on day 3 with DMEM/F12 media, 10% FBS, and 100 ng/mL hIGF-1. Human IGF-1 was used because it has a similar homology to bovine IGF-1 [255]. The media and IGF-1 were changed daily. Chondrocytes were isolated from 5 alginate/HA beads for analysis at day 1, 4, and 8 by the addition of 4 mL of 0.1M ethylenediaminetetraacetic acid (EDTA) for 30 minutes at 37^{o}C. A cell pellet was formed by centrifugation and then resuspended in PBS and split for RNA and DNA isolation.

5.2.2.3 RNA Isolation

Total RNA was isolated from chondrocytes by following the instructions provided in the RNeasy Plus Mini Kit. Total RNA was eluted into 30 μL of RNase free water and detected using a NanoDrop ND-1000 Spectrophotometer (NanoDrop Technologies, Wilmington, DE).

5.2.2.4 DNA Isolation and Quantification

Total DNA was isolated from chondrocytes using a DNeasy Blood and Tissue Kit by following the details in the manual instructions. Total DNA was eluted in 400 μL of an AE buffer and then incubated with PicoGreen supplied from a Quant-iT PicoGreen dsDNA Assay kit. The samples were excited at 480 nm and evaluated at an emission of 520 nm using a fluorescence microplate reader (Molecular Devices SpectraMax M5, Sunnyvale, CA). A standard curve was prepared from a known concentration of DNA provided in the kit and this curve was used to quantify nanograms of DNA per bead.

5.2.2.5 Histology

All samples were collected and fixed in 4% paraformaldehyde and 0.1 M sodium cacodylate buffer containing 10 mM $CaCl_2$ (pH 7.4) for 24 hours at 4^{o}C. The beads were washed with 0.1 M sodium cacodylate buffer with 10 mM $CaCl_2$ (pH 7.4) for 24 hours at room temperature. Afterwards, the beads were dehydrated in a series of ethanol concentrations (40-100%) with a final Citrisolv Hybrid wash. The samples were embedded in Paraplast X-tra paraffin and cut into 4 μm thickness sections, which were placed onto charged microscope slides and kept at 4^{o}C until staining.

5.2.2.6 Histochemical Staining

Sections were oven dried for 2 hours at 60^{o}C, deparaffinized in Citrisolv Hybrid two times for 3 minutes, rehydrated in 100% and 95% ethanol for 1 minute each, and rinsed in distilled water. Sections were stained with Safranin-O (0.1%) and counter stained with Fast Green (0.001%).

5.2.2.7 Immunohistochemistry

Sections were prepared as previously described [272]. The following antibodies were used to stains for the presence of CD44, IGF-1, type II collagen, and type I collagen. The primary antibodies are: anti-CD44, anti-hIGF-1, anti-type II collagen, and anti-type I collagen. The antibodies for CD44 and type I collagen were diluted 1:100. The antibodies for IGF-1 and type II collagen were diluted 1:200. A HISTOSTAIN®-SP Kit was used to reveal the presence of CD44, type II collagen, and type I collagen by using a horseradish peroxidase (HRP)-strepavidin-biotin system. This complex formation was detected by a 3,3'-diaminobenzidine tetrahydrochloride (DAB) chromogen. For IGF-

1, a HRP conjugated secondary goat antibody was used at a dilution of 500 times and detected by a histochemical substrate (Liquid DAB Substrate Kit). All samples were counterstained with hematoxylin, dehydrated in 95% and 100% ethanol twice for 1 minute each, cleared in Citrisolv Hybrid twice for 1 minute, and coverslipped using Permount. To show non-specific staining, samples were not incubated with the primary antibody and then incubated with the secondary antibody for each protein (negative staining control).

5.2.2.8 Quantitative Reverse Transcriptase-Polymerase Chain Reaction (qRT-PCR)

Isolated mRNA was reverse transcribed using a cDNA Archive Kit. Quantitative RT-PCR was performed by combining the cDNA solution with a Universal Master Mix, as well as oligonucleotide primers and probes that were created for the genes of interest (IGF-1, IGF-1R, IGFBP-3, CD44, type II collagen, and type I collagen) and the endogenous gene control (glyceraldehyde 3 phosphate dehydrogenase, GAPDH). The same primer and probes for IGF-1, IGF-1R, IGFBP-3, type II collagen, type I collagen, and GAPDH were used from previous work [253, 272]. The sequences for the forward primer, reverse primer, and probe for CD44 are 5' CGGGTTCATAGAAGGGCATGT 3', 5' TGTTCGCAGCACAGATGGA 3', and 5' ATTCCCCGGATCCAC 3'. The reaction was conducted on an ABI Prism 7000 sequence detector (Applied Biosystems), using thermal conditions of 2 minutes at 50^{o}C, 30 minutes at 60^{o}C, 5 minutes at 95^{o}C, and 40 cycles of 20 seconds at 94^{o}C and 1 minutes at 62^{o}C. The expression for each gene was analyzed for all the groups in the study using a relative comparative method, which were normalized to GAPDH. The calibration for the data obtained for each gene

expression sample set was analyzed to the 0 mg/mL HA sample at day 1. This calibrator was chosen to represent the gene expressions data appropriately.

5.2.2.9 Release of IGF-1 in Alginate/HA Hydrogels

Cell free 0, 0.05, 0.50, and 5.00 mg/mL HA alginate solutions (200 μL) were each injected into 12 mm diameter size transwell inserts. The solutions were immersed in a 100 mM solution of calcium chloride for 30 minutes. The alginate/HA gel was rinsed in phenol free DMEM/F-12 with 15mM HEPES, 50 μg/mL ascorbic-2-phosphate, and 1 mg/mL BSA for 30 minutes. Finally, the gel inserts were immersed in the same media used for rinsing and equilibrated for 3 days in a cell culture incubator. After 3 days, the inserts were put into 12-well plates containing 2 mL of the same media used earlier along with 2 μg of hIGF-1. Fresh media (450 μL) was placed on top of the gel. At the following time points, 100 μL of the solution on top of the gels was removed and placed in -20 ^{o}C freezer until analysis: 0, 2, 4, 6, 8, 10, 12, 24, and 48 hours. The removed media was replaced with fresh 100 μL DMEM/F-12. Samples were tested for hIGF-1 content by a hIGF-1 Elisa Kit.

5.2.2.10 Statistical Analysis

Data from all studies were analyzed using ANOVA and Tukey's multiple-comparison test. The means and standard deviations are reported in each figure.

5.3 Results

5.3.1 Hyaluronic Acid Entanglement in Alginate

Proliferation was monitored by chondrocytes embedded in the alginate/HA beads. DNA was isolated and measured at each time point for all the groups (Figure 5.1). The

levels of DNA were not significantly different amongst the groups at day 1, 4, or 8. However, there was an increasing trend in DNA from day 1 to 8 for all the groups.

To confirm that hyaluronic acid was being retained in the alginate beads, they were weighed as well as stained with Safranin-O and Fast Green. The water content of the alginate/HA beads for all the groups were approximately 96% throughout the whole experiment. The incorporation of hyaluronic acid increased the bead dry weight (Figure 5.2). All the groups were significantly different from each other ($p < 0.01$) except for the 0 and 0.05 mg/mL HA groups at each time point. Additionally, the groups individually maintained steady weights during the time course of the experiment.

The Safranin-O and Fast Green stained histology sections showed that chondrocytes were thoroughly dispersed in the alginate/HA beads, which can be seen by their gray stained nuclei (Figure 5.3). Safranin-O/Fast Green stain turns alginate into an intense orange color, while making the proteoglycans and glycosaminoglycans appear as a fainter orange hue [261]. Seen in Figure 5.3 at day 1, the orange stain becomes lighter as the incorporation of hyaluronic acid increases. By day 8, the orange color became darker for the alginate/HA beads. Clustering of chondrocytes was observed around the circumference for all the alginate/HA beads (not shown), which was similar in appearance to previous work [272].

5.3.2 CD44 mRNA Expression

In order to ensure that hyaluronic acid was interacting with the embedded chondrocytes in the alginate/HA beads, CD44 mRNA expression was analyzed (Figure 5.4). At day 1, all the chondrocytes expressed CD44 at similar levels. By day 4, only the chondrocytes that were embedded in alginate/HA beads expressed CD44 ($p < 0.01$). The

continued 2 fold increase in CD44 expression was also observed by the chondrocytes at day 8.

5.3.3 Endogenous mRNA Expression of IGF-1 Signaling Molecules

The embedded chondrocytes in all the alginate/HA beads expressed IGF-1 throughout the 8 day study (Figure 5.5). The 0 mg/mL HA case had a 6 fold increase in expression of IGF-1, while the 0.05, 0.50, and 5.00 mg/mL HA groups all had a 2 fold increase from day 1 to 4. The 0 mg/mL HA group had the highest level of IGF-1 expression compared to the other groups at day 4 ($p < 0.01$). From day 4 to 8, the chondrocytes embedded in the 0 mg/mL HA beads maintained their level of IGF-1 expression. A 5 fold increase of expression was seen by the 0.05 mg/mL HA beads, while the other two groups, 0.50 and 5.00 mg/mL HA, both had a 2 fold increase in IGF-1 expression from day 4 to 8. At day 8, the 0.05 mg/mL HA group had the highest level of IGF-1 expression compared to the other groups ($p < 0.01$). The 0.50 mg/mL HA case had higher IGF-1 expression ($p < 0.01$) than the 0 and 5.00 mg/mL HA samples, which did not have significant differences in expression levels.

IGF-1R expression was observed from all the groups during the 8 day period (Figure 5.6). At day 1, the expression levels for all the alginate/HA groups did not differ significantly. Throughout the experiment, the only group that experienced fluctuations of IGF-1R expression was the 0 mg/mL HA group. There was a 3 fold increase in IGF-1R expression from day 1 to 4 and then a 3.5 fold decrease in IGF-1R expression from day 4 to 8. At day 4 and 8, the 0 mg/mL HA group had expression levels that were significantly different from the groups with hyaluronic acid ($p < 0.01$).

During the 8 day study, the expression of IGFBP-3 decreased for all sample groups (Figure 5.7). The 0.05 mg/mL HA group had the highest level of IGFBP-3 expression compared to the other cases at day 1 ($p < 0.01$). However, by day 4 the expression levels had more variance among the groups. The 0 mg/mL and 0.50 mg/mL HA group both had a 1.5 fold increase in IGFBP-3 expression. The other two groups, 0.05 mg/mL and 5.00 mg/mL HA, had a decrease in expression with a 6.6 and 0.6 fold change, respectively. The 0 mg/mL HA group had the highest expression level at day 4 followed by the 0.50 mg/mL HA case ($p < 0.01$). There was no difference in IGFBP-3 expression between the 0.05 and 5.00 mg/mL HA group. By day 8, all the groups expressed equal levels of IGFBP-3.

5.3.4 mRNA Expression of Phenotypic Matrix Proteins

All the chondrocytes embedded in the alginate/HA beads expressed type II collagen during the 8 day study (Figure 5.8). The 0 and 5.00 mg/mL HA group at day 1 had similar levels of type II collagen expression. Additionally, the 0.05 and 0.50 mg/mL HA group were not significantly different but had higher type II collagen expression levels compare to the 0 and 5.00 mg/mL HA cases ($p < 0.01$). Similar trends were found at day 4 for all the groups ($p < 0.01$). The 0, 0.05, and 0.50 mg/mL HA groups decreased in type II collagen expression by 0.8, 1.5, and 1.5 fold difference respectively from day 1 to 4. The 5.00 mg/mL HA group was the only case that did not change in expression level. From day 4 to 8, the type II collagen expression levels decreased for all the groups. The most change was experienced by the 0 mg/mL HA group with a 5 fold difference, which had the lowest expression of type II collagen ($p < 0.01$). The 0.05, 0.50, and 5.00

mg/mL HA groups had similar levels of expression with fold changes of 2.7, 3.7, and 1.5 from day 4 to 8, respectively.

Type I collagen was also expressed by all the samples throughout the study (Figure 5.9). From day 1 to 8, all the groups significantly increased in type I collagen expression. The expression levels were similar amongst the groups at day 1. Additionally, there were no significant differences in type I collagen expression between the samples at day 4. By day 8, the 0 mg/mL HA group had a 34 fold increase in type I collagen, which was the lowest compared to alginate beads that contained hyaluronic acid ($p < 0.01$). The largest increase in type I collagen expression was by the 0.05 mg/mL HA group with a 78 fold change. Type I collagen expression was increased by 40 fold for the 0.5 mg/mL HA group and by a 52 fold for the 5 mg/mL HA group.

5.3.5 CD44, IGF-1, Type II Collagen, and Type I Collagen Protein Expression

Immunohistochemistry was performed for all the groups at each time point in order to confirm that the embedded chondrocytes were synthesizing the proteins of interest. All the proteins increased in abundance by day 8 and were located primarily surrounding the chondrocyte clusters (Figure 5.10). CD44 stained strongly within the chondrocyte clusters, while IGF-1 was found to be present outside the clusters as well. Type II collagen staining seemed to be greater than type I collagen staining for all the groups.

5.3.6 Release of IGF-1 in Alginate/HA Hydrogels

All the alginate/HA groups released less than 2% of the initial total IGF-1 amount (2 μg) (Figure 5.11). The 0, 0.05, and 0.50 mg/mL HA groups released approximately 10

ng more IGF-1 compared to the 5.00 mg/mL HA case. At 24 and 48 hours the 5.00 mg/mL HA group had significantly lower amounts of IGF-1 released compared to all the other cases ($p < 0.01$). Steady state release of IGF-1 was achieved by 48 hours for all the groups.

5.4 Discussion

We have shown in earlier works that in a 3-D alginate hydrogel system, delivering exogenous IGF-1 to the embedded chondrocytes alters the endogenous expression of upstream IGF-1 signaling molecules, such as IGF-1 and IGF-1R [272]. We were therefore interested to investigate how incorporating hyaluronic acid, a chondrocyte adhesion moiety, within alginate hydrogels would affect the endogenous expression of IGF-1 signaling molecules. Thus, in the present study, we varied the amount of hyaluronic acid in alginate to investigate the following objectives: (1) effect of hyaluronic acid on endogenous IGF-1, IGF-1R, and IGFBP-3 and (2) effect of hyaluronic acid on chondrocyte phenotypic expression.

As alginate hydrogels have a high porosity, there is a concern that hyaluronic acid may diffuse out of the alginate beads. Previous work shows that at 2.4% w/v alginate, hyaluronic acid has a higher retention ability compared to lower alginate concentrations [283]. Additionally, the incorporation of chondrocytes in alginate beads also decreases the potential release of hyaluronic acid [280, 283]. In order to confirm that in this system, hyaluronic acid did not leach out of the alginate beads, we measured bead dry weight (Figure 5.2) and stained with Safranin-O/Fast Green (Figure 5.3). The dry weights of the beads at all time points was higher for the groups that contained 0.50 and 5.00 mg/mL HA compared to the 0 and 0.05 mg/mL HA groups. As all the groups had

similar levels of DNA content at each time point and the alginate concentration was the same in the experiment, the higher dry weights imply that the alginate beads retained HA. This data is consistent with the Safranin-O/Fast Green stained bead images which show proteoglycans and glycosaminoglycans in an orange hue but in contrast to alginate, it is a much lighter orange shade. At day 1, it can be seen that as the HA content increases the stain becomes a lighter orange color, indicating that the free HA is entangled in the alginate beads. However, by day 8 all the images become a darker orange hue, indicating that there is some loss of HA from the beads as the study progressed. The loss of HA is also indicated by the lack of change in dry weights of the beads from day 1 to day 8 for all the groups. In this experiment, chondrocytes proliferated and formed matrix protein clusters on the bead periphery. These cluster formations can increase the dry weights but since the dry weights did not fluctuate, this indicates that some HA could have leached out of the bead.

The mRNA expression of CD44, further confirmed that HA was present in the beads (Figure 5.4). Chondrocytes with and without free HA produced CD44 proteins as seen by immunohistochemical staining (Figure 5.10). However, variations were seen in chondrocyte CD44 mRNA expression. At day 1 all the groups expressed CD44 but by day 4 only the groups that contained HA expressed high levels of CD44. This trend continued till day 8, indicating that HA was still present in the beads and additionally the chondrocytes are interacting with HA. It was interesting to see that despite the varying concentrations of HA in the construct, chondrocytes expressed similar levels of CD44 mRNA throughout the 8 day study. A continuous expression of CD44 is expected since chondrocytes are attachment cells and hyaluronic acid is present in the alginate beads.

The 0.05 mg/mL HA concentration seems to be enough to allow for chondrocyte adherence to hyaluronic acid. When hyaluronic acid attaches onto CD44, chondrocytes have the ability to internalize HA via endocytosis [277]. However, in order to continually attach to the free hyaluronic acid, chondrocytes must continue to express CD44. Therefore, this might be why we see a constant steady level of CD44 expression. This steady state level could possibly be a saturating point for CD44 expression and it seems to be reached by chondrocytes surrounded with a HA concentration of 0.05 mg/mL. We speculate that a decrease in CD44 expression may be observed if HA concentration is further lowered.

We have found in earlier experiments that incubating chondrocytes with exogenous IGF-1 depresses endogenous expression of IGF-1 [272]. In this particular study, the objective was to determine how the incorporation of hyaluronic acid affects chondrocyte interaction with delivered IGF-1. Our data showed that hyaluronic acid influenced IGF-1 expression by day 8 (Figure 5.5). The synthesis of IGF-1 proteins was confirmed by immunohistochemistry for all the groups at day 8 (Figure 5.10). However, the IGF-1 mRNA expression decreased as higher amounts of hyaluronic acid was added to the alginate beads. Since the amount of IGF-1 retentation is similar for the 0, 0.05, and 0.50 mg/mL HA groups, it seems that hyaluronic acid interaction with the chondrocytes can increase the mRNA expression of IGF-1. Interestingly, the 5.00 mg/mL HA group had similar IGF-1 expression levels compared to the 0 mg/mL HA group. In a high HA concentration (5.00 mg/mL), IGF-1 becomes entrapped in the hydrogel (Figure 5.11). A similar result was seen in cartilage explants, when exposured to free hyaluronic acid led to retention of IGF-1 [284]. Therefore, the chondrocytes are able to sense the presence of

IGF-1 and decrease their need to express endogenous IGF-1. It seems that once a certain dosage of free hyaluronic acid is reached, there is a well concentrated entrapped supply of IGF-1 to the chondrocytes. As a result chondrocytes start to have IGF-1 expression levels similar to samples that contain no hyaluronic acid.

Chondrocyte interaction with IGF-1 is primarily through its own specific receptor, IGF-1R [272, 285]. A correlation in IGF-1 expression and IGF-1R expression could then be expected. Since the chondrocytes were incubated with exogenous IGF-1, there should be an increase in expression of the receptor for the control group as seen in previous studies [272, 285]. While an increase is observed by day 4, which is expected, a decrease occurs in IGF-1R expression by day 8 (Figure 5.6). While this sudden decrease in expression is unclear, the fluctuation in expression shows that exogenous IGF-1 is affecting the receptor expression. However, for the groups that have hyaluronic acid, there is no change in IGF-1R expression throughout the study. We speculate that hyaluronic acid might have a role in the regulation of IGF-1R in the presence of exogenous IGF-1. While this is the first reported study to investigate IGF-1R expression by embedded chondrocytes in the presence of IGF-1 and HA, the interaction of hyaluronic acid with IGF-1R can be confirmed by a previous study involving chondrocyte treatment with interleukin-1 (IL-1). Here it was found that when chondrocytes were treated with IL-1, the presence of HA actually increased IGF-1R protein levels [286]. However, the details of how HA interacts with IGF-1 signaling has still yet to be fully understood.

In regards to IGFBP-3 expression, hyaluronic acid does not seem to have an impact on IGFBP-3 expression, since it decreased for all the groups by day 8 (Figure

5.7). This lack of expression further indicates that IGFBP-3 is not a controlling factor for intake of exogenous IGF-1 by embedded chondrocytes as found in previous work [272].

Chondrocytes continued to express type II collagen, a primary phenotypic marker, throughout the study for all the groups (Figure 5.8). Though there is a decrease in mRNA expression from day 1 to 8, the immunohistochemistry stains indicate that type II collagen was being highly produced for all the groups at day 8 (Figure 5.10). Therefore, indicating that the chondrocytes are maintaining their phenotype. Despite the continuous expression of type II collagen, there was also expression of type I collagen, indicating a fibroblastic phenotype. The protein expression of type I collagen was less intense than type II collagen at day 8 (Figure 5.10). However, type I collagen mRNA expression increased for all the groups throughout the experiment (Figure 5.9). The expression of type I collagen has been found to occur by chondrocytes embedded in 2.0% w/v alginate with or without exogenous IGF-1 [272]. However, type I collagen expression is lower for chondrocytes when exposed to IGF-1. In this experiment, hyaluronic acid seems to further increase chondrocyte type I collagen expression by day 8 when in contact with excess IGF-1. Even without IGF-1, it has been found that hyaluronic acid increases type I collagen expression [282]. This indicates that hyaluronic acid possibly overpowers the affect of exogenous IGF-1 by making the chondrocytes retain more of a fibroblastic phenotype.

Incorporation of hyaluronic acid has been shown to affect how exogenous IGF-1 interacts with embedded chondrocytes in alginate hydrogel. This is to be expected because of the importance that attachment proteins play in articular cartilage function. Hyaluronic acid seems to be able to entrap IGF-1 and therefore control its delivery to

chondrocytes and thus altering embedded chondrocyte IGF-1 expression. While normally IGF-1R expression by chondrocytes would be increased when delivered IGF-1, in the presence of hyaluronic acid there is minimal change. This could indicate a possible interaction between hyaluronic acid and IGF-1R. Hyaluronic acid seemed to have a huge influence over the affect of exogenous IGF-1 by chondrocytes because of the increase in type I collagen, indicating a more fibroblastic phenotype. Overall, these results show that the expression of upstream IGF-1 signaling molecules by chondrocytes is sensitive by the addition of free hyaluronic acid as well as its phenotypic function, especially when embedded in a 3-D alginate hydrogel.

5.5 Conclusions

From the results we obtained from this study, in the presence of exogenous IGF-1 we found that hyaluronic acid affects chondrocyte phenotypic function as well as IGF-1 expression and IGF-1R expression. Hyaluronic acid has been known to increase chondrocyte expression of type I collagen and in this study similar results were observed. The concentration of hyaluronic acid within alginate allowed for chondrocyte interaction and retention of exogenous IGF-1. Therefore, HA was shown to control the expression of IGF-1 by the embedded chondrocytes. Additionally, the presence of hyaluronic acid might be interacting with IGF-1R and altering the receptor expression despite the presence of excess IGF-1. We further concluded that IGFBP-3 expression is changed minimally by the introduction of hyaluronic acid and does not seem to play a vital role in IGF-1 signaling for embedded chondrocytes. From the data collected in this experiment, there are potentially some regulatory mechanisms that are shared between the HA and IGF-1 pathways. However, future work will be necessary to determine these details.

Overall, we have shown that it is important to understand how construct properties can affect chondrocyte endogenous expression of upstream IGF-1 signaling molecules in order to create a properly engineered articular cartilage.

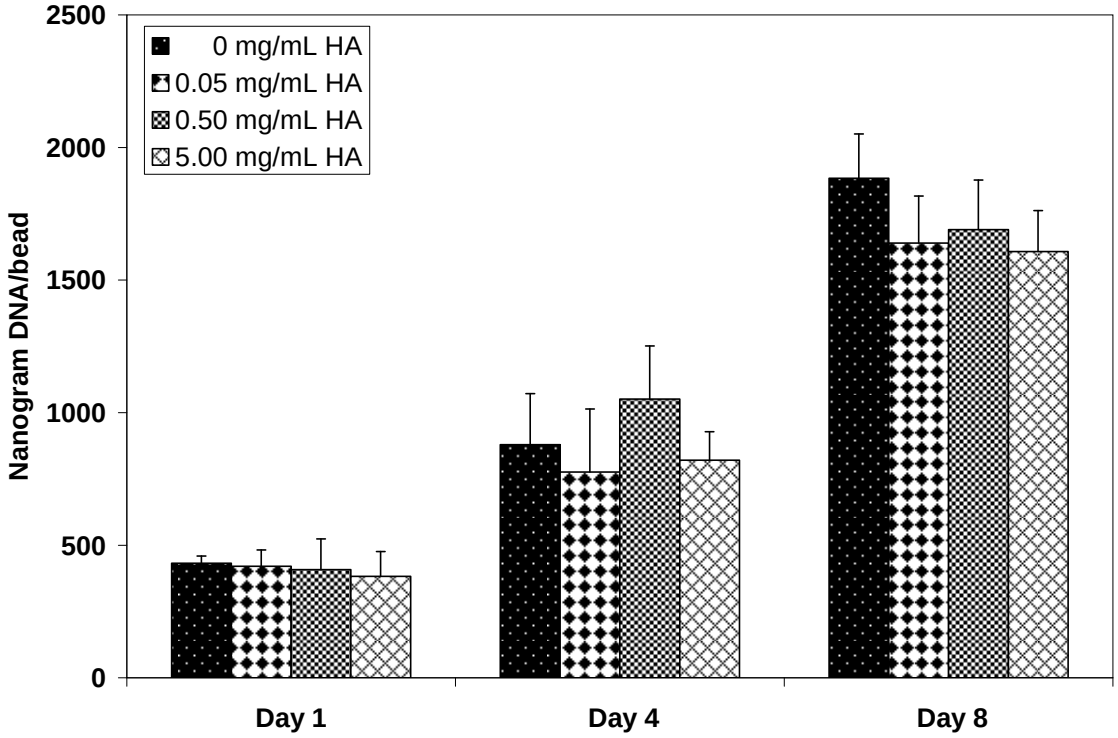

Figure 5.1. Nanogram DNA levels per bead for all sample groups over the experimental time course of 8 days. There is no significant difference in DNA levels among each of groups at each time point. The means and standard deviations are reported ($n = 3$).

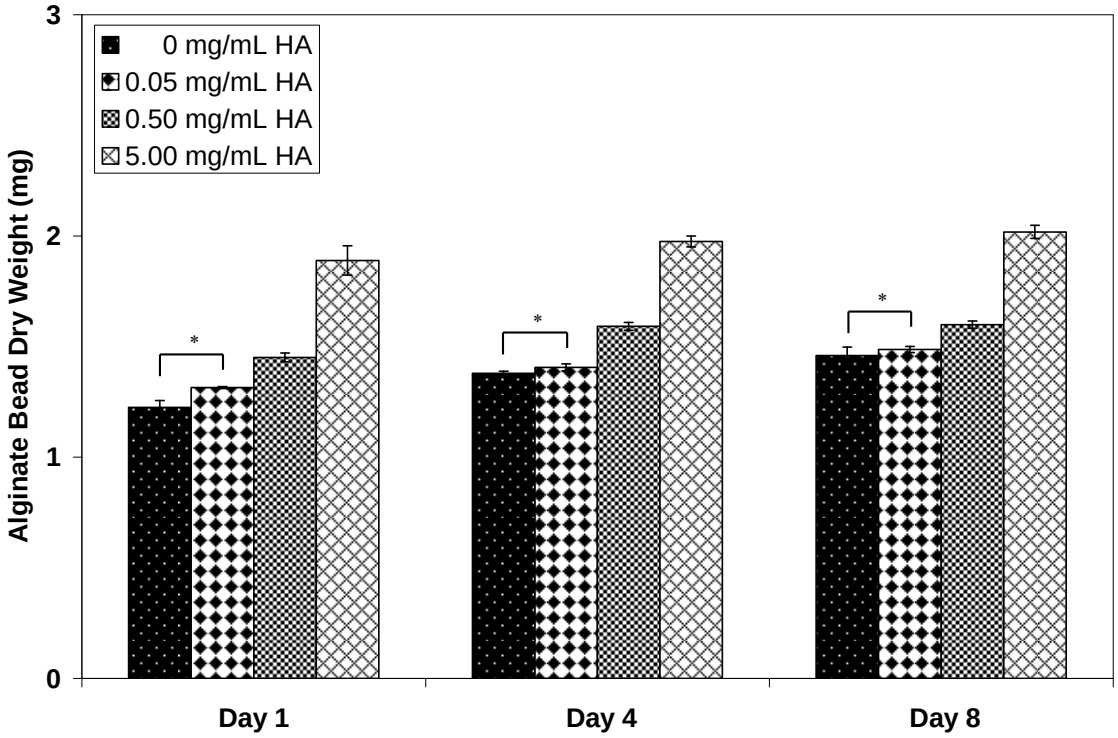

Figure 5.2. The alginate/HA bead dry weights were measured for the following groups during the time course of the experiment: 0, 0.05, 0.50, and 5.00 mg/mL HA. The means and standard deviations are reported ($n = 3$, $*$ indicates $p < 0.01$).

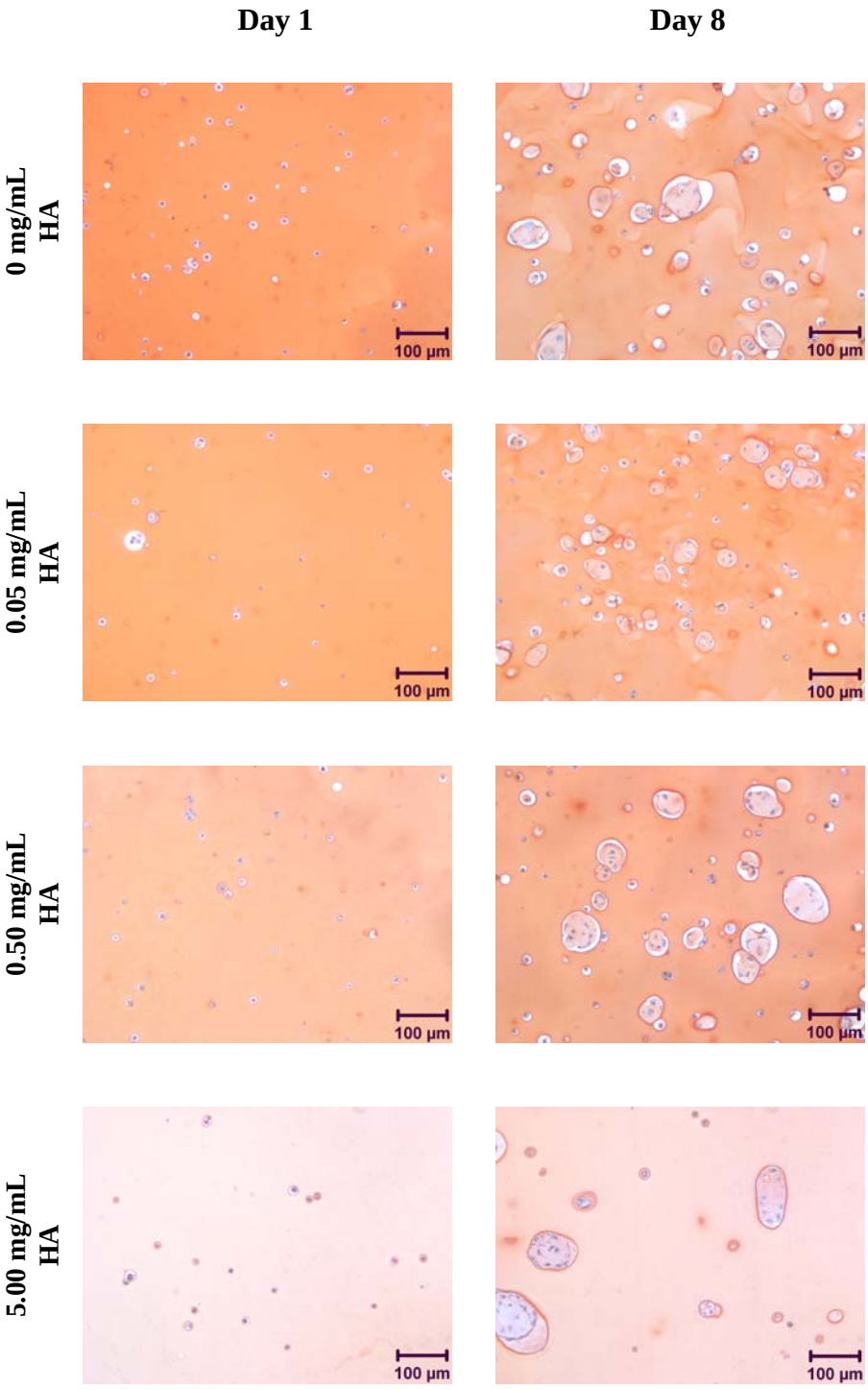

Figure 5.3. Safranin-O and Fast Green stained sections at day 1 and day 8 for 0 mg/mL HA, 0.05 mg/mL HA, 0.50 mg/mL HA, and 5.00 mg/mL HA. Alginate stains into an intense orange color, hyaluronic acid becomes a lighter orange hue, and chondrocytes a shade of gray. Scale bars are located on the bottom right corner of each image.

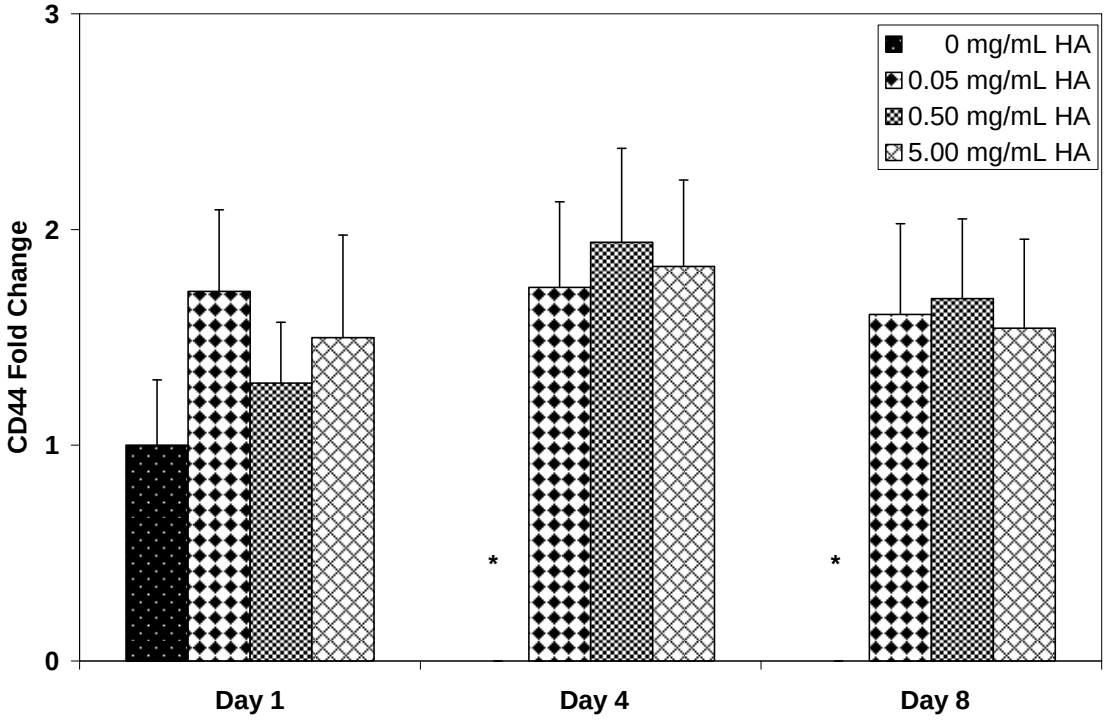

Figure 5.4. CD44 mRNA expression for all sample groups over 8 days. Chondrocytes only expressed CD44 in the groups that contained hyaluronic acid in the alginate beads at day 4 and 8. There was no statistical difference in CD44 expression when there were different hyaluronic acid concentrations. The means and standard deviations are reported ($n = 3$, $*$ indicates $p < 0.01$).

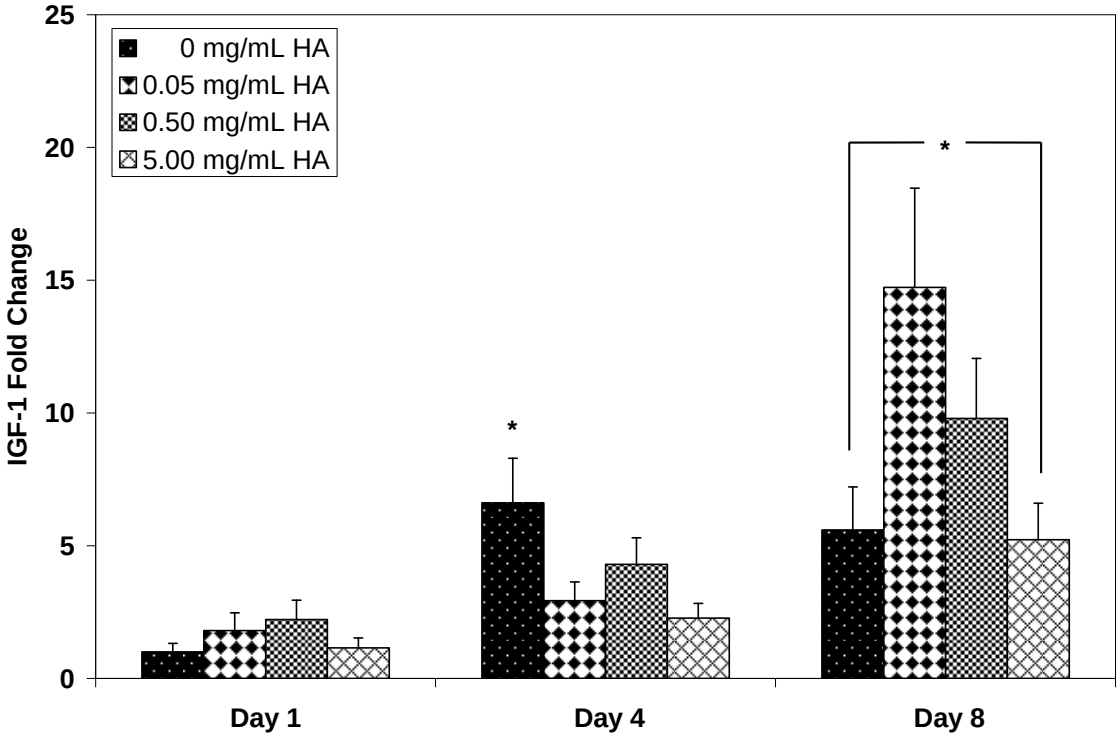

Figure 5.5. Chondrocytes in all bead groups expressed IGF-1 at day 1, 4, and 8. Results indicate that at day 8, the 0 and 5.00 mg/mL HA samples had similar as well as the lowest level of IGF-1 expression compared to the 0.05 and 0.50 mg/mL HA groups. The highest level of expression was from the 0.05 mg/mL HA beads, followed by the 0.50 mg/mL HA group. The means and standard deviations are reported ($n = 3$, $*$ indicates $p < 0.01$).

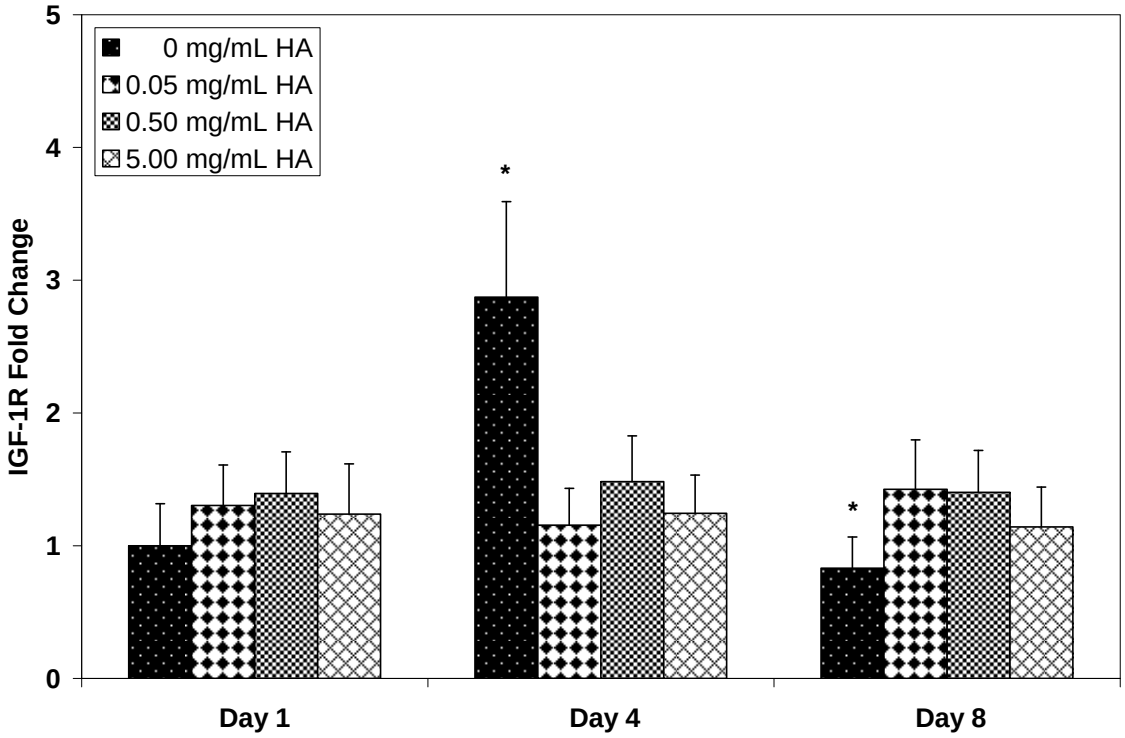

Figure 5.6. All the groups expressed IGF-1R throughout the study. By day 8, the IGF-1R expression was lowest for the 0 mg/mL HA group compared to the other samples. The means and standard deviations are reported ($n = 3$, $*$ indicates $p < 0.01$).

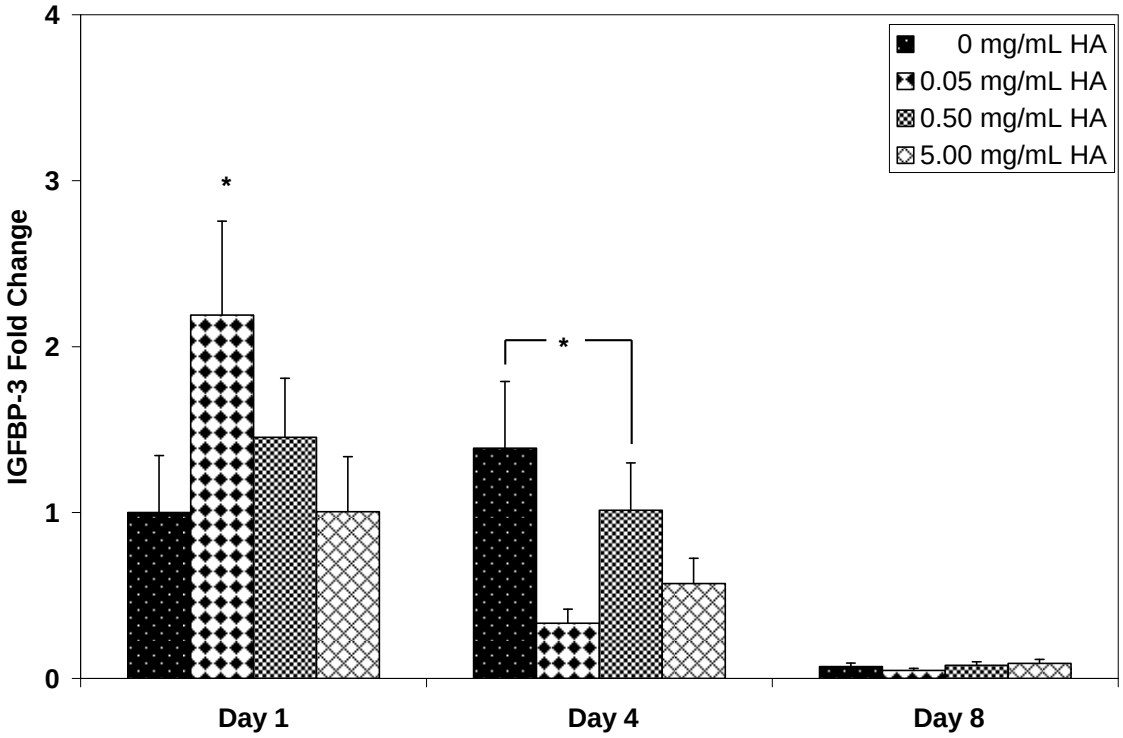

Figure 5.7. IGFBP-3 mRNA expression for all sample groups over 8 days. A decrease in IGFBP-3 expression occurred for all groups by 8 days. The means and standard deviations are reported ($n = 3$, $*$ indicates $p < 0.01$).

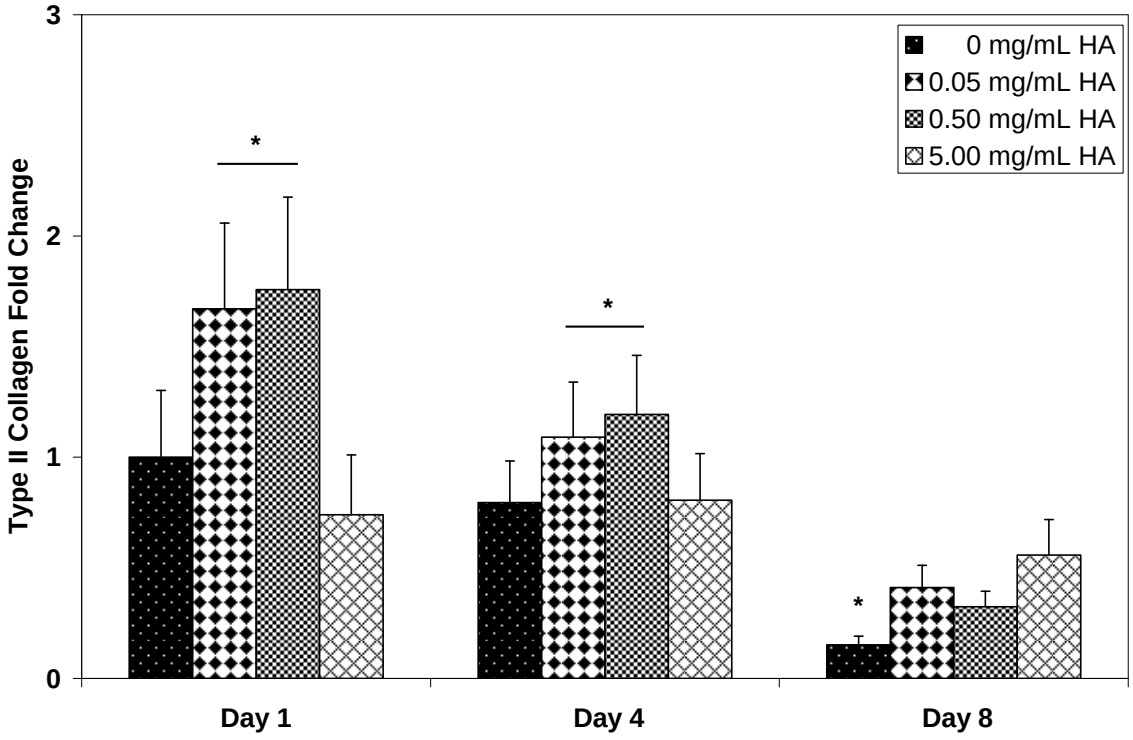

Figure 5.8. Type II collagen mRNA expression was sustained throughout the 8 day study for all the sample groups. However, a decreasing trend occurred by all the groups from day 1 to 8. At day 8, the 0 mg/mL HA case had the lowest type II collagen expression compared to the groups that contained hyaluronic acid. The means and standard deviations are reported ($n = 3$, $*$ indicates $p < 0.01$).

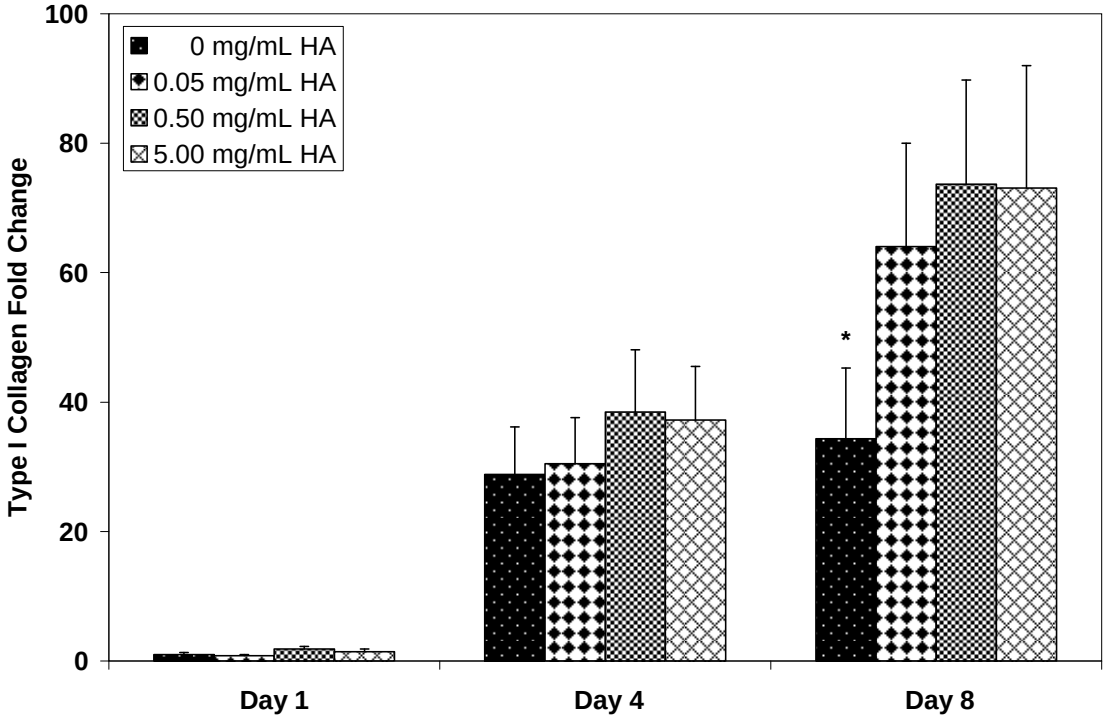

Figure 5.9. Type I collagen mRNA expression for all sample groups over 8 days. A higher level of expression occurred in the beads that contained hyaluronic acid versus the 0 mg/mL HA group by the day 8 time point. The means and standard deviations are reported ($n = 3$, $*$ indicates $p < 0.01$).

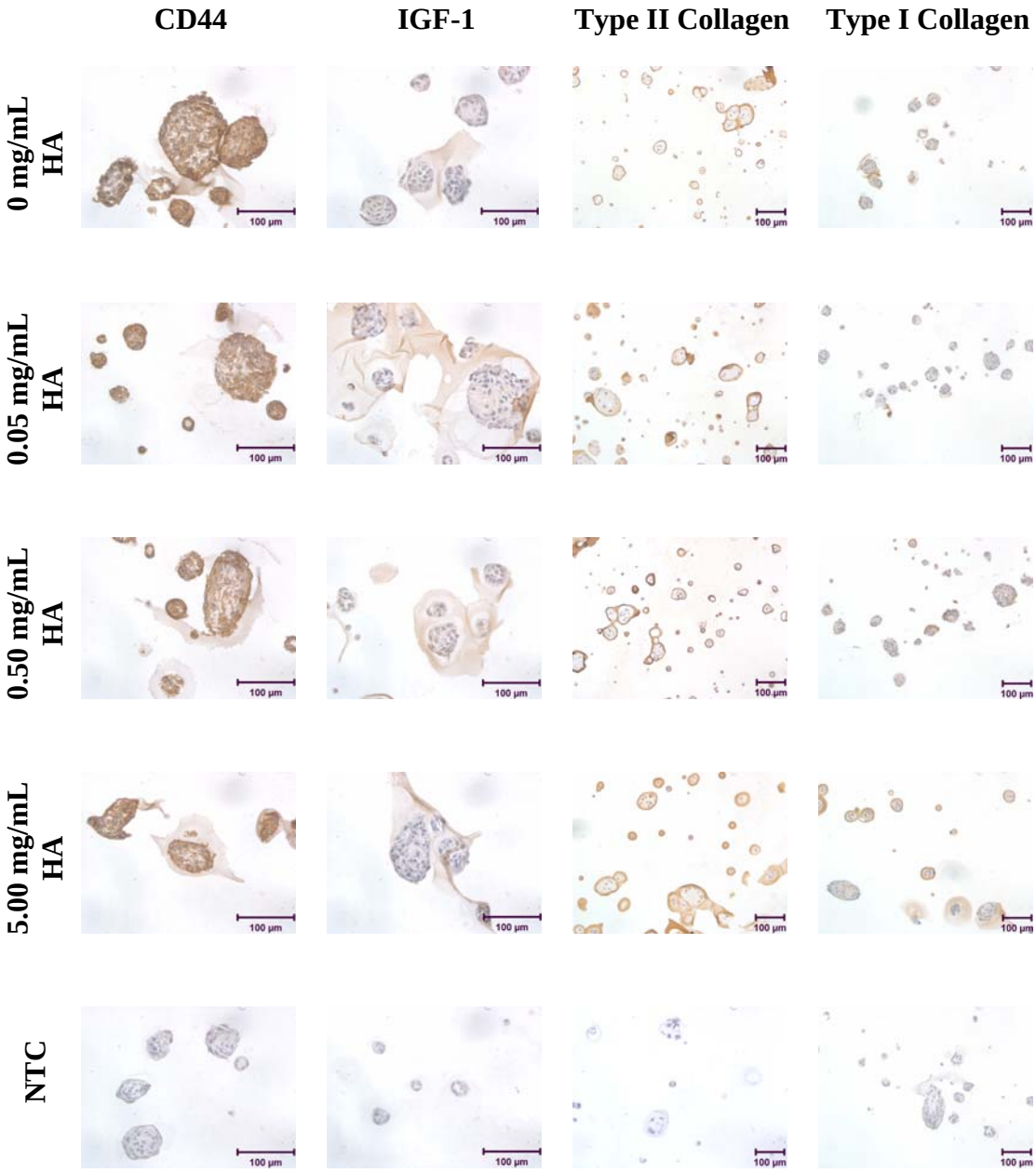

Figure 5.10. Immunohistochemistry staining at day 8 for CD44, IGF-1, type II collagen, and type I collagen. The 0, 0.05, 0.50, and 5.00 mg/mL HA groups are all represented here, as well as the negative staining control (NTC). Most of the staining occurred around the cluster of chondrocytes. Scale bars are located on the bottom right corner of each image.

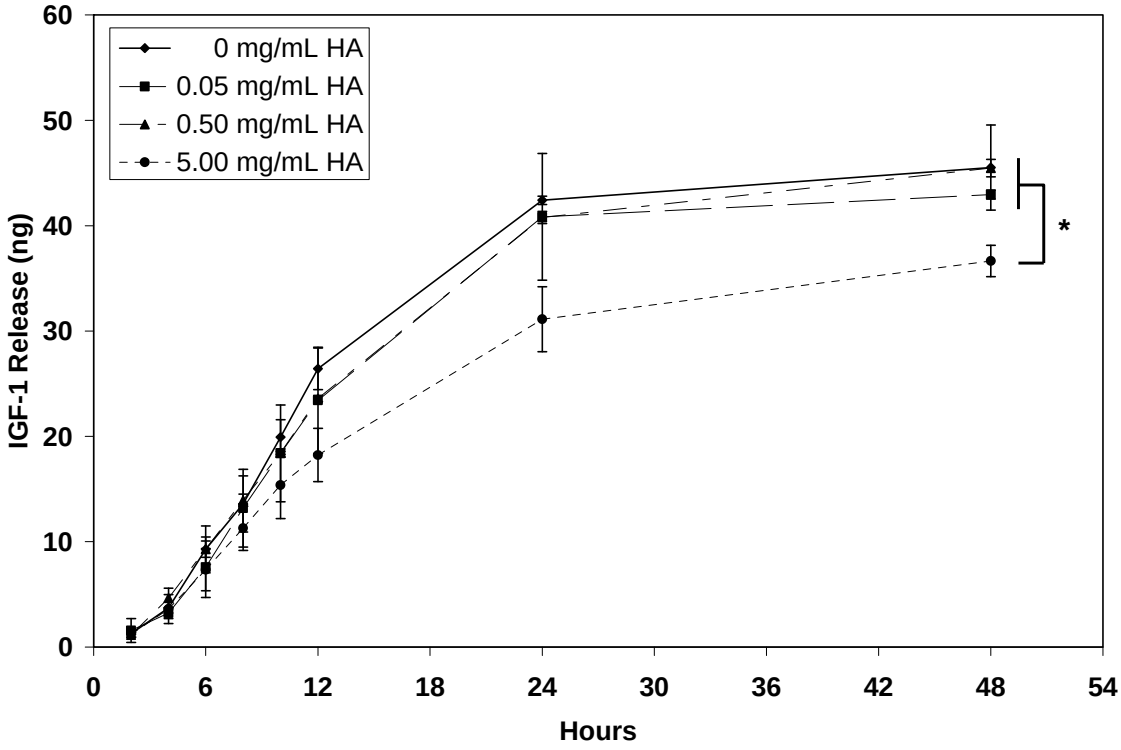

Figure 5.11. IGF-1 diffusion through 0 mg/mL and 5.00 mg/mL HA alginate hydrogels. The 0 mg/mL HA released twice as much IGF-1 compared to the 5.00 mg/mL HA gels. The means and standard deviations are reported ($n = 3$, $*$ indicates $p < 0.01$).

6 *In Vivo* Investigation of IGF-1 Delivery Effects on Chondrocytes Embedded in an Alginate/Hyaluronic Acid Hydrogel

6.1 Introduction

Articular cartilage is a delicate tissue and unfortunately it does not have the reparative capacity to heal when it has become damaged or diseased. The limited ability for cartilage to restore itself to a healthy state has led tissue engineers to determine innovative methods to aid in cartilage regeneration. Most of the approaches involve utilizing a biomaterial as a drug delivery vehicle for growth factors and/or scaffold for chondrocytes or stem cells [3, 287-289]. Therefore, biomaterial interactions are an important attribute to understand when creating an engineered cartilage construct.

Alginate hydrogels are commonly used as a scaffold because it can maintain chondrocyte phenotype and viability [103, 106, 116, 132, 230, 250]. The lack of amine groups on alginate chains provides a simple environment with minimal interaction to embedded chondrocytes [251, 252]. Therefore, allowing researchers to investigate how the addition of specific components affects chondrocyte signaling. For instance, in our previous work we introduced insulin-like growth factor-1 (IGF-1) to an alginate hydrogel with embedded chondrocytes [272]. By exogenously delivering IGF-1, this resulted in down-regulating chondrocytic IGF-1 expression [272]. Interestingly, by incorporating hyaluronic acid (HA) into alginate hydrogels an anchoring site for the chondrocytes was established that ultimately hindered the diffusion of free IGF-1 (Figure 5.11). As a result, increasing concentrations of HA was able to decrease IGF-1 expression. From these *in vitro* experiments, the impact of HA on chondrocyte IGF-1 signaling can be observed. It

is known that *in vitro* and *in vivo* studies do not always correlate as there are many more variables to influence the construct in an *in vivo* environment. Therefore, these interesting results led us to investigate how HA and IGF-1 would impact chondrocytes embedded in alginate hydrogels in an *in vivo* scenario.

Previous *in vivo* work has shown that chondrocytes in alginate hydrogels are implantable in animal models and can aid in cartilage growth [291, 292]. Additionally, hyaluronic acid hydrogels have also been tested to determine their capacity to grow cartilaginous tissue [293-295]. However, a combination of alginate and hyaluronic acid hydrogels with IGF-1 delivery as a potential cartilage construct has been minimally studied *in vivo* [296]. The limited knowledge available has led us to investigate how an initial batch delivery of IGF-1 affects an *in vivo* transplanted hydrogel construct that is composed of alginate with varied HA concentrations with embedded chondrocytes. Therefore, the objectives of this *in vivo* study were to determine how chondrocytes are influenced by HA concentration and IGF-1 delivery by observing cell proliferation as well as glycosaminoglycan, IGF-1, type II collagen, and type I collagen protein production..

6.2 Materials and Methods

6.2.1 Materials

The following items were purchased from Invitrogen (Carlsbad, CA): Dulbecco's Modified Eagle Medium: Nutrient Mixture F-12 Ham (DMEM/F12), penicillin/streptomycin, fungizone/amphotericin B, HISTOSTAIN®-SP Kit, and Liquid DAB Substrate Kit. The ascorbic-2-phosphate, bovine serum albumin, sodium bicarbonate, alginic acid sodium salt from brown algae, hyaluronic acid sodium salt from

Streptococcus equi (53747, 1.63 x 10^6 Da), and sodium cacodylate were purchased from Sigma-Aldrich (St. Louis, MO). ITS+ Universal Culture Supplement Premix was purchased from BD Biosciences (San Jose, CA). *Collagenase P* was purchased from Roche (Basel, Switzerland). The human insulin-like growth factor-1 (hIGF-1) and anti-IGF-1 was obtained from R&D Systems (Minneapolis, MN). The anti-type II collagen (ab300), anti-type I collagen (ab6308), and HRP conjugated goat secondary antibody (ab6885) were purchased from Abcam (Cambridge, MA). The Citrisolv Hybrid, Fast Green, hematoxylin, and eosin were purchased from Fisher Scientific (Pittsburgh, PA). The Safranin-O was obtained from Poly Scientific (Bay Shore, NY). The 12 mm diameter polyester membrane transwell inserts with 3 μm pore size were obtained from Corning Incorporation (Corning, NY).

6.2.2 Methods

6.2.2.1 Cartilage Extraction and Chondrocyte Isolation

Slices of cartilage were removed from the metatarsal phalangeal joints of 2-3 week old calves after 6 hours of slaughter (RanchoVeal, Petaluma, CA). The pieces were rinsed in DMEM/F12 with 50 μg/mL ascorbic-2-phosphate, 1 mg/mL bovine serum albumin, 2.6 mg/mL sodium bicarbonate, 2.5 μg/mL fungizone/amphotericin B, and 0.1% penicillin/streptomycin. Cartilage was incubated overnight in 0.2% *collagenase P* at 37 ^{o}C and then filtered through a 70 μm nylon mesh to isolate primary chondrocytes.

6.2.2.2 Chondrocyte Encapsulation and Culture

Alginate hydrogels at a 2.0% w/v concentration were made by mixing and heating alginic acid, 0.15 M sodium chloride, and 0.025 M HEPES into deionized water (pH 7.4).

Hyaluronic acid was also added to the alginate solution at three different concentrations (0, 0.5, and 5.0 mg/mL). The final alginate/hyaluronic acid solution was sterilized using a 0.22 μm syringe filter and then mixed with chondrocytes at a density of 7,000,000 cells/mL. This solution was injected at a volume of 200 μL into transwell inserts. The constructs was placed in 4 mL of 100 mM calcium chloride and then rinsed with DMEM/F12 for 30 minutes before being removed from the insert and placed in a 6 well plate with DMEM/F12 with 10% heat activated FBS (placed in 57^{o}C for 1 hour). After 3 day of culture, all the constructs was placed in DMEM/F12 with ITS+ (1:100 dilution). Each group was placed in either 0 μg hIGF-1 (-) or 5 μg hIGF-1 (+) for 24 hours before surgery.

6.2.2.3 Implantation

The work described in this study was approved by the University of Maryland College Park IACUC (#R-07-93) as well as the University of California Davis Medical Center IACUC (#13234). Male SCID mice (Charles River Laboratories, Wilmington, MA) that are 4-6 weeks old were anesthetized using Isoflurane 1-3% and the surgical site was shaven with clippers and scrubbed with Betadine solution. An incision of ~12mm was made through the full thickness of the skin on the ventral and dorsal side of the mouse. Two subcutaneous pockets were created by blunt dissection on the ventral and dorsal side of the mouse. The constructs were cut in half and were inserted into the sites as semi-circle constructs (4 total samples in each mouse). The skin was closed by sterile surgical clips. Carprofen was administered at 5 mg/mL S.C. during the procedure to eliminate any post operation pain. The mice were kept warm until recovered from

anesthesia and returned to the cage. After 7, 14, and 21 days the mice were euthanized by carbon dioxide through inhalation and the constructs were collected for analysis.

6.2.2.4 Histology

The constructs were physically stable before implantation however they broke into smaller pieces upon retrieval. All samples were fixed in 4% paraformaldehyde and 0.1 M sodium cacodylate buffer containing 10 mM $CaCl_2$ (pH 7.4) for 24 hours at 4^{o}C. The beads were washed with 0.1 M sodium cacodylate buffer with 10 mM $CaCl_2$ (pH 7.4) for 24 hours at room temperature. Afterwards, the beads were dehydrated in a series of ethanol concentrations (70-100%) with a final xylene wash. The samples were embedded in paraffin and cut into 6 μm thickness sections, which were placed onto charged microscope slides and kept at 4^{o}C until staining.

6.2.2.5 Histochemical Staining

Sections were oven dried for 2 hours at 60^{o}C, deparaffinized in Citisolv Hybrid and then rehydrated in ethanol (100% and 70%), and rinsed in distilled water. Sections were stained with Hematoxylin and Eosin (H&E) and Safranin-O (0.1%) with Fast Green (0.001%) counter stain. All samples were dehydrated, cleared in Citrisolv Hybrid, and coverslipped with mounting medium.

6.2.2.6 Immunohistochemistry

Sections were oven dried, deparaffinized, and rehydrated as described above. The following antibodies were used to stains for the presence of IGF-1, type II collagen, and type I collagen. All the primary antibodies were all diluted to 1:100. The secondary goat

antibody used for IGF-1 was diluted 1:250. A HISTOSTAIN®-SP Kit and DAB Substrate Kit was used to reveal the presence of type II collagen and type I collagen by using a hydrogen peroxidase (HRP)-strepavidin-biotin system. For IGF-1 detection, only the Liquid DAB Substrate Kit was used. All samples were counterstained with hematoxylin, dehydrated, cleared in Citrisolv Hybrid, and coverslipped with mounting medium. To show non-specific staining, samples were not incubated with the primary antibody and then incubated with the secondary antibody for each protein (negative staining control, NTC).

6.2.2.7 Histomorphometrical Analysis

For all the groups at each timepoint, sixteen randomly chosen Safranin-O/Fast Green stained images were captured using a Zeiss Axiovert 40 CFL inverted microscope (Carl Zeiss, Oberkochen, Germany). Chondrocytes were counted on each image and reported as cell count per image area. Additionally, measurements were taken of glycosaminoglycan (GAG) production as GAG area minus cell area per image area for each slide. The measurements were calculated using the SPOT Advanced software (Diagnostic Instruments Inc., Sterling Heights, MI). Figures 6.1 is a representative image of cell counting and GAG measurements.

6.2.2.8 Statistical Analysis

Data from all studies were analyzed using ANOVA and Tukey's multiple-comparison test. The means and standard deviations are reported in each figure.

6.3 Results

6.3.1 Cell Morphology, Viability, and Proliferation

Chondrocyte morphology and viability was observed from H&E stained images. For all the groups at each time point, chondrocytes maintained their rounded morphology as well as viability (Figure 6.2 is a representative image). Additionally, all the chondrocytes were uniformly distributed throughout the construct. Chondrocytes were counted from Safranin-O/Fast Green stained images (nuclei stained gray) and reported as cell count/μm^2 x 10^6 (Figure 6.3). Initially, the 0.5 mg/mL HA (-) and 5.0 mg/mL HA (-) has significantly higher cell counts compared to the rest of the groups ($p < 0.05$). By day 14, most of the samples had an increase in cell number with the highest fold increase of ~3 by the 0 mg/mL HA (-) and 5.0 mg/mL HA (+) groups from day 7. As a result these groups were found to be significantly higher in cell count from the other cases ($p < 0.05$). The number of chondrocytes decreased by 2 fold for the 0 mg/mL HA (-) and 5.0 mg/mL HA (+) groups. However, the 0.5 mg/mL HA (+) group had a 2.2-fold increase from day 14 to 21 while all the groups maintained similar cell counts. Ultimately, the 0 mg/mL HA (-) group had the lowest number of chondrocytes and the 0.5 mg/mL HA (+) group contained the highest number of chondrocytes by day 21 compared to all the groups ($p < 0.05$).

6.3.2 Glycosaminoglycan Production

Safranin-O/Fast Green stain turns glycosaminoglycan molecules into a light orange hue compared to alginate which becomes a very bright orange color [256]. For each image, the glycosaminoglycan area was measured and reported as GAG area/μm^2 x

10^3 (Figure 6.4). At day 7, all the groups did not have significantly different GAG areas ($p < 0.05$). By day 14, most of the samples increased in GAG production. The 0 mg/mL HA (-) and (+) case increased GAG area by 3 and 3.7 fold, respectively. A 1.7 and 1.8 fold increase in GAG was observed for the 0.5 mg/mL HA (-) and (+) group. The greatest GAG area was calculated for the 5.0 mg/mL HA (-) and (+) groups at day 14, which increased by 4.4 and 5.4 fold. IGF-1 did not create significant differences ffor the 5.0 mg/mL HA cases at day 14. However, the 0, 0.5, and 5.0 mg/mL HA cases were significantly different from one another ($p < 0.05$). By day 21, the 0 mg/mL HA (-) and (+) group as well as the 5.0 mg/mL HA (-) and (+) group maintained similar levels of GAG compared to their respective groups at day 14. An increase in GAG area was observed by the 0.5 mg/mL HA group by 1.9 and 2.5 fold for the (-) and (+) samples respectively. Similarly to day 14, IGF-1 did not create differences in GAG area for each group but HA concentration created variations in measured GAG area at day 21 ($p < 0.05$).

A ratio of GAG area to cell count was calculated to determine how much GAG was produced per chondrocyte in a given area (Figure 6.5). The results showed that at day 7, the 0 mg/mL HA (-) group had the highest ratio compared to the rest of the samples ($p < 0.05$). By day 14, IGF-1 did not influence the ratios for the 0, 0.5, and 5.0 mg/mL HA groups. GAG area/chondrocyte was significantly different amongst the 0, 0.5, and 5.0 mg/mL HA cases ($p < 0.05$). The highest GAG area/cell count ratio was calculated for the 5.0 mg/mL HA case ($p < 0.05$). At day 21, the 0 mg/mL HA (+) and 0.5 mg/mL HA (+) group had the lowest ratio compared to all the groups at this time point ($p < 0.05$). Throughout the study, the 0 mg/mL HA (+) and 0.5 mg/mL HA (+)

cases had similar ratio levels while all the other groups increased by either day 14 or 21. The 5.0 mg/mL HA (-) and (+) group had a 2.8 and 2 fold increase respectively from day 7 to 14 and maintained their ratio from day 14 to 21. The 0 mg/mL HA (-) and 0.5 mg/mL HA (-) samples showed ratios that had an increasing trend throughout the study.

6.3.3 Immunohistochemistry Analysis

For each group at day 21, representative immunohistochemistry stained images for IGF-1, type II collagen, and type I collagen can be seen in Figure 6.6. The presence of each protein is indicated by a brown color as a result of using DAB. IGF-1 staining was observed for all the groups. Specifically, with or without pre-culture of IGF-1, as the HA concentration increased the staining intensity decreased. When comparing the 0, 0.5, and 5.0 mg/mL HA groups individually, IGF-1 staining was less in the samples that were delivered with IGF-1 compared to the free IGF-1 samples. All the samples had a significant presence of type II collagen by 21 days and had similar amounts of type II collagen. Type I collagen staining was observed for all the samples as well. However, the staining was less intense in all the groups compared to the type II collagen stained images. The presence of type I collagen seemed to increase with HA concentration for the groups that were not cultured with exogenous IGF-1. An opposing trend is seen for the samples that are exposed to excess IGF-1; by increasing HA concentration the type I collagen staining intensity decreased.

6.4 Discussion

Hyaluronic acid is an extracellular matrix protein that is present in cartilage and therefore it has been utilized as a biomaterial for cartilage repair [294, 295, 297-300].

The ability for hyaluronic acid to interact with various components such as cells and proteins makes it an important molecule to investigate. Our previous work has shown that hyaluronic acid in an alginate hydrogel has the ability to retain IGF-1 (Figure 5.11). This allows for increased interaction between the exogenous IGF-1 with the embedded chondrocytes and was able to down-regulate the endogenous expression of IGF-1. This intriguing *in vitro* outcome led us to explore how HA and IGF-1 affect chondrocytes within a 3-D hydrogel *in vivo*.

Chondrocytes maintained their viability indicating that they were stable in the hydrogels during the 27 day *in vivo* experiment (Figure 6.2). Additionally, throughout the study chondrocytes were observed to proliferate modestly (Figure 6.3). By day 7, the 0.5 mg/mL HA and 5.0 mg/mL HA groups without IGF-1 had the highest cell counts. Indicating that HA has an affect on initial chondrocyte proliferation but its influence on the chondrocytes can be diminished by pre-culturing the samples with IGF-1. By day 14 most of the samples reached similar cell count numbers except for the 0 mg/mL HA (-) and 5.0 mg/mL HA (+) groups which were higher by at least 2-fold. When observing the changes that occurred from day 7 to 21, for most of the samples the cell counts increased by a maximum of 2-fold except for the 0.5 mg/mL HA (+) group which had a 4-fold increase. It seems that by day 21, the 0 mg/mL HA (-) group had the lowest cell count indicating hyaluronic acid and pre-culturing with IGF-1 has an impact on the overall proliferate capacity of chondrocytes *in vivo*. Since the highest cell count was observed by the 0.5 mg/mL HA (+) group, this possibly suggests that concentration of HA is a critical factor for chondrocyte proliferation.

In regards to glycosaminoglycan production, by day 14 and 21 there are considerable differences among the 0, 0.5, and 5.0 mg/mL HA groups with no variations between the (-) and (+) cases for each group (Figure 6.4). These results imply that HA has a greater impact than pre-culturing with IGF-1 has a minimal influence on overall GAG production. At the later timepoints the 5.0 mg/mL HA group had the highest GAG area. By day 21, it seems that there is a correlation between GAG area and HA concentration as seen by the increasing trend between HA concentration and GAG area. Previous works have shown that incorporation of hyaluronic acid in a construct has a positive influence on GAG production *in vivo* [298, 301]. This data further supports that HA has the abilty to control the synthesis of GAG.

When observing the cell count and GAG area for each group, it was interesting to see how much GAG area was produced per chondrocyte (Figure 6.5). At day 21, results indicate that for the 0 mg/mL HA and 0.5 mg/mL HA cases pre-culturing IGF-1 affects GAG production per chondrocyte. Additionally, the 0 and 0.5 mg/mL HA (-) cases along with the 5.0 mg/mL HA (-) and (+) samples had similar GAG areas. These observations were not noticeable in Figure 6.4. The result in Figure 6.5 indicates that in 0 mg/mL and 0.5 mg/mL HA cases, IGF-1 hinders the amount of GAG produced per chondrocyte. By pre-culturing IGF-1 to the alginate/HA constructs, the chondrocytes decreased their total GAG production. Therefore, indicating that exogenous IGF-1 delivery impacts chondrocyte GAG activity with low levels of HA in alginate hydrogels. However, by incorporating a high HA concentration of 5.0 mg/mL, IGF-1 delivery did not change GAG production per chondrocyte. This could be due to interactions that occur at high concentrations of HA with IGF-1, which could overcome the impact of IGF-1 on GAG

synthesis by chondrocytes. We speculate that at high concentrations of HA leads to increased specific (e.g., binding) interactions with IGF-1 or chondrocytes and as a result increases GAG production per chondrocyte. Therefore, we were able to observe similar levels of GAG per chondrocyte for the 5.0 mg/mL HA group regardless of IGF-1.

The initial culturing of the constructs with exogenous IGF-1 led to interesting IGF-1 immunohistochemical results (Figure 6.6). In particular, incorporating more hyaluronic acid in the alginate constructs downregulated IGF-1 production. Furthermore, the synthesis of IGF-1 was further diminished in the 0, 0.5, and 5.0 mg/mL HA cases with the introduction of exogenous IGF-1. Indicating that HA and/or pre-culturing with IGF-1 decreases endogenous IGF-1 synthesis.

All the constructs produced type II collagen as seen by the images taken at day 21 in Figure 6.6, thus showing that the chondrocytes were phenotypically stable throughout the study. Interesting trends were observed for the type I collagen images (Figure 6.6). By increasing HA concentration, chondrocytes upregulated type I collagen synthesis indicating that hyaluronic acid enables chondrocytes to maintain a fibroblastic phenotype. However by pre-incubating the samples with IGF-1, the affects of HA was reversed as seen by the decreasing type I collagen staining with increasing HA. Therefore, indicating that exogenous IGF-1 can counteract the negative affect of HA concentration on type I collagen synthesis.

The goal of this study was to show how hyaluronic acid and exogenous delivery of IGF-1 were able to influence chondrocytes embedded in alginate hydrogels *in vivo*. Chondrocytes were influenced by HA concentration, specifically without IGF-1 delivery the total glycosaminoglycan production and type I collagen staining was upregulated as

HA content increased while IGF-1 staining decreased. When the constructs were pre-cultured with IGF-1, total glycosaminoglycan content was not affected, IGF-1 synthesis decreased further, and type I collagen staining decreased. Interestingly, there were no trends observed for chondrocyte proliferation or type II collagen staining. The fact that all the samples produced considerable amounts of type II collagen by day 21 suggests that the construct properties are beneficial for maintaining chondrocyte function *in vivo*. However, the results specifically observed from this study indicated that the 5.0 mg/mL HA (+) case is the best group because of the high production of GAG with minimal type I collagen staining. Overall, this *in vivo* study clearly shows that HA concentration and IGF-1 can modify chondrocyte expression through their interactions.

6.5 Conclusions

Hyaluronic acid concentration in an alginate hydrogel can change the production of extracellular matrix proteins, such as GAGs and collagens, in an *in vivo* environment. Additionally, pre-culturing constructs with IGF-1 also affects how chondrocytes respond to HA *in vivo*. In this particular study, delivering exogenous IGF-1 along with increasing HA produced the highest GAG amounts while minimizing the production of fibroblastic type I collagen protein. Though the specifics in how HA and IGF-1 interact with one another still need to be investigated, the overall results validate the importance of balancing components in a construct and understanding how each factor influences one another *in vivo* to create a proper tissue engineering construct for articular cartilage repair.

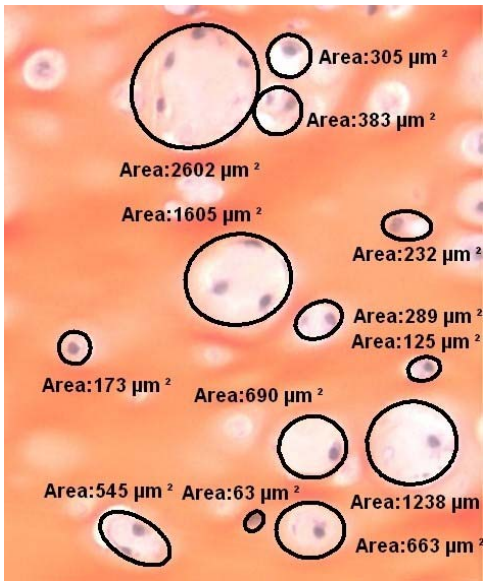

Figure 6.1. A representative image of how the glycosaminoglycan areas were measured from a Safranin-O/Fast Green stained image.

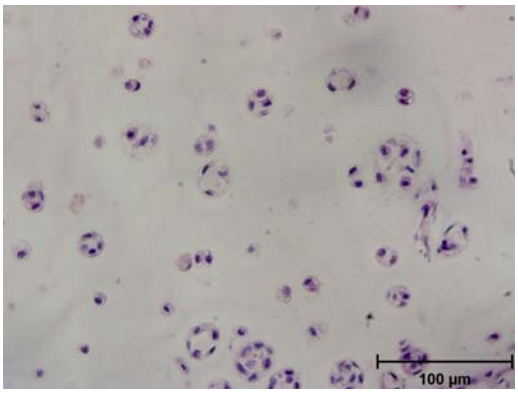

Figure 6.2. H&E image from 0 mg/mL HA group with IGF-1 pre-culture at day 21. Chondrocytes were evenly distributed in the hydrogel and maintained their viability and rounded morphology throughout the experiment.

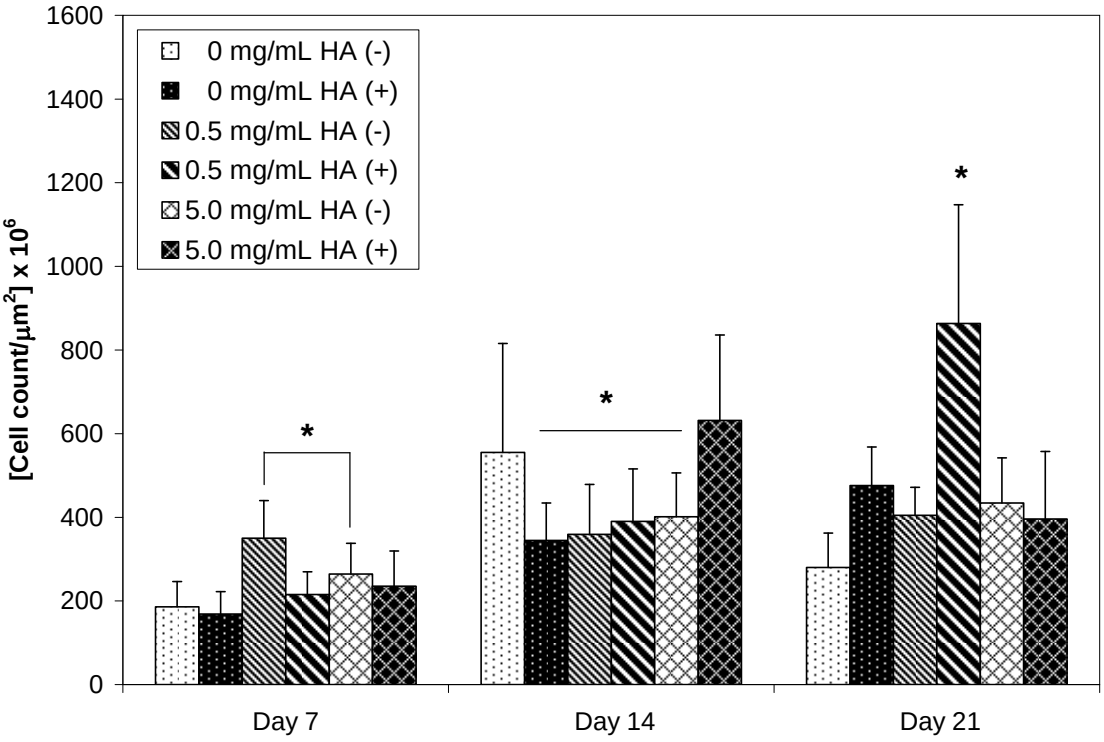

Figure 6.3. Chondrocytes were counted on Safranin-O/Fast Green stained images to determine cell proliferation throughout the study. Cell count per slide area was graphed for all the groups at day 7, 14, and 21. Chondrocytes were able to proliferate in all the cases. However by day 21, the 0.05 mg/mL HA (+) group had the greatest number of chondrocytes per area and the 0 mg/mL HA (-) group had the lowest. The means and standard deviations are reported ($n = 16$; $*$ indicates $p < 0.05$).

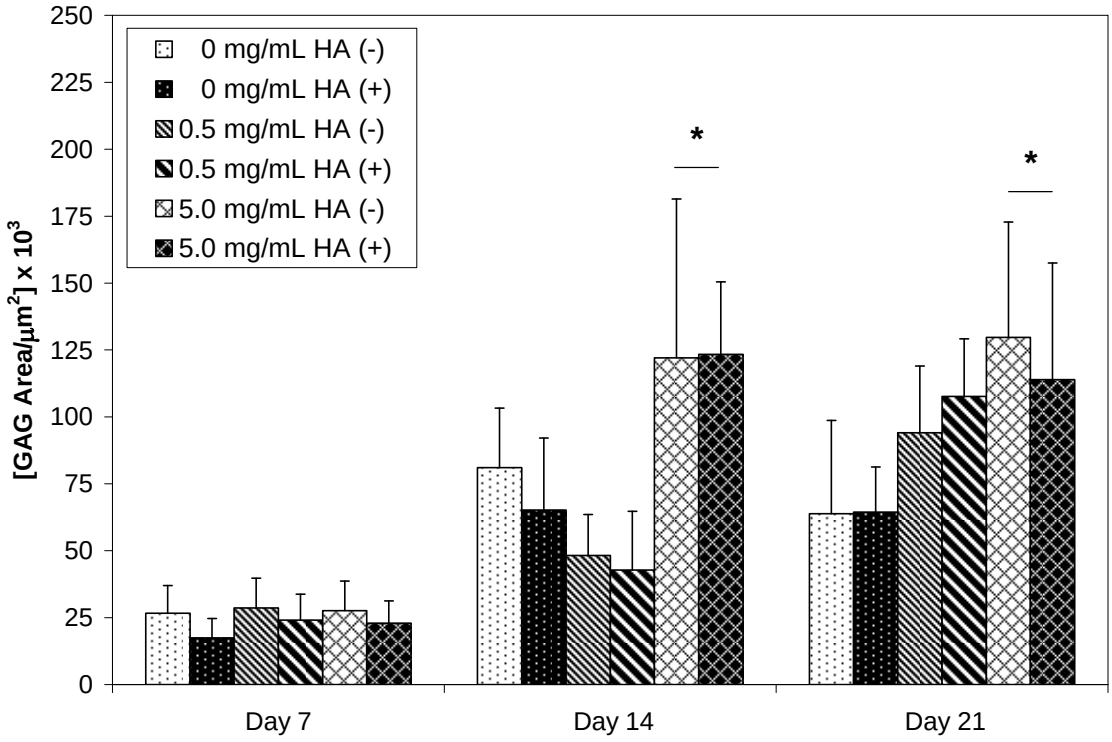

Figure 6.4. Glycosaminoglycan area was measured from Safranin-O/Fast Green stained samples. The total GAG area was calculated per slide area for each case at each timepoint. At day 21, the GAG area increased with higher HA content. The greatest GAG amount was measured in the 5.0 mg/mL HA group. The means and standard deviations are reported ($n = 16$; $*$ indicates $p < 0.05$).

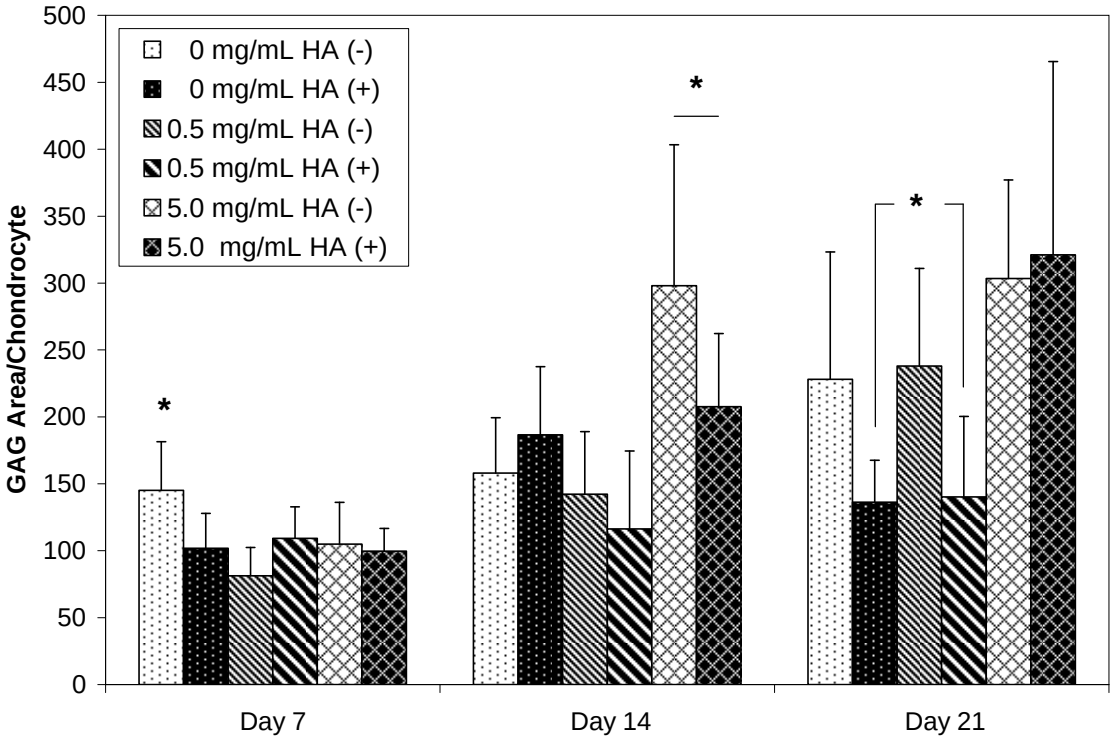

Figure 6.5. The total GAG area per cell count was calculated for each group at day 7, 14, and 21. At day 21, the GAG production per chondrocyte was lowest in the 0 mg/mL HA and 0.5 mg/mL HA groups that were pre-cultured with IGF-1 (+). The means and standard deviations are reported ($n = 16$; $*$ indicates $p < 0.05$).

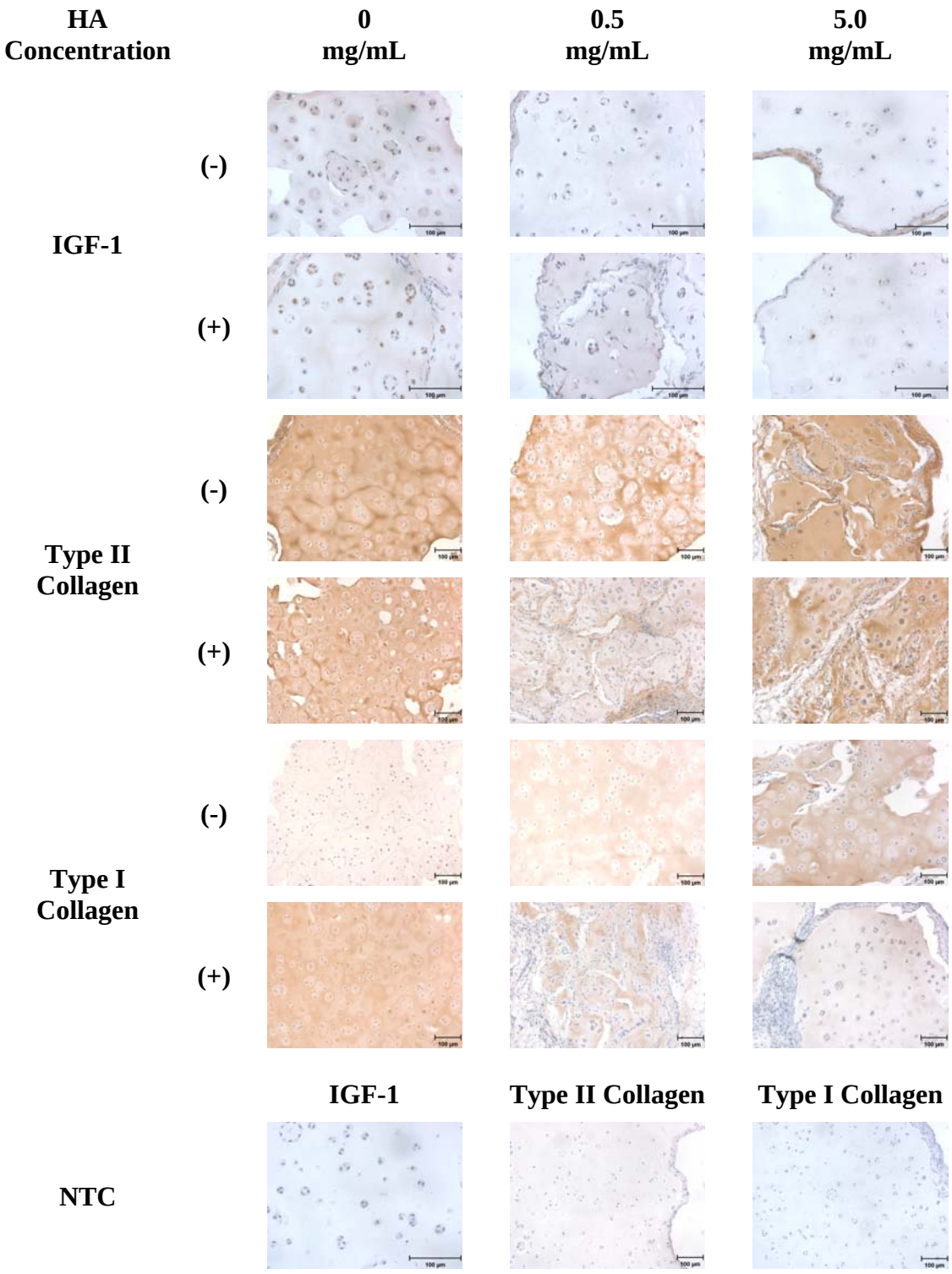

Figure 6.6. Immunohistochemical staining of IGF-1, type II collagen, and type I collagen for all the groups at day 7, 14, and 21. The 0, 0.5, and 5.0 mg/mL HA groups are all represented here, as well as the negative staining control (NTC). The scale bars are located on the bottom right hand corner for each image.

7 Summary

The poor intrinsic ability for articular cartilage to repair itself after becoming diseased or damaged has resulted in applying tissue engineering applications to aid in healing. In order to create a proper construct, chondrocyte signaling within a biomaterial needs to be fully understood. In this particular work, the overall goal was to investigate how construct properties alter IGF-1 signaling by chondrocytes *in vitro* and *in vivo*.

The first objective was to vary alginate concentration, which alters the water content of the hydrogel. Additionally, the paracrine signaling distance was modified by changing the density of chondrocytes embedded in each alginate hydrogel bead. We investigated the effects of these fabrication parameters, alginate concentration and cell density, on chondrocyte IGF-1 expression and phenotypic type II collagen expression over 8 days using quantitative reverse-transcriptase polymerase chain reaction (qRT-PCR). IGF-1 expression was greater for the 100,000 versus 25,000 cell density case, therefore showing the impact of paracrine signaling distance. At the 100,000 cell density case, IGF-1 expression was significantly altered by alginate concentration with the highest expression occurring in 2.0% w/v alginate. Type II collagen expression was observed to be the highest in the 100,000 cell density and 2.0% w/v alginate case. The results suggest that high cell density at high alginate concentration can significantly affect the endogenous IGF-1 expression as well as type II collagen expression by chondrocytes. From these findings, the 2.0% w/v alginate with 100,000 chondrocytes per bead was used as a basis for the other objectives.

The second objective was to examine the effects of IGF-1 delivery to chondrocytes embedded in a 3-D scaffold specifically the endogenous expression of the

upstream IGF-1 signaling molecules: IGF-1, IGF-1R, and IGFBP-3. The lack of amine groups on alginate hydrogels allows us to clearly investigate solely on how exogenous IGF-1 affects chondrocyte signaling. Three different IGF-1 concentrations were incubated with the chondrocytes: 0, 10, 50, and 100 ng/mL. IGF-1 delivery to the construct led to an increase in glycosaminoglycan as well as type II collagen production by 8 days. Additionally, type II collagen expression was the highest along with type I collagen expression being the lowest for chondrocytes exposed to IGF-1. IGF-1 expression was higher for chondrocytes incubated without IGF-1 compared to the IGF-1 delivered groups. This result was expected as chondrocytes are attempting to overcome the lack of IGF-1 signal by increasing their endogenous expression of IGF-1. The presence of IGF-1 led chondrocytes to express higher levels of IGF-1R, or alternatively a greater turnover rate of IGF-1R so as to potentially bind more available IGF-1. IGFBP-3 did not appear to be largely influenced by IGF-1 delivery with an observed decrease in expression. Therefore, indicating that IGF-1R is a key factor in regulating IGF-1 signaling. These results confirm the significant role of IGF-1 in chondrocyte function as endogenous expression. Interestingly, similar expression levels and protein production occurred for all the IGF-1 concentrations. Therefore, the highest IGF-1 concentration at 100 ng/mL was utilized in the following experiments.

The third objective was to investigate how an extracellular matrix protein alters IGF-1 signaling of chondrocytes embedded in an alginate hydrogel. Hyaluronic acid is a large glycosaminoglycan present in cartilage. Chondroctyes adhere to this molecule through the receptor CD44. In this particular study, varying concentrations of hyaluronic acid (0, 0.05, 0.50, and 5.00 mg/mL) were incorporated into alginate hydrogels. We have

previously determined the effects of IGF-1 delivery on chondrocyte signaling. Therefore, we investigated how hyaluronic acid affects IGF-1 delivery on chondrocyte IGF-1 signaling. IGF-1 expression was highest for alginate containing 0.50 mg/mL hyaluronic acid while the lowest was observed for the 0 mg/mL and 5.00 mg/mL hyaluronic acid cases. It seems that at low hyaluronic acid concentrations, hyaluronic acid interaction with chondrocytes results in higher endogenous IGF-1 expression. However at a high concentration of hyaluronic acid the retention of free IGF-1 molecules in alginate hydrogels was significant, which allowed for continuous interaction of IGF-1 to the chondrocytes. These results indicate that hyaluronic acid can vary the expression levels of IGF-1. Additionally, the expression of IGF-1R was also influenced by hyaluronic acid because unlike the previous study, IGF-1 and IGF-1R did not correlate in expression. IGFBP-3 expression was minimally affected by hyaluronic acid. Hyaluronic acid did not signfignicantly alter type II collagen expression. However, hyaluronic acid increased chondrocyte expression of type I collagen. The results show that incorporation of hyaluronic acid can affect how exogenous IGF-1 interacts with embedded chondrocytes in alginate hydrogel. These *in vitro* results were intriguing and therefore led us to investigate our model *in vivo*.

Finally, the fourth objective was to determine how chondrocytes are influenced by construct properties *in vivo*. Chondrocytes were embedded in 2.0% w/v alginate hydrogels with varying hyaluronic acid concentrations (0, 0.5, and 5.0 mg/mL). These constructs were delivered with or without IGF-1 (1 μg/mL) and then subcutaneously implanted in SCID mice. IGF-1 pre-culture was found to have a strong impact on how much glycosmainoglycan is produced per chondrocyte in the 0 mg/mL and 0.5 mg/mL

cases but little influence on the 5.0 mg/mL group by day 21. By incorporating more hyaluronic acid in the alginate constructs resulted in downregulation of IGF-1 production. Furthermore, the synthesis of IGF-1 was further diminished in the 0 and 0.5, and 5.0 mg/mL HA cases with the introduction of exogenous IGF-1. Therefore, indicating that pre-culturing with IGF-1 has a significant influence on endogenous IGF-1 synthesis. Chondrocytes were phenotypically stable in the all the constructs during the *in vivo* study. A decrease in type I collagen occurred as hyaluronic acid concentration increased. However by pre-incubating the samples with IGF-1, the affects of hyaluronic acid was reversed. Therefore, showing that exogenous IGF-1 can counteract the affect of HA concentration on type I collagen synthesis. These results indicate that the ideal construct would be 5.0 mg/mL hyaluronic acid with IGF-1 because of the high amounts of glycosmaminoglycan production with minimal type I collagen staining. This *in vivo* study clearly shows that HA concentration and IGF-1 content are able to counter act each other.

This work shows how construct properties are able to influence chondrocyte expression of upstream IGF-1 signaling molecules by observing how alginate concentration, cell density, exogenous IGF-1 delivery, and hyaluronic acid concentration affect endogenous IGF-1 signaling both *in vitro* and *in vivo*. Overall, in order to properly engineer articular cartilage it is important to create a balance in construct components by understanding how various factors influence one another.

8 Conclusions

Articular cartilage does not have an innate ability to repair. Unfortunately, as a result complete regeneration of damaged articular cartilage is very difficult. The most

widely used medical approach currently for small lesions is Carticel® which implants autologous chondrocytes into the defect site. Another product is NeoCart®, which is in a clinical trial phase, which utilizes autologous chondrocytes with a scaffold for implantation. These products have shown promise to minimize pain to patients and allow them to be more physically active. However, their long term affects are unclear and their ability to actually completely heal cartilage is unknown. For these reasons, engineering articular cartilage is still of relative importance and therefore research is still being continuously conducted. In order to achieve the ultimate goal of creating a construct that will be able to form into cartilage, the details of the construct must be fully understood. Therefore, in this work we investigated how various molecules influence chondrocyte expression, specifically upstream IGF-1 signaling molecules, type II collagen, and type I collagen. From the results found, it is clear that by just adding one element into a construct, there was significant variance in mRNA and protein expression levels of IGF-1, IGF-1R, type II collagen, and type I collagen. Overall, this work depicts the importance of studying how embedded chondrocytes in 3-D microenvironments express signaling molecules. We hope that future works will investigate how construct properties can further change chondrocyte endogenous signaling and function.

9 Future Works

The work that has been completed thus far opens up a numerous number of possible future studies. The intricate detail of IGF-1 signaling by chondrocytes is still under investigation and it is of great interest to tissue engineers. In this particular work we focused on how the expression of upstream IGF-1 signaling molecules changed by only altering a few construct properties. Therefore, a future goal of this project could be to determine how the constructs can be modified further to enhance chondrocyte IGF-1 signaling.

Perhaps first investigate the intracellular pathways, MAPK, PI3K, p38, and JNK, for IGF-1 more closely as well as type II collagen signaling. This can provide more details of how endogenous IGF-1 and type II collagen signaling are correlated with each other. Additionally, how construct properties specifically change IGF-1 signaling.

Another goal would be to utilize mesenchymal stem cells (MSCs). There is a tremendous amount of interest in MSCs for cartilage repair because of its ability to differentiate into chondrocytes as well as being highly proliferative, which does not seem to occur by chondrocytes. It would be interesting to determine how IGF-1 affects MSCs to differentiate into chondrocytes. Chondrocytes can be transfected with DNA plasmid that induces higher IGF-1 protein production. These chondrocytes can then be incubated with MSCs and IGF-1 signaling can be monitored at the gene and protein level by both cell types. By placing these cells in a construct, the biomaterial properties can be changed to determine how to enhance MSCs to differentiate (e.g., express type II collagen) and also increase their interaction with chondrocytes expressing IGF-1.

While the overall goal is to create a tissue engineering construct that will be able to regenerate articular cartilage, we believe that it is very important to study the basic details of cell signaling. Therefore, our current future goals are focused on how to enhance IGF-1 and type II collagen signaling in chondrocytes or MSCs so that a better construct for articular cartilage repair can be created.

10 Bibliography

1. Poole, A.R., T. Kojima, T. Yasuda, F. Mwale, M. Kobayashi, and S. Laverty, *Composition and structure of articular cartilage: a template for tissue repair.* Clin Orthop Relat Res, 2001(391 Suppl): p. S26-33.
2. Ulrich-Vinther, M., M.D. Maloney, E.M. Schwarz, R. Rosier, and R.J. O'Keefe, *Articular cartilage biology.* J Am Acad Orthop Surg, 2003. **11**(6): p. 421-30.
3. Randolph, M.A., K. Anseth, and M.J. Yaremchuk, *Tissue engineering of cartilage.* Clin Plast Surg, 2003. **30**(4): p. 519-37.
4. Newman, A.P., *Articular cartilage repair.* Am J Sports Med, 1998. **26**(2): p. 309-24.
5. Almarza, A.J. and K.A. Athanasiou, *Design characteristics for the tissue engineering of cartilaginous tissues.* Ann Biomed Eng, 2004. **32**(1): p. 2-17.
6. Woodfield, T.B., J.M. Bezemer, J.S. Pieper, C.A. van Blitterswijk, and J. Riesle, *Scaffolds for tissue engineering of cartilage.* Crit Rev Eukaryot Gene Expr, 2002. **12**(3): p. 209-36.
7. Goessler, U.R., K. Hormann, and F. Riedel, *Tissue engineering with chondrocytes and function of the extracellular matrix (Review).* Int J Mol Med, 2004. **13**(4): p. 505-13.
8. Riesle, J., A.P. Hollander, R. Langer, L.E. Freed, and G. Vunjak-Novakovic, *Collagen in tissue-engineered cartilage: types, structure, and crosslinks.* J Cell Biochem, 1998. **71**(3): p. 313-27.
9. Temenoff, J.S. and A.G. Mikos, *Review: tissue engineering for regeneration of articular cartilage.* Biomaterials, 2000. **21**(5): p. 431-40.
10. Ishida, O., Y. Tanaka, I. Morimoto, M. Takigawa, and S. Eto, *Chondrocytes are regulated by cellular adhesion through CD44 and hyaluronic acid pathway.* J Bone Miner Res, 1997. **12**(10): p. 1657-63.
11. van der Kraan, P.M., P. Buma, T. van Kuppevelt, and W.B. van den Berg, *Interaction of chondrocytes, extracellular matrix and growth factors: relevance for articular cartilage tissue engineering.* Osteoarthritis Cartilage, 2002. **10**(8): p. 631-7.
12. Holland, T.A. and A.G. Mikos, *Advances in drug delivery for articular cartilage.* J Control Release, 2003. **86**(1): p. 1-14.
13. Chubinskaya, S. and K.E. Kuettner, *Regulation of osteogenic proteins by chondrocytes.* Int J Biochem Cell Biol, 2003. **35**(9): p. 1323-40.
14. Darling, E.M. and K.A. Athanasiou, *Growth factor impact on articular cartilage subpopulations.* Cell Tissue Res, 2005: p. 1-11.
15. Hickey, D.G., S.R. Frenkel, and P.E. Di Cesare, *Clinical applications of growth factors for articular cartilage repair.* Am J Orthop, 2003. **32**(2): p. 70-6.
16. Hunter, T., *Signaling--2000 and beyond.* Cell, 2000. **100**(1): p. 113-27.
17. Martin, G.S., *Cell signaling and cancer.* Cancer Cell, 2003. **4**(3): p. 167-74.
18. Dhanasekaran, N., *Cell signaling: an overview.* Oncogene, 1998. **17**(11 Reviews): p. 1329-30.
19. Brumley, L.M. and R.B. Marchase, *Receptor synthesis and routing to the plasma membrane.* Am J Med Sci, 1991. **302**(4): p. 238-43.

20. Geiger, B., A. Bershadsky, R. Pankov, and K.M. Yamada, *Transmembrane crosstalk between the extracellular matrix--cytoskeleton crosstalk.* Nat Rev Mol Cell Biol, 2001. **2**(11): p. 793-805.
21. Lotz, M., *Cytokines in cartilage injury and repair.* Clin Orthop Relat Res, 2001(391 Suppl): p. S108-15.
22. Hering, T.M., *Regulation of chondrocyte gene expression.* Front Biosci, 1999. **4**: p. D743-61.
23. Lee, J.W., W.N. Qi, and S.P. Scully, *The involvement of beta1 integrin in the modulation by collagen of chondrocyte-response to transforming growth factor-beta1*. J Orthop Res, 2002. **20**(1): p. 66-75.
24. Loeser, R.F., *Integrins and cell signaling in chondrocytes.* Biorheology, 2002. **39**(1-2): p. 119-24.
25. Loeser, R.F., C.S. Carlson, and M.P. McGee, *Expression of beta 1 integrins by cultured articular chondrocytes and in osteoarthritic cartilage.* Exp Cell Res, 1995. **217**(2): p. 248-57.
26. Glowacki, J., E. Trepman, and J. Folkman, *Cell shape and phenotypic expression in chondrocytes.* Proc Soc Exp Biol Med, 1983. **172**(1): p. 93-8.
27. Salter, D.M., D.E. Hughes, R. Simpson, and D.L. Gardner, *Integrin expression by human articular chondrocytes.* Br J Rheumatol, 1992. **31**(4): p. 231-4.
28. Enomoto, M., P.S. Leboy, A.S. Menko, and D. Boettiger, *Beta 1 integrins mediate chondrocyte interaction with type I collagen, type II collagen, and fibronectin.* Exp Cell Res, 1993. **205**(2): p. 276-85.
29. Kurtis, M.S., B.P. Tu, O.A. Gaya, J. Mollenhauer, W. Knudson, R.F. Loeser, C.B. Knudson, and R.L. Sah, *Mechanisms of chondrocyte adhesion to cartilage: role of beta1-integrins, CD44, and annexin V.* J Orthop Res, 2001. **19**(6): p. 1122-30.
30. Cao, L., V. Lee, M.E. Adams, C. Kiani, Y. Zhang, W. Hu, and B.B. Yang, *beta-Integrin-collagen interaction reduces chondrocyte apoptosis.* Matrix Biol, 1999. **18**(4): p. 343-55.
31. Shakibaei, M., T. John, P. De Souza, R. Rahmanzadeh, and H.J. Merker, *Signal transduction by beta1 integrin receptors in human chondrocytes in vitro: collaboration with the insulin-like growth factor-I receptor.* Biochem J, 1999. **342 Pt 3**: p. 615-23.
32. Curtis, A.J., C.K. Ng, C.J. Handley, and H.C. Robinson, *Effect of insulin-like growth factor-I on the synthesis and distribution of link protein and hyaluronan in explant cultures of articular cartilage.* Biochim Biophys Acta, 1992. **1135**(3): p. 309-17.
33. Blunk, T., A.L. Sieminski, K.J. Gooch, D.L. Courter, A.P. Hollander, A.M. Nahir, R. Langer, G. Vunjak-Novakovic, and L.E. Freed, *Differential effects of growth factors on tissue-engineered cartilage.* Tissue Eng, 2002. **8**(1): p. 73-84.
34. Bhakta, N.R., A.M. Garcia, E.H. Frank, A.J. Grodzinsky, and T.I. Morales, *The insulin-like growth factors (IGFs) I and II bind to articular cartilage via the IGF-binding proteins.* J Biol Chem, 2000. **275**(8): p. 5860-6.
35. Wang, J., D. Elewaut, E.M. Veys, and G. Verbruggen, *Insulin-like growth factor 1-induced interleukin-1 receptor II overrides the activity of interleukin-1 and controls the homeostasis of the extracellular matrix of cartilage.* Arthritis Rheum, 2003. **48**(5): p. 1281-91.

36. Morales, T.I., *The role and content of endogenous insulin-like growth factor-binding proteins in bovine articular cartilage.* Arch Biochem Biophys, 1997. **343**(2): p. 164-72.
37. Claeys, I., G. Simonet, J. Poels, T. Van Loy, L. Vercammen, A. De Loof, and J. Vanden Broeck, *Insulin-related peptides and their conserved signal transduction pathway.* Peptides, 2002. **23**(4): p. 807-16.
38. Bunn, R.C. and J.L. Fowlkes, *Insulin-like growth factor binding protein proteolysis.* Trends Endocrinol Metab, 2003. **14**(4): p. 176-81.
39. Dupont, J., S.E. Dunn, J.C. Barrett, and D. LeRoith, *Microarray analysis and identification of novel molecules involved in insulin-like growth factor-1 receptor signaling and gene expression.* Recent Prog Horm Res, 2003. **58**: p. 325-42.
40. Dupont, J. and M. Holzenberger, *Biology of insulin-like growth factors in development.* Birth Defects Res C Embryo Today, 2003. **69**(4): p. 257-71.
41. Nakajima, H., T. Goto, O. Horikawa, T. Kikuchi, and M. Shinmei, *Characterization of the cells in the repair tissue of full-thickness articular cartilage defects.* Histochem Cell Biol, 1998. **109**(4): p. 331-8.
42. Jones, J.I. and D.R. Clemmons, *Insulin-like growth factors and their binding proteins: biological actions.* Endocr Rev, 1995. **16**(1): p. 3-34.
43. Matsumoto, T., S.E. Gargosky, K. Iwasaki, and R.G. Rosenfeld, *Identification and characterization of insulin-like growth factors (IGFs), IGF-binding proteins (IGFBPs), and IGFBP proteases in human synovial fluid.* J Clin Endocrinol Metab, 1996. **81**(1): p. 150-5.
44. Clemmons, D.R., *IGF binding proteins: regulation of cellular actions.* Growth Regul, 1992. **2**(2): p. 80-7.
45. Morales, T.I., *The insulin-like growth factor binding proteins in uncultured human cartilage: increases in insulin-like growth factor binding protein 3 during osteoarthritis.* Arthritis Rheum, 2002. **46**(9): p. 2358-67.
46. Malemud, C.J., *Cytokines as therapeutic targets for osteoarthritis.* BioDrugs, 2004. **18**(1): p. 23-35.
47. Miyazawa, K., M. Shinozaki, T. Hara, T. Furuya, and K. Miyazono, *Two major Smad pathways in TGF-beta superfamily signalling.* Genes Cells, 2002. **7**(12): p. 1191-204.
48. Zimmerman, C.M. and R.W. Padgett, *Transforming growth factor beta signaling mediators and modulators.* Gene, 2000. **249**(1-2): p. 17-30.
49. Heldin, C.H., K. Miyazono, and P. ten Dijke, *TGF-beta signalling from cell membrane to nucleus through SMAD proteins.* Nature, 1997. **390**(6659): p. 465-71.
50. Balemans, W. and W. Van Hul, *Extracellular regulation of BMP signaling in vertebrates: a cocktail of modulators.* Dev Biol, 2002. **250**(2): p. 231-50.
51. Reddi, A.H., *Bone morphogenetic proteins: from basic science to clinical applications.* J Bone Joint Surg Am, 2001. **83-A Suppl 1**(Pt 1): p. S1-6.
52. Reddi, A.H., *Interplay between bone morphogenetic proteins and cognate binding proteins in bone and cartilage development: noggin, chordin and DAN.* Arthritis Res, 2001. **3**(1): p. 1-5.
53. Miyazono, K., *Positive and negative regulation of TGF-beta signaling.* J Cell Sci, 2000. **113 (Pt 7)**: p. 1101-9.

54. Miyazono, K., K. Kusanagi, and H. Inoue, *Divergence and convergence of TGF-beta/BMP signaling.* J Cell Physiol, 2001. **187**(3): p. 265-76.
55. Li, T.F., R.J. O'Keefe, and D. Chen, *TGF-beta signaling in chondrocytes.* Front Biosci, 2005. **10**: p. 681-8.
56. van Beuningen, H.M., P.M. van der Kraan, O.J. Arntz, and W.B. van den Berg, *Protection from interleukin 1 induced destruction of articular cartilage by transforming growth factor beta: studies in anatomically intact cartilage in vitro and in vivo.* Ann Rheum Dis, 1993. **52**(3): p. 185-91.
57. Qi, W.N. and S.P. Scully, *Effect of type II collagen in chondrocyte response to TGF-beta 1 regulation.* Exp Cell Res, 1998. **241**(1): p. 142-50.
58. Pedrozo, H.A., Z. Schwartz, R. Gomez, A. Ornoy, W. Xin-Sheng, S.L. Dallas, L.F. Bonewald, D.D. Dean, and B.D. Boyan, *Growth plate chondrocytes store latent transforming growth factor (TGF)-beta 1 in their matrix through latent TGF-beta 1 binding protein-1.* J Cell Physiol, 1998. **177**(2): p. 343-54.
59. Hynes, R.O., *Cell adhesion: old and new questions.* Trends Cell Biol, 1999. **9**(12): p. M33-7.
60. Morales, T.I., *Transforming growth factor-beta 1 stimulates synthesis of proteoglycan aggregates in calf articular cartilage organ cultures.* Arch Biochem Biophys, 1991. **286**(1): p. 99-106.
61. Guerne, P.A., A. Sublet, and M. Lotz, *Growth factor responsiveness of human articular chondrocytes: distinct profiles in primary chondrocytes, subcultured chondrocytes, and fibroblasts.* J Cell Physiol, 1994. **158**(3): p. 476-84.
62. Bitzer, M., G. von Gersdorff, D. Liang, A. Dominguez-Rosales, A.A. Beg, M. Rojkind, and E.P. Bottinger, *A mechanism of suppression of TGF-beta/SMAD signaling by NF-kappa B/RelA.* Genes Dev, 2000. **14**(2): p. 187-97.
63. Schneiderbauer, M.M., C.M. Dutton, and S.P. Scully, *Signaling "cross-talk" between TGF-beta1 and ECM signals in chondrocytic cells.* Cell Signal, 2004. **16**(10): p. 1133-40.
64. Cook, S.D., R.L. Barrack, L.P. Patron, and S.L. Salkeld, *Osteogenic protein-1 in knee arthritis and arthroplasty.* Clin Orthop Relat Res, 2004(428): p. 140-5.
65. Luyten, F.P., Y.M. Yu, M. Yanagishita, S. Vukicevic, R.G. Hammonds, and A.H. Reddi, *Natural bovine osteogenin and recombinant human bone morphogenetic protein-2B are equipotent in the maintenance of proteoglycans in bovine articular cartilage explant cultures.* J Biol Chem, 1992. **267**(6): p. 3691-5.
66. Reddi, A.H., *Morphogenesis and tissue engineering of bone and cartilage: inductive signals, stem cells, and biomimetic biomaterials.* Tissue Eng, 2000. **6**(4): p. 351-9.
67. Brunet, L.J., J.A. McMahon, A.P. McMahon, and R.M. Harland, *Noggin, cartilage morphogenesis, and joint formation in the mammalian skeleton.* Science, 1998. **280**(5368): p. 1455-7.
68. Frenkel, S.R., P.B. Saadeh, B.J. Mehrara, G.S. Chin, D.S. Steinbrech, B. Brent, G.K. Gittes, and M.T. Longaker, *Transforming growth factor beta superfamily members: role in cartilage modeling.* Plast Reconstr Surg, 2000. **105**(3): p. 980-90.
69. Nishida, Y., C.B. Knudson, K.E. Kuettner, and W. Knudson, *Osteogenic protein-1 promotes the synthesis and retention of extracellular matrix within bovine*

articular cartilage and chondrocyte cultures. Osteoarthritis Cartilage, 2000. **8**(2): p. 127-36.
70. Vinall, R.L., S.H. Lo, and A.H. Reddi, *Regulation of articular chondrocyte phenotype by bone morphogenetic protein 7, interleukin 1, and cellular context is dependent on the cytoskeleton.* Exp Cell Res, 2002. **272**(1): p. 32-44.
71. Lietman, S.A., M. Yanagishita, T.K. Sampath, and A.H. Reddi, *Stimulation of proteoglycan synthesis in explants of porcine articular cartilage by recombinant osteogenic protein-1 (bone morphogenetic protein-7).* J Bone Joint Surg Am, 1997. **79**(8): p. 1132-7.
72. Heldin, C.H., *Platelet-derived growth factor--an introduction.* Cytokine Growth Factor Rev, 2004. **15**(4): p. 195-6.
73. Betsholtz, C., *Biology of platelet-derived growth factors in development.* Birth Defects Res C Embryo Today, 2003. **69**(4): p. 272-85.
74. Schafer, S.J., F.P. Luyten, M. Yanagishita, and A.H. Reddi, *Proteoglycan metabolism is age related and modulated by isoforms of platelet-derived growth factor in bovine articular cartilage explant cultures.* Arch Biochem Biophys, 1993. **302**(2): p. 431-8.
75. Harvey, A.K., S.T. Stack, and S. Chandrasekhar, *Differential modulation of degradative and repair responses of interleukin-1-treated chondrocytes by platelet-derived growth factor.* Biochem J, 1993. **292 (Pt 1)**: p. 129-36.
76. Sah, R.L., A.C. Chen, A.J. Grodzinsky, and S.B. Trippel, *Differential effects of bFGF and IGF-I on matrix metabolism in calf and adult bovine cartilage explants.* Arch Biochem Biophys, 1994. **308**(1): p. 137-47.
77. Chin, J.E., C.A. Hatfield, R.F. Krzesicki, and W.F. Herblin, *Interactions between interleukin-1 and basic fibroblast growth factor on articular chondrocytes. Effects on cell growth, prostanoid production, and receptor modulation.* Arthritis Rheum, 1991. **34**(3): p. 314-24.
78. Klooster, A.R. and S.M. Bernier, *Tumor necrosis factor alpha and epidermal growth factor act additively to inhibit matrix gene expression by chondrocyte.* Arthritis Res Ther, 2005. **7**(1): p. R127-38.
79. Huh, Y.H., S.H. Kim, S.J. Kim, and J.S. Chun, *Differentiation status-dependent regulation of cyclooxygenase-2 expression and prostaglandin E2 production by epidermal growth factor via mitogen-activated protein kinase in articular chondrocytes.* J Biol Chem, 2003. **278**(11): p. 9691-7.
80. Enomoto, H., I. Inoki, K. Komiya, T. Shiomi, E. Ikeda, K. Obata, H. Matsumoto, Y. Toyama, and Y. Okada, *Vascular endothelial growth factor isoforms and their receptors are expressed in human osteoarthritic cartilage.* Am J Pathol, 2003. **162**(1): p. 171-81.
81. Pufe, T., W. Petersen, B. Tillmann, and R. Mentlein, *The splice variants VEGF121 and VEGF189 of the angiogenic peptide vascular endothelial growth factor are expressed in osteoarthritic cartilage.* Arthritis Rheum, 2001. **44**(5): p. 1082-8.
82. Neufeld, G., T. Cohen, S. Gengrinovitch, and Z. Poltorak, *Vascular endothelial growth factor (VEGF) and its receptors.* Faseb J, 1999. **13**(1): p. 9-22.

83. Pulsatelli, L., P. Dolzani, T. Silvestri, L. Frizziero, A. Facchini, and R. Meliconi, *Vascular endothelial growth factor activities on osteoarthritic chondrocytes.* Clin Exp Rheumatol, 2005. **23**(4): p. 487-93.
84. Pfander, D., T. Cramer, G. Weseloh, O. Pullig, D. Schuppan, M. Bauer, and B. Swoboda, *Hepatocyte growth factor in human osteoarthritic cartilage.* Osteoarthritis Cartilage, 1999. **7**(6): p. 548-59.
85. Moo, V., J. Sieper, V. Herzog, and B.M. Muller, *Regulation of expression of cytokines and growth factors in osteoarthritic cartilage explants.* Clin Rheumatol, 2001. **20**(5): p. 353-8.
86. Attur, M.G., M. Dave, M. Akamatsu, M. Katoh, and A.R. Amin, *Osteoarthritis or osteoarthrosis: the definition of inflammation becomes a semantic issue in the genomic era of molecular medicine.* Osteoarthritis Cartilage, 2002. **10**(1): p. 1-4.
87. Pfander, D., N. Heinz, P. Rothe, H.D. Carl, and B. Swoboda, *Tenascin and aggrecan expression by articular chondrocytes is influenced by interleukin 1beta: a possible explanation for the changes in matrix synthesis during osteoarthritis.* Ann Rheum Dis, 2004. **63**(3): p. 240-4.
88. Stabellini, G., M. De Mattei, C. Calastrini, N. Gagliano, C. Moscheni, M. Pasello, A. Pellati, C. Bellucci, and M. Gioia, *Effects of interleukin-1beta on chondroblast viability and extracellular matrix changes in bovine articular cartilage explants.* Biomed Pharmacother, 2003. **57**(7): p. 314-9.
89. Vosshenrich, C.A. and J.P. Di Santo, *Interleukin signaling.* Curr Biol, 2002. **12**(22): p. R760-3.
90. Legendre, F., J. Dudhia, J.P. Pujol, and P. Bogdanowicz, *JAK/STAT but not ERK1/ERK2 pathway mediates interleukin (IL)-6/soluble IL-6R down-regulation of Type II collagen, aggrecan core, and link protein transcription in articular chondrocytes. Association with a down-regulation of SOX9 expression.* J Biol Chem, 2003. **278**(5): p. 2903-12.
91. Blanco, F.J., R.L. Ochs, H. Schwarz, and M. Lotz, *Chondrocyte apoptosis induced by nitric oxide.* Am J Pathol, 1995. **146**(1): p. 75-85.
92. Olee, T., S. Hashimoto, J. Quach, and M. Lotz, *IL-18 is produced by articular chondrocytes and induces proinflammatory and catabolic responses.* J Immunol, 1999. **162**(2): p. 1096-100.
93. Seguin, C.A. and S.M. Bernier, *TNFalpha suppresses link protein and type II collagen expression in chondrocytes: Role of MEK1/2 and NF-kappaB signaling pathways.* J Cell Physiol, 2003. **197**(3): p. 356-69.
94. Malemud, C.J., *Fundamental pathways in osteoarthritis: an overview.* Front Biosci, 1999. **4**: p. D659-61.
95. Wajant, H., K. Pfizenmaier, and P. Scheurich, *Tumor necrosis factor signaling.* Cell Death Differ, 2003. **10**(1): p. 45-65.
96. Baud, V. and M. Karin, *Signal transduction by tumor necrosis factor and its relatives.* Trends Cell Biol, 2001. **11**(9): p. 372-7.
97. Scherle, P.A., M.A. Pratta, W.S. Feeser, E.J. Tancula, and E.C. Arner, *The effects of IL-1 on mitogen-activated protein kinases in rabbit articular chondrocytes.* Biochem Biophys Res Commun, 1997. **230**(3): p. 573-7.
98. Olney, R.C., D.M. Wilson, M. Mohtai, P.J. Fielder, and R.L. Smith, *Interleukin-1 and tumor necrosis factor-alpha increase insulin-like growth factor-binding*

protein-3 (IGFBP-3) production and IGFBP-3 protease activity in human articular chondrocytes. J Endocrinol, 1995. **146**(2): p. 279-86.
99. Hoffman, A.S., *Hydrogels for biomedical applications.* Adv Drug Deliv Rev, 2002. **54**(1): p. 3-12.
100. Lee, K.Y. and D.J. Mooney, *Hydrogels for tissue engineering.* Chem Rev, 2001. **101**(7): p. 1869-79.
101. Gutowska, A., B. Jeong, and M. Jasionowski, *Injectable gels for tissue engineering.* Anat Rec, 2001. **263**(4): p. 342-9.
102. Benya, P.D. and J.D. Shaffer, *Dedifferentiated chondrocytes reexpress the differentiated collagen phenotype when cultured in agarose gels.* Cell, 1982. **30**(1): p. 215-24.
103. Elisseeff, J.H., A. Lee, H.K. Kleinman, and Y. Yamada, *Biological response of chondrocytes to hydrogels.* Ann N Y Acad Sci, 2002. **961**: p. 118-22.
104. Alsberg, E., K.W. Anderson, A. Albeiruti, J.A. Rowley, and D.J. Mooney, *Engineering growing tissues.* Proc Natl Acad Sci U S A, 2002. **99**(19): p. 12025-30.
105. Grunder, T., C. Gaissmaier, J. Fritz, R. Stoop, P. Hortschansky, J. Mollenhauer, and W.K. Aicher, *Bone morphogenetic protein (BMP)-2 enhances the expression of type II collagen and aggrecan in chondrocytes embedded in alginate beads.* Osteoarthritis Cartilage, 2004. **12**(7): p. 559-67.
106. Chubinskaya, S., K. Huch, M. Schulze, L. Otten, M.B. Aydelotte, and A.A. Cole, *Gene expression by human articular chondrocytes cultured in alginate beads.* J Histochem Cytochem, 2001. **49**(10): p. 1211-20.
107. Starkman, B.G., J.D. Cravero, M. Delcarlo, and R.F. Loeser, *IGF-I stimulation of proteoglycan synthesis by chondrocytes requires activation of the PI 3-kinase pathway but not ERK MAPK.* Biochem J, 2005. **389**(Pt 3): p. 723-9.
108. Almqvist, K.F., L. Wang, J. Wang, D. Baeten, M. Cornelissen, R. Verdonk, E.M. Veys, and G. Verbruggen, *Culture of chondrocytes in alginate surrounded by fibrin gel: characteristics of the cells over a period of eight weeks.* Ann Rheum Dis, 2001. **60**(8): p. 781-90.
109. Perka, C., R.S. Spitzer, K. Lindenhayn, M. Sittinger, and O. Schultz, *Matrix-mixed culture: new methodology for chondrocyte culture and preparation of cartilage transplants.* J Biomed Mater Res, 2000. **49**(3): p. 305-11.
110. Qi, W.N. and S.P. Scully, *Type II collagen modulates the composition of extracellular matrix synthesized by articular chondrocytes.* J Orthop Res, 2003. **21**(2): p. 282-9.
111. Flechtenmacher, J., K. Huch, E.J. Thonar, J.A. Mollenhauer, S.R. Davies, T.M. Schmid, W. Puhl, T.K. Sampath, M.B. Aydelotte, and K.E. Kuettner, *Recombinant human osteogenic protein 1 is a potent stimulator of the synthesis of cartilage proteoglycans and collagens by human articular chondrocytes.* Arthritis Rheum, 1996. **39**(11): p. 1896-904.
112. Clancy, R.M., J. Rediske, X. Tang, N. Nijher, S. Frenkel, M. Philips, and S.B. Abramson, *Outside-in signaling in the chondrocyte. Nitric oxide disrupts fibronectin-induced assembly of a subplasmalemmal actin/rho A/focal adhesion kinase signaling complex.* J Clin Invest, 1997. **100**(7): p. 1789-96.

113. Girotto, D., S. Urbani, P. Brun, D. Renier, R. Barbucci, and G. Abatangelo, *Tissue-specific gene expression in chondrocytes grown on three-dimensional hyaluronic acid scaffolds.* Biomaterials, 2003. **24**(19): p. 3265-75.
114. Miralles, G., R. Baudoin, D. Dumas, D. Baptiste, P. Hubert, J.F. Stoltz, E. Dellacherie, D. Mainard, P. Netter, and E. Payan, *Sodium alginate sponges with or without sodium hyaluronate: in vitro engineering of cartilage.* J Biomed Mater Res, 2001. **57**(2): p. 268-78.
115. Elisseeff, J., W. McIntosh, K. Fu, B.T. Blunk, and R. Langer, *Controlled-release of IGF-I and TGF-beta1 in a photopolymerizing hydrogel for cartilage tissue engineering.* J Orthop Res, 2001. **19**(6): p. 1098-104.
116. Fisher, J.P., S. Jo, A.G. Mikos, and A.H. Reddi, *Thermoreversible hydrogel scaffolds for articular cartilage engineering.* J Biomed Mater Res A, 2004. **71**(2): p. 268-74.
117. Park, Y., M.P. Lutolf, J.A. Hubbell, E.B. Hunziker, and M. Wong, *Bovine primary chondrocyte culture in synthetic matrix metalloproteinase-sensitive poly(ethylene glycol)-based hydrogels as a scaffold for cartilage repair.* Tissue Eng, 2004. **10**(3-4): p. 515-22.
118. Langer, R., *Tissue engineering.* Mol Ther, 2000. **1**(1): p. 12-5.
119. Bonassar, L.J. and C.A. Vacanti, *Tissue engineering: the first decade and beyond.* J Cell Biochem Suppl, 1998. **30-31**: p. 297-303.
120. Hutmacher, D.W., *Scaffold design and fabrication technologies for engineering tissues--state of the art and future perspectives.* J Biomater Sci Polym Ed, 2001. **12**(1): p. 107-24.
121. Lee, K.Y. and D.J. Mooney, *Hydrogels for tissue engineering.* Chemical Reviews, 2001. **101**(7): p. 1869-1879.
122. Vinall, R.L., S.H. Lo, and A.H. Reddi, *Regulation of articular chondrocyte phenotype by bone morphogenetic protein 7, interleukin 1, and cellular context is dependent on the cytoskeleton.* Experimental Cell Research, 2002. **272**(1): p. 32-44.
123. Hung, C.T., E.G. Lima, R.L. Mauck, E. Taki, M.A. LeRoux, H.H. Lu, R.G. Stark, X.E. Guo, and G.A. Ateshian, *Anatomically shaped osteochondral constructs for articular cartilage repair.* Journal of Biomechanics, 2003. **36**(12): p. 1853-1864.
124. Rahfoth, B., J. Weisser, F. Sternkopf, T. Aigner, K. von der Mark, and R. Brauer, *Transplantation of allograft chondrocytes embedded in agarose gel into cartilage defects of rabbits.* Osteoarthritis Cartilage, 1998. **6**(1): p. 50-65.
125. Seal, B.L., T.C. Otero, and A. Panitch, *Polymeric biomaterials for tissue and organ regeneration.* Materials Science & Engineering R-Reports, 2001. **34**(4-5): p. 147-230.
126. Dillon, G.P., X. Yu, A. Sridharan, J.P. Ranieri, and R.V. Bellamkonda, *The influence of physical structure and charge on neurite extension in a 3D hydrogel scaffold.* J Biomater Sci Polym Ed, 1998. **9**(10): p. 1049-69.
127. Wang, L., R.M. Shelton, P.R. Cooper, M. Lawson, J.T. Triffitt, and J.E. Barralet, *Evaluation of sodium alginate for bone marrow cell tissue engineering.* Biomaterials, 2003. **24**(20): p. 3475-81.
128. Davis, T.A., B. Volesky, and A. Mucci, *A review of the biochemistry of heavy metal biosorption by brown algae.* Water Res, 2003. **37**(18): p. 4311-30.

129. Rowley, J.A., G. Madlambayan, and D.J. Mooney, *Alginate hydrogels as synthetic extracellular matrix materials.* Biomaterials, 1999. **20**(1): p. 45-53.
130. Hoffman, A.S., *Hydrogels for biomedical applications.* Advanced Drug Delivery Reviews, 2002. **54**(1): p. 3-12.
131. Shapiro, L. and S. Cohen, *Novel alginate sponges for cell culture and transplantation.* Biomaterials, 1997. **18**(8): p. 583-90.
132. Guo, J.F., G.W. Jourdian, and D.K. MacCallum, *Culture and growth characteristics of chondrocytes encapsulated in alginate beads.* Connect Tissue Res, 1989. **19**(2-4): p. 277-97.
133. Pariente, J.L., B.S. Kim, and A. Atala, *In vitro biocompatibility evaluation of naturally derived and synthetic biomaterials using normal human bladder smooth muscle cells.* Journal of Urology, 2002. **167**(4): p. 1867-1871.
134. Shimizu, T., M. Yamato, A. Kikuchi, and T. Okano, *Cell sheet engineering for myocardial tissue reconstruction.* Biomaterials, 2003. **24**(13): p. 2309-16.
135. Liu, H., Y.W. Lee, and M.F. Dean, *Re-expression of differentiated proteoglycan phenotype by dedifferentiated human chondrocytes during culture in alginate beads.* Biochim Biophys Acta, 1998. **1425**(3): p. 505-15.
136. Glicklis, R., L. Shapiro, R. Agbaria, J.C. Merchuk, and S. Cohen, *Hepatocyte behavior within three-dimensional porous alginate scaffolds.* Biotechnol Bioeng, 2000. **67**(3): p. 344-53.
137. Mosahebi, A., M. Simon, M. Wiberg, and G. Terenghi, *A novel use of alginate hydrogel as Schwann cell matrix.* Tissue Eng, 2001. **7**(5): p. 525-34.
138. Leach, J.B., K.A. Bivens, C.W. Patrick, and C.E. Schmidt, *Photocrosslinked hyaluronic acid hydrogels: Natural, biodegradable tissue engineering scaffolds.* Biotechnology and Bioengineering, 2003. **82**(5): p. 578-589.
139. Hayashi, T., *Biodegradable Polymers for Biomedical Uses.* Progress in Polymer Science, 1994. **19**(4): p. 663-702.
140. Aigner, J., J. Tegeler, P. Hutzler, D. Campoccia, A. Pavesio, C. Hammer, E. Kastenbauer, and A. Naumann, *Cartilage tissue engineering with novel nonwoven structured biomaterial based on hyaluronic acid benzyl ester.* Journal of Biomedical Materials Research, 1998. **42**(2): p. 172-181.
141. Halbleib, M., T. Skurk, C. de Luca, D. von Heimburg, and H. Hauner, *Tissue engineering of white adipose tissue using hyaluronic acid-based scaffolds. I: in vitro differentiation of human adipocyte precursor cells on scaffolds.* Biomaterials, 2003. **24**(18): p. 3125-3132.
142. VandeVord, P.J., H.W.T. Matthew, S.P. DeSilva, L. Mayton, B. Wu, and P.H. Wooley, *Evaluation of the biocompatibility of a chitosan scaffold in mice.* Journal of Biomedical Materials Research, 2002. **59**(3): p. 585-590.
143. Suh, J.K.F. and H.W.T. Matthew, *Application of chitosan-based polysaccharide biomaterials in cartilage tissue engineering: a review.* Biomaterials, 2000. **21**(24): p. 2589-2598.
144. Li, J., J. Pan, L. Zhang, X. Guo, and Y. Yu, *Culture of primary rat hepatocytes within porous chitosan scaffolds.* J Biomed Mater Res, 2003. **67A**(3): p. 938-43.
145. Kawase, M., N. Michibayashi, Y. Nakashima, N. Kurikawa, K. Yagi, and T. Mizoguchi, *Application of glutaraldehyde-crosslinked chitosan as a scaffold for hepatocyte attachment.* Biol Pharm Bull, 1997. **20**(6): p. 708-10.

146. Seol, Y.J., J.Y. Lee, Y.J. Park, Y.M. Lee, Y. Ku, I.C. Rhyu, S.J. Lee, S.B. Han, and C.P. Chung, *Chitosan sponges as tissue engineering scaffolds for bone formation.* Biotechnol Lett, 2004. **26**(13): p. 1037-1041.
147. Nettles, D.L., S.H. Elder, and J.A. Gilbert, *Potential Use of Chitosan as a Cell Scaffold Material for Cartilage Tissue Engineering.* Tissue Eng, 2002. **8**(6): p. 1009-1016.
148. Lee, C.H., A. Singla, and Y. Lee, *Biomedical applications of collagen.* Int J Pharm, 2001. **221**(1-2): p. 1-22.
149. Drury, J.L. and D.J. Mooney, *Hydrogels for tissue engineering: scaffold design variables and applications.* Biomaterials, 2003. **24**(24): p. 4337-51.
150. Ma, L., C. Gao, Z. Mao, J. Shen, X. Hu, and C. Han, *Thermal dehydration treatment and glutaraldehyde cross-linking to increase the biostability of collagen-chitosan porous scaffolds used as dermal equivalent.* J Biomater Sci Polym Ed, 2003. **14**(8): p. 861-74.
151. Langer, R. and J.P. Vacanti, *Tissue engineering.* Science, 1993. **260**(5110): p. 920-6.
152. Falanga, V., D. Margolis, O. Alvarez, M. Auletta, F. Maggiacomo, M. Altman, J. Jensen, M. Sabolinski, and J. Hardin-Young, *Rapid healing of venous ulcers and lack of clinical rejection with an allogeneic cultured human skin equivalent. Human Skin Equivalent Investigators Group.* Arch Dermatol, 1998. **134**(3): p. 293-300.
153. Noah, E.M., J. Chen, X. Jiao, I. Heschel, and N. Pallua, *Impact of sterilization on the porous design and cell behavior in collagen sponges prepared for tissue engineering.* Biomaterials, 2002. **23**(14): p. 2855-61.
154. Nehrer, S., H.A. Breinan, A. Ramappa, H.P. Hsu, T. Minas, S. Shortkroff, C.B. Sledge, I.V. Yannas, and M. Spector, *Chondrocyte-seeded collagen matrices implanted in a chondral defect in a canine model.* Biomaterials, 1998. **19**(24): p. 2313-28.
155. Risbud, M.V., E. Karamuk, V. Schlosser, and J. Mayer, *Hydrogel-coated textile scaffolds as candidate in liver tissue engineering: II. Evaluation of spheroid formation and viability of hepatocytes.* Journal of Biomaterials Science-Polymer Edition, 2003. **14**(7): p. 719-731.
156. Orwin, E.J. and A. Hubel, *In vitro culture characteristics of corneal epithelial, endothelial, and keratocyte cells in a native collagen matrix.* Tissue Engineering, 2000. **6**(4): p. 307-319.
157. Payne, R.G., M.J. Yaszemski, A.W. Yasko, and A.G. Mikos, *Development of an injectable, in situ crosslinkable, degradable polymeric carrier for osteogenic cell populations. Part 1. Encapsulation of marrow stromal osteoblasts in surface crosslinked gelatin microparticles.* Biomaterials, 2002. **23**(22): p. 4359-4371.
158. Awad, H.A., M.Q. Wickham, H.A. Leddy, J.M. Gimble, and F. Guilak, *Chondrogenic differentiation of adipose-derived adult stem cells in agarose, alginate, and gelatin scaffolds.* Biomaterials, 2004. **25**(16): p. 3211-3222.
159. Risbud, M., M. Endres, J. Ringe, R. Bhonde, and M. Sittinger, *Biocompatible hydrogel supports the growth of respiratory epithelial cells: Possibilities in tracheal tissue engineering.* Journal of Biomedical Materials Research, 2001. **56**(1): p. 120-127.

160. Altman, G.H., F. Diaz, C. Jakuba, T. Calabro, R.L. Horan, J. Chen, H. Lu, J. Richmond, and D.L. Kaplan, *Silk-based biomaterials.* Biomaterials, 2003. **24**(3): p. 401-16.
161. Minoura, N., S. Aiba, Y. Gotoh, M. Tsukada, and Y. Imai, *Attachment and growth of cultured fibroblast cells on silk protein matrices.* J Biomed Mater Res, 1995. **29**(10): p. 1215-21.
162. Sofia, S., M.B. McCarthy, G. Gronowicz, and D.L. Kaplan, *Functionalized silk-based biomaterials for bone formation.* J Biomed Mater Res, 2001. **54**(1): p. 139-48.
163. Thomson, R.C., M.C. Wake, M.J. Yaszemski, and A.G. Mikos, *Biodegradable polymer scaffolds to regenerate organs.* Biopolymers Ii, 1995. **122**: p. 245-274.
164. Gunatillake, P.A. and R. Adhikari, *Biodegradable synthetic polymers for tissue engineering.* Eur Cell Mater, 2003. **5**: p. 1-16; discussion 16.
165. Yang, S., K.F. Leong, Z. Du, and C.K. Chua, *The design of scaffolds for use in tissue engineering. Part I. Traditional factors.* Tissue Eng, 2001. **7**(6): p. 679-89.
166. Freed, L.E., J.C. Marquis, A. Nohria, J. Emmanual, A.G. Mikos, and R. Langer, *Neocartilage Formation Invitro and Invivo Using Cells Cultured on Synthetic Biodegradable Polymers.* Journal of Biomedical Materials Research, 1993. **27**(1): p. 11-23.
167. Shinoka, T., P.X. Ma, D. Shum-Tim, C.K. Breuer, R.A. Cusick, G. Zund, R. Langer, J.P. Vacanti, and J.E. Mayer, Jr., *Tissue-engineered heart valves. Autologous valve leaflet replacement study in a lamb model.* Circulation, 1996. **94**(9 Suppl): p. II164-8.
168. Kaihara, S., S. Kim, B.S. Kim, D.J. Mooney, K. Tanaka, and J.P. Vacanti, *Survival and function of rat hepatocytes cocultured with nonparenchymal cells or sinusoidal endothelial cells on biodegradable polymers under flow conditions.* J Pediatr Surg, 2000. **35**(9): p. 1287-90.
169. Mooney, D.J., C.L. Mazzoni, C. Breuer, K. McNamara, D. Hern, J.P. Vacanti, and R. Langer, *Stabilized polyglycolic acid fibre-based tubes for tissue engineering.* Biomaterials, 1996. **17**(2): p. 115-24.
170. Agrawal, C.M. and R.B. Ray, *Biodegradable polymeric scaffolds for musculoskeletal tissue engineering.* J Biomed Mater Res, 2001. **55**(2): p. 141-50.
171. Ishaug-Riley, S.L., L.E. Okun, G. Prado, M.A. Applegate, and A. Ratcliffe, *Human articular chondrocyte adhesion and proliferation on synthetic biodegradable polymer films.* Biomaterials, 1999. **20**(23-24): p. 2245-56.
172. Yang, F., R. Murugan, S. Ramakrishna, X. Wang, Y.X. Ma, and S. Wang, *Fabrication of nano-structured porous PLLA scaffold intended for nerve tissue engineering.* Biomaterials, 2004. **25**(10): p. 1891-900.
173. Park, S.S., H.R. Jin, D.H. Chi, and R.S. Taylor, *Characteristics of tissue-engineered cartilage from human auricular chondrocytes.* Biomaterials, 2004. **25**(12): p. 2363-9.
174. Middleton, J.C. and A.J. Tipton, *Synthetic biodegradable polymers as orthopedic devices.* Biomaterials, 2000. **21**(23): p. 2335-46.
175. El-Amin, S.F., H.H. Lu, Y. Khan, J. Burems, J. Mitchell, R.S. Tuan, and C.T. Laurencin, *Extracellular matrix production by human osteoblasts cultured on*

biodegradable polymers applicable for tissue engineering. Biomaterials, 2003. **24**(7): p. 1213-21.
176. Kim, B.S., J. Nikolovski, J. Bonadio, E. Smiley, and D.J. Mooney, *Engineered smooth muscle tissues: Regulating cell phenotype with the scaffold.* Experimental Cell Research, 1999. **251**(2): p. 318-328.
177. Teng, Y.D., E.B. Lavik, X. Qu, K.I. Park, J. Ourednik, D. Zurakowski, R. Langer, and E.Y. Snyder, *Functional recovery following traumatic spinal cord injury mediated by a unique polymer scaffold seeded with neural stem cells.* Proc Natl Acad Sci U S A, 2002. **99**(5): p. 3024-9.
178. Mooney, D.J., G. Organ, J.P. Vacanti, and R. Langer, *Design and fabrication of biodegradable polymer devices to engineer tubular tissues.* Cell Transplant, 1994. **3**(2): p. 203-10.
179. Dai, N.T., M.R. Williamson, N. Khammo, E.F. Adams, and A.G. Coombes, *Composite cell support membranes based on collagen and polycaprolactone for tissue engineering of skin.* Biomaterials, 2004. **25**(18): p. 4263-71.
180. Barralet, J.E., L.L. Wallace, and A.J. Strain, *Tissue engineering of human biliary epithelial cells on polyglycolic acid/polycaprolactone scaffolds maintains long-term phenotypic stability.* Tissue Eng, 2003. **9**(5): p. 1037-45.
181. Park, Y.J., J.Y. Lee, Y.S. Chang, J.M. Jeong, J.K. Chung, M.C. Lee, K.B. Park, and S.J. Lee, *Radioisotope carrying polyethylene oxide-polycaprolactone copolymer micelles for targetable bone imaging.* Biomaterials, 2002. **23**(3): p. 873-9.
182. Ciapetti, G., L. Ambrosio, L. Savarino, D. Granchi, E. Cenni, N. Baldini, S. Pagani, S. Guizzardi, F. Causa, and A. Giunti, *Osteoblast growth and function in porous poly epsilon -caprolactone matrices for bone repair: a preliminary study.* Biomaterials, 2003. **24**(21): p. 3815-24.
183. Ng, K.W., D.W. Hutmacher, J.T. Schantz, C.S. Ng, H.P. Too, T.C. Lim, T.T. Phan, and S.H. Teoh, *Evaluation of ultra-thin poly(epsilon-caprolactone) films for tissue-engineered skin.* Tissue Eng, 2001. **7**(4): p. 441-55.
184. Fisher, J.P., T.A. Holland, D. Dean, and A.G. Mikos, *Photoinitiated cross-linking of the biodegradable polyester poly(propylene fumarate). Part II. In vitro degradation.* Biomacromolecules, 2003. **4**(5): p. 1335-42.
185. Peter, S.J., M.J. Miller, A.W. Yasko, M.J. Yaszemski, and A.G. Mikos, *Polymer concepts in tissue engineering.* J Biomed Mater Res, 1998. **43**(4): p. 422-7.
186. Suggs, L.J. and A.G. Mikos, *Development of poly(propylene fumarate-co-ethylene glycol) as an injectable carrier for endothelial cells.* Cell Transplant, 1999. **8**(4): p. 345-50.
187. Shung, A.K., E. Behravesh, S. Jo, and A.G. Mikos, *Crosslinking characteristics of and cell adhesion to an injectable poly(propylene fumarate-co-ethylene glycol) hydrogel using a water-soluble crosslinking system.* Tissue Eng, 2003. **9**(2): p. 243-54.
188. Davis, K.A. and K.S. Anseth, *Controlled release from crosslinked degradable networks.* Crit Rev Ther Drug Carrier Syst, 2002. **19**(4-5): p. 385-423.
189. Heller, J., J. Barr, S.Y. Ng, K.S. Abdellauoi, and R. Gurny, *Poly(ortho esters): synthesis, characterization, properties and uses.* Adv Drug Deliv Rev, 2002. **54**(7): p. 1015-39.

190. Andriano, K.P., Y. Tabata, Y. Ikada, and J. Heller, *In vitro and in vivo comparison of bulk and surface hydrolysis in absorbable polymer scaffolds for tissue engineering.* J Biomed Mater Res, 1999. **48**(5): p. 602-12.
191. Vacanti, J.P., M.A. Morse, W.M. Saltzman, A.J. Domb, A. Perez-Atayde, and R. Langer, *Selective cell transplantation using bioabsorbable artificial polymers as matrices.* J Pediatr Surg, 1988. **23**(1 Pt 2): p. 3-9.
192. Langer, R., *Biomaterials in drug delivery and tissue engineering: one laboratory's experience.* Acc Chem Res, 2000. **33**(2): p. 94-101.
193. Kumar, N., R.S. Langer, and A.J. Domb, *Polyanhydrides: an overview.* Adv Drug Deliv Rev, 2002. **54**(7): p. 889-910.
194. Uhrich, K.E., A. Gupta, T.T. Thomas, C.T. Laurencin, and R. Langer, *Synthesis and Characterization of Degradable Poly(Anhydride-Co-Imides).* Macromolecules, 1995. **28**(7): p. 2184-2193.
195. Muggli, D.S., A.K. Burkoth, and K.S. Anseth, *Crosslinked polyanhydrides for use in orthopedic applications: degradation behavior and mechanics.* J Biomed Mater Res, 1999. **46**(2): p. 271-8.
196. Qiu, L.Y. and K.J. Zhu, *Novel biodegradable polyphosphazenes containing glycine ethyl ester and benzyl ester of amino acethydroxamic acid as cosubstituents: Syntheses, characterization, and degradation properties.* Journal of Applied Polymer Science, 2000. **77**(13): p. 2987-2995.
197. Laurencin, C.T., M.E. Norman, H.M. Elgendy, S.F. el-Amin, H.R. Allcock, S.R. Pucher, and A.A. Ambrosio, *Use of polyphosphazenes for skeletal tissue regeneration.* J Biomed Mater Res, 1993. **27**(7): p. 963-73.
198. Laurencin, C.T., S.F. El-Amin, S.E. Ibim, D.A. Willoughby, M. Attawia, H.R. Allcock, and A.A. Ambrosio, *A highly porous 3-dimensional polyphosphazene polymer matrix for skeletal tissue regeneration.* J Biomed Mater Res, 1996. **30**(2): p. 133-8.
199. Langone, F., S. Lora, F.M. Veronese, P. Caliceti, P.P. Parnigotto, F. Valenti, and G. Palma, *Peripheral nerve repair using a poly(organo)phosphazene tubular prosthesis.* Biomaterials, 1995. **16**(5): p. 347-53.
200. Tangpasuthadol, V., S.M. Pendharkar, and J. Kohn, *Hydrolytic degradation of tyrosine-derived polycarbonates, a class of new biomaterials. Part I: study of model compounds.* Biomaterials, 2000. **21**(23): p. 2371-8.
201. Choueka, J., J.L. Charvet, K.J. Koval, H. Alexander, K.S. James, K.A. Hooper, and J. Kohn, *Canine bone response to tyrosine-derived polycarbonates and poly(L-lactic acid).* J Biomed Mater Res, 1996. **31**(1): p. 35-41.
202. Lee, S.J., J.S. Choi, K.S. Park, G. Khang, Y.M. Lee, and H.B. Lee, *Response of MG63 osteoblast-like cells onto polycarbonate membrane surfaces with different micropore sizes.* Biomaterials, 2004. **25**(19): p. 4699-707.
203. Cai, J., S. Bo, R. Cheng, L. Jiang, and Y. Yang, *Analysis of interfacial phenomena of aqueous solutions of polyethylene oxide and polyethylene glycol flowing in hydrophilic and hydrophobic capillary viscometers.* J Colloid Interface Sci, 2004. **276**(1): p. 174-81.
204. Novikova, L.N., L.N. Novikov, and J.O. Kellerth, *Biopolymers and biodegradable smart implants for tissue regeneration after spinal cord injury.* Current Opinion in Neurology, 2003. **16**(6): p. 711-715.

205. Sawhney, A.S., C.P. Pathak, and J.A. Hubbell, *Bioerodible Hydrogels Based on Photopolymerized Poly(Ethylene Glycol)-Co-Poly(Alpha-Hydroxy Acid) Diacrylate Macromers.* Macromolecules, 1993. **26**(4): p. 581-587.
206. Sims, C.D., P.E. Butler, R. Casanova, B.T. Lee, M.A. Randolph, W.P. Lee, C.A. Vacanti, and M.J. Yaremchuk, *Injectable cartilage using polyethylene oxide polymer substrates.* Plast Reconstr Surg, 1996. **98**(5): p. 843-50.
207. Bourke, S.L. and J. Kohn, *Polymers derived from the amino acid L-tyrosine: polycarbonates, polyarylates and copolymers with poly(ethylene glycol).* Adv Drug Deliv Rev, 2003. **55**(4): p. 447-66.
208. Bryant, S.J. and K.S. Anseth, *Controlling the spatial distribution of ECM components in degradable PEG hydrogels for tissue engineering cartilage.* J Biomed Mater Res, 2003. **64A**(1): p. 70-9.
209. Desai, N.P., A. Sojomihardjo, Z. Yao, N. Ron, and P. Soon-Shiong, *Interpenetrating polymer networks of alginate and polyethylene glycol for encapsulation of islets of Langerhans.* J Microencapsul, 2000. **17**(6): p. 677-90.
210. Ganta, S.R., N.P. Piesco, P. Long, R. Gassner, L.F. Motta, G.D. Papworth, D.B. Stolz, S.C. Watkins, and S. Agarwal, *Vascularization and tissue infiltration of a biodegradable polyurethane matrix.* J Biomed Mater Res, 2003. **64A**(2): p. 242-8.
211. Gorna, K. and S. Gogolewski, *Preparation, degradation, and calcification of biodegradable polyurethane foams for bone graft substitutes.* J Biomed Mater Res, 2003. **67A**(3): p. 813-27.
212. Zhang, J., B.A. Doll, E.J. Beckman, and J.O. Hollinger, *A biodegradable polyurethane-ascorbic acid scaffold for bone tissue engineering.* J Biomed Mater Res, 2003. **67A**(2): p. 389-400.
213. Grad, S., L. Kupcsik, K. Gorna, S. Gogolewski, and M. Alini, *The use of biodegradable polyurethane scaffolds for cartilage tissue engineering: potential and limitations.* Biomaterials, 2003. **24**(28): p. 5163-71.
214. McDevitt, T.C., K.A. Woodhouse, S.D. Hauschka, C.E. Murry, and P.S. Stayton, *Spatially organized layers of cardiomyocytes on biodegradable polyurethane films for myocardial repair.* J Biomed Mater Res, 2003. **66A**(3): p. 586-95.
215. Anseth, K.S., A.T. Metters, S.J. Bryant, P.J. Martens, J.H. Elisseeff, and C.N. Bowman, *In situ forming degradable networks and their application in tissue engineering and drug delivery.* Journal of Controlled Release, 2002. **78**(1-3): p. 199-209.
216. Kim, B.S., C.E. Baez, and A. Atala, *Biomaterials for tissue engineering.* World J Urol, 2000. **18**(1): p. 2-9.
217. Dar, A., M. Shachar, J. Leor, and S. Cohen, *Cardiac tissue engineering - Optimization of cardiac cell seeding and distribution in 3D porous alginate scaffolds.* Biotechnology and Bioengineering, 2002. **80**(3): p. 305-312.
218. Sachlos, E. and J.T. Czernuszka, *Making tissue engineering scaffolds work. Review: the application of solid freeform fabrication technology to the production of tissue engineering scaffolds.* Eur Cell Mater, 2003. **5**: p. 29-39; discussion 39-40.
219. Lu, L., X. Zhu, R.G. Valenzuela, B.L. Currier, and M.J. Yaszemski, *Biodegradable polymer scaffolds for cartilage tissue engineering.* Clin Orthop, 2001(391 Suppl): p. S251-70.

220. Chen, G.P., T. Ushida, and T. Tateishi, *Development of biodegradable porous scaffolds for tissue engineering.* Materials Science & Engineering C-Biomimetic and Supramolecular Systems, 2001. **17**(1-2): p. 63-69.
221. Griffith, L.G., *Polymeric biomaterials.* Acta Materialia, 2000. **48**(1): p. 263-277.
222. Yang, S., K.F. Leong, Z. Du, and C.K. Chua, *The design of scaffolds for use in tissue engineering. Part II. Rapid prototyping techniques.* Tissue Eng, 2002. **8**(1): p. 1-11.
223. Shive, M.S. and J.M. Anderson, *Biodegradation and biocompatibility of PLA and PLGA microspheres.* Adv Drug Deliv Rev, 1997. **28**(1): p. 5-24.
224. Ziats, N.P., K.M. Miller, and J.M. Anderson, *In vitro and in vivo interactions of cells with biomaterials.* Biomaterials, 1988. **9**(1): p. 5-13.
225. Anderson, J.M. and K.M. Miller, *Biomaterial biocompatibility and the macrophage.* Biomaterials, 1984. **5**(1): p. 5-10.
226. von Burkersroda, F., L. Schedl, and A. Gopferich, *Why degradable polymers undergo surface erosion or bulk erosion.* Biomaterials, 2002. **23**(21): p. 4221-4231.
227. Yoon, D.M. and J.P. Fisher, *Polymeric Scaffolds for Tissue Engineering Applications*. Third ed. The Biomedical Engineering Handbook: Tissue Engineering and Artificial Organs, ed. J.D. Bronzino. 2006, Boca Raton: CRC Press. 37-1 - 37-18.
228. Vacanti, C.A., R. Langer, B. Schloo, and J.P. Vacanti, *Synthetic polymers seeded with chondrocytes provide a template for new cartilage formation.* Plast Reconstr Surg, 1991. **88**(5): p. 753-9.
229. Murphy, C.L. and A. Sambanis, *Effect of oxygen tension and alginate encapsulation on restoration of the differentiated phenotype of passaged chondrocytes.* Tissue Eng, 2001. **7**(6): p. 791-803.
230. van Susante, J.L., P. Buma, H.M. van Beuningen, W.B. van den Berg, and R.P. Veth, *Responsiveness of bovine chondrocytes to growth factors in medium with different serum concentrations.* J Orthop Res, 2000. **18**(1): p. 68-77.
231. Genes, N.G., J.A. Rowley, D.J. Mooney, and L.J. Bonassar, *Effect of substrate mechanics on chondrocyte adhesion to modified alginate surfaces.* Arch Biochem Biophys, 2004. **422**(2): p. 161-7.
232. Lin, Z., C. Willers, J. Xu, and M.H. Zheng, *The chondrocyte: biology and clinical application.* Tissue Eng, 2006. **12**(7): p. 1971-84.
233. Yoon, D.M. and J.P. Fisher, *Chondrocyte Signaling and Artificial Matrices for Articular Cartilage Engineering*. Tissue Engineering: Special Edition of the Advances in Experimental Medicine and Biology, ed. J.P. Fisher. Vol. 585. 2006, New York: Springer. 67-86.
234. Loeser, R.F., S. Chubinskaya, C. Pacione, and H.J. Im, *Basic fibroblast growth factor inhibits the anabolic activity of insulin-like growth factor 1 and osteogenic protein 1 in adult human articular chondrocytes.* Arthritis Rheum, 2005. **52**(12): p. 3910-7.
235. Yasuda, A., K. Kojima, K.W. Tinsley, H. Yoshioka, Y. Mori, and C.A. Vacanti, *In vitro culture of chondrocytes in a novel thermoreversible gelation polymer scaffold containing growth factors.* Tissue Eng, 2006. **12**(5): p. 1237-45.

236. McQuillan, D.J., C.J. Handley, M.A. Campbell, S. Bolis, V.E. Milway, and A.C. Herington, *Stimulation of proteoglycan biosynthesis by serum and insulin-like growth factor-I in cultured bovine articular cartilage.* Biochem J, 1986. **240**(2): p. 423-30.
237. Schalkwijk, J., L.A. Joosten, W.B. van den Berg, J.J. van Wyk, and L.B. van de Putte, *Insulin-like growth factor stimulation of chondrocyte proteoglycan synthesis by human synovial fluid.* Arthritis Rheum, 1989. **32**(1): p. 66-71.
238. Hunziker, E.B., T.M. Quinn, and H.J. Hauselmann, *Quantitative structural organization of normal adult human articular cartilage.* Osteoarthritis Cartilage, 2002. **10**(7): p. 564-72.
239. Lin, Z., C. Willers, J. Xu, and M.H. Zheng, *The Chondrocyte: Biology and Clinical Application.* Tissue Eng, 2006.
240. Yasuda, A., K. Kojima, K.W. Tinsley, H. Yoshioka, Y. Mori, and C.A. Vacanti, *In Vitro Culture of Chondrocytes in a Novel Thermoreversible Gelation Polymer Scaffold Containing Growth Factors.* Tissue Eng, 2006.
241. Hodgkinson, S.C., L. Moore, J.R. Napier, S.R. Davis, J.J. Bass, and P.D. Gluckman, *Characterization of insulin-like growth factor binding proteins in ovine tissue fluids.* J Endocrinol, 1989. **120**(3): p. 429-38.
242. Baxter, R.C. and J.L. Martin, *Binding proteins for the insulin-like growth factors: structure, regulation and function.* Prog Growth Factor Res, 1989. **1**(1): p. 49-68.
243. Martin, J.A. and J.A. Buckwalter, *The role of chondrocyte-matrix interactions in maintaining and repairing articular cartilage.* Biorheology, 2000. **37**(1-2): p. 129-40.
244. Schneiderman, R., N. Rosenberg, J. Hiss, P. Lee, F. Liu, R.L. Hintz, and A. Maroudas, *Concentration and size distribution of insulin-like growth factor-I in human normal and osteoarthritic synovial fluid and cartilage.* Arch Biochem Biophys, 1995. **324**(1): p. 173-88.
245. Eviatar, T., H. Kauffman, and A. Maroudas, *Synthesis of insulin-like growth factor binding protein 3 in vitro in human articular cartilage cultures.* Arthritis Rheum, 2003. **48**(2): p. 410-7.
246. Chevalier, X. and J.A. Tyler, *Production of binding proteins and role of the insulin-like growth factor I binding protein 3 in human articular cartilage explants.* Br J Rheumatol, 1996. **35**(6): p. 515-22.
247. Yoon, D.M. and J.P. Fisher, *Chondrocyte signaling and artificial matrices for articular cartilage engineering.* Adv Exp Med Biol, 2006. **585**: p. 67-86.
248. Nixon, A.J., R.A. Saxer, and B.D. Brower-Toland, *Exogenous insulin-like growth factor-I stimulates an autoinductive IGF-I autocrine/paracrine response in chondrocytes.* J Orthop Res, 2001. **19**(1): p. 26-32.
249. Porter, R.M., R.M. Akers, R.D. Howard, and K. Forsten-Williams, *Alginate Encapsulation Impacts the Insulin-like Growth Factor-I System of Monolayer-Expanded Equine Articular Chondrocytes and Cell Response to Interleukin-1beta.* Tissue Eng, 2007.
250. Hauselmann, H.J., R.J. Fernandes, S.S. Mok, T.M. Schmid, J.A. Block, M.B. Aydelotte, K.E. Kuettner, and E.J. Thonar, *Phenotypic stability of bovine articular chondrocytes after long-term culture in alginate beads.* J Cell Sci, 1994. **107 (Pt 1)**: p. 17-27.

251. Smetana, K., Jr., *Cell biology of hydrogels.* Biomaterials, 1993. **14**(14): p. 1046-50.
252. Smidsrod, O. and G. Skjak-Braek, *Alginate as immobilization matrix for cells.* Trends Biotechnol, 1990. **8**(3): p. 71-8.
253. Yoon, D.M., E.C. Hawkins, S. Francke-Carroll, and J.P. Fisher, *Effect of construct properties on encapsulated chondrocyte expression of insulin-like growth factor-1.* Biomaterials, 2007. **28**(2): p. 299-306.
254. van Osch, G.J., W.B. van den Berg, E.B. Hunziker, and H.J. Hauselmann, *Differential effects of IGF-1 and TGF beta-2 on the assembly of proteoglycans in pericellular and territorial matrix by cultured bovine articular chondrocytes.* Osteoarthritis Cartilage, 1998. **6**(3): p. 187-95.
255. Honegger, A. and R.E. Humbel, *Insulin-like growth factors I and II in fetal and adult bovine serum. Purification, primary structures, and immunological cross-reactivities.* J Biol Chem, 1986. **261**(2): p. 569-75.
256. Rosenberg, L., *Chemical basis for the histological use of safranin O in the study of articular cartilage.* J Bone Joint Surg Am, 1971. **53**(1): p. 69-82.
257. Favre, E., M. Leonard, A. Laurent, and E. Dellacherie, *Diffusion of polyethyleneglycols in calcium alginate hydrogels.* Colloids and Surfaces a-Physicochemical and Engineering Aspects, 2001. **194**(1-3): p. 197-206.
258. Nauman, J.V., P.G. Campbell, F. Lanni, and J.L. Anderson, *Diffusion of insulin-like growth factor-I and ribonuclease through fibrin gels.* Biophys J, 2007. **92**(12): p. 4444-50.
259. Leddy, H.A., H.A. Awad, and F. Guilak, *Molecular diffusion in tissue-engineered cartilage constructs: effects of scaffold material, time, and culture conditions.* J Biomed Mater Res B Appl Biomater, 2004. **70**(2): p. 397-406.
260. Loeser, R.F., G. Shanker, C.S. Carlson, J.F. Gardin, B.J. Shelton, and W.E. Sonntag, *Reduction in the chondrocyte response to insulin-like growth factor 1 in aging and osteoarthritis: studies in a non-human primate model of naturally occurring disease.* Arthritis Rheum, 2000. **43**(9): p. 2110-20.
261. Chubinskaya, S., A. Hakimiyan, C. Pacione, A. Yanke, L. Rappoport, T. Aigner, D.C. Rueger, and R.F. Loeser, *Synergistic effect of IGF-1 and OP-1 on matrix formation by normal and OA chondrocytes cultured in alginate beads.* Osteoarthritis Cartilage, 2007. **15**(4): p. 421-30.
262. Trippel, S.B., *Growth factor actions on articular cartilage.* J Rheumatol Suppl, 1995. **43**: p. 129-32.
263. O'Connor, W.J., T. Botti, S.N. Khan, and J.M. Lane, *The use of growth factors in cartilage repair.* Orthop Clin North Am, 2000. **31**(3): p. 399-410.
264. Luyten, F.P., V.C. Hascall, S.P. Nissley, T.I. Morales, and A.H. Reddi, *Insulin-like growth factors maintain steady-state metabolism of proteoglycans in bovine articular cartilage explants.* Arch Biochem Biophys, 1988. **267**(2): p. 416-25.
265. Tyler, J.A., *Insulin-like growth factor 1 can decrease degradation and promote synthesis of proteoglycan in cartilage exposed to cytokines.* Biochem J, 1989. **260**(2): p. 543-8.
266. Bryant, S.J., C.R. Nuttelman, and K.S. Anseth, *The effects of crosslinking density on cartilage formation in photocrosslinkable hydrogels.* Biomed Sci Instrum, 1999. **35**: p. 309-14.

267. Kuo, Y.C. and I.N. Ku, *Effects of gel concentration, human fibronectin, and cation supplement on the tissue-engineered cartilage.* Biotechnol Prog, 2007. **23**(1): p. 238-45.
268. Mahmoudifar, N. and P.M. Doran, *Effect of seeding and bioreactor culture conditions on the development of human tissue-engineered cartilage.* Tissue Eng, 2006. **12**(6): p. 1675-85.
269. Porter, R.M., R.M. Akers, R.D. Howard, and K. Forsten-Williams, *Alginate encapsulation impacts the insulin-like growth factor-I system of monolayer-expanded equine articular chondrocytes and cell response to interleukin-1beta.* Tissue Eng, 2007. **13**(6): p. 1333-45.
270. Saini, S. and T.M. Wick, *Concentric cylinder bioreactor for production of tissue engineered cartilage: effect of seeding density and hydrodynamic loading on construct development.* Biotechnol Prog, 2003. **19**(2): p. 510-21.
271. Yen, C.N., Y.R. Lin, M.D. Chang, C.W. Tien, Y.C. Wu, C.J. Liao, and Y.C. Hu, *Use of porous alginate sponges for substantial chondrocyte expansion and matrix production: effects of seeding density.* Biotechnol Prog, 2008. **24**(2): p. 452-7.
272. Yoon, D.M. and J.P. Fisher, *Effects of exogenous IGF-1 delivery on the early expression of IGF-1 signaling molecules by alginate embedded chondrocytes.* Tissue Eng Part A, 2008. **14**(7): p. 1263-73.
273. Holmes, M.W., M.T. Bayliss, and H. Muir, *Hyaluronic acid in human articular cartilage. Age-related changes in content and size.* Biochem J, 1988. **250**(2): p. 435-41.
274. Kamada, H., K. Masuda, A.L. D'Souza, M.E. Lenz, D. Pietryla, L. Otten, and E.J. Thonar, *Age-related differences in the accumulation and size of hyaluronan in alginate culture.* Arch Biochem Biophys, 2002. **408**(2): p. 192-9.
275. Knudson, C.B. and W. Knudson, *Hyaluronan and CD44: modulators of chondrocyte metabolism.* Clin Orthop Relat Res, 2004(427 Suppl): p. S152-62.
276. Hua, Q., C.B. Knudson, and W. Knudson, *Internalization of hyaluronan by chondrocytes occurs via receptor-mediated endocytosis.* J Cell Sci, 1993. **106 (Pt 1)**: p. 365-75.
277. Knudson, W. and R.F. Loeser, *CD44 and integrin matrix receptors participate in cartilage homeostasis.* Cell Mol Life Sci, 2002. **59**(1): p. 36-44.
278. Akmal, M., A. Singh, A. Anand, A. Kesani, N. Aslam, A. Goodship, and G. Bentley, *The effects of hyaluronic acid on articular chondrocytes.* J Bone Joint Surg Br, 2005. **87**(8): p. 1143-9.
279. Yoo, H.S., E.A. Lee, J.J. Yoon, and T.G. Park, *Hyaluronic acid modified biodegradable scaffolds for cartilage tissue engineering.* Biomaterials, 2005. **26**(14): p. 1925-33.
280. Gerard, C., C. Catuogno, C. Amargier-Huin, L. Grossin, P. Hubert, P. Gillet, P. Netter, E. Dellacherie, and E. Payan, *The effect of alginate, hyaluronate and hyaluronate derivatives biomaterials on synthesis of non-articular chondrocyte extracellular matrix.* J Mater Sci Mater Med, 2005. **16**(6): p. 541-51.
281. Nishimoto, S., M. Takagi, S. Wakitani, T. Nihira, and T. Yoshida, *Effect of chondroitin sulfate and hyaluronic acid on gene expression in a three-dimensional culture of chondrocytes.* J Biosci Bioeng, 2005. **100**(1): p. 123-6.

282. Chung, C., I.E. Erickson, R.L. Mauck, and J.A. Burdick, *Differential behavior of auricular and articular chondrocytes in hyaluronic acid hydrogels.* Tissue Eng Part A, 2008. **14**(7): p. 1121-31.
283. Lindenhayn, K., C. Perka, R. Spitzer, H. Heilmann, K. Pommerening, J. Mennicke, and M. Sittinger, *Retention of hyaluronic acid in alginate beads: aspects for in vitro cartilage engineering.* J Biomed Mater Res, 1999. **44**(2): p. 149-55.
284. Homandberg, G.A., V. Ummadi, and H. Kang, *The role of insulin-like growth factor-I in hyaluronan mediated repair of cultured cartilage explants.* Inflamm Res, 2004. **53**(8): p. 396-404.
285. Davies, L.C., E.J. Blain, S.J. Gilbert, B. Caterson, and V.C. Duance, *The potential of IGF-1 and TGFbeta1 for promoting "adult" articular cartilage repair: an in vitro study.* Tissue Eng Part A, 2008. **14**(7): p. 1251-61.
286. Karna, E., W. Miltyk, A. Surazynski, and J.A. Palka, *Protective effect of hyaluronic acid on interleukin-1-induced deregulation of beta1-integrin and insulin-like growth factor-I receptor signaling and collagen biosynthesis in cultured human chondrocytes.* Mol Cell Biochem, 2008. **308**(1-2): p. 57-64.
287. Chung, C. and J.A. Burdick, *Engineering cartilage tissue.* Adv Drug Deliv Rev, 2008. **60**(2): p. 243-62.
288. Sohier, J., L. Moroni, C. van Blitterswijk, K. de Groot, and J.M. Bezemer, *Critical factors in the design of growth factor releasing scaffolds for cartilage tissue engineering.* Expert Opin Drug Deliv, 2008. **5**(5): p. 543-66.
289. Elisseeff, J., *Injectable cartilage tissue engineering.* Expert Opin Biol Ther, 2004. **4**(12): p. 1849-59.
290. Schmidt, M.B., E.H. Chen, and S.E. Lynch, *A review of the effects of insulin-like growth factor and platelet derived growth factor on in vivo cartilage healing and repair.* Osteoarthritis Cartilage, 2006. **14**(5): p. 403-12.
291. Madry, H., G. Kaul, M. Cucchiarini, U. Stein, D. Zurakowski, K. Remberger, M.D. Menger, D. Kohn, and S.B. Trippel, *Enhanced repair of articular cartilage defects in vivo by transplanted chondrocytes overexpressing insulin-like growth factor I (IGF-I).* Gene Ther, 2005. **12**(15): p. 1171-9.
292. Nunamaker, E.A., E.K. Purcell, and D.R. Kipke, *In vivo stability and biocompatibility of implanted calcium alginate disks.* J Biomed Mater Res A, 2007. **83**(4): p. 1128-37.
293. Barbucci, R., S. Lamponi, A. Borzacchiello, L. Ambrosio, M. Fini, P. Torricelli, and R. Giardino, *Hyaluronic acid hydrogel in the treatment of osteoarthritis.* Biomaterials, 2002. **23**(23): p. 4503-13.
294. Chung, C., J. Mesa, M.A. Randolph, M. Yaremchuk, and J.A. Burdick, *Influence of gel properties on neocartilage formation by auricular chondrocytes photoencapsulated in hyaluronic acid networks.* J Biomed Mater Res A, 2006. **77**(3): p. 518-25.
295. Grigolo, B., L. Roseti, M. Fiorini, M. Fini, G. Giavaresi, N.N. Aldini, R. Giardino, and A. Facchini, *Transplantation of chondrocytes seeded on a hyaluronan derivative (hyaff-11) into cartilage defects in rabbits.* Biomaterials, 2001. **22**(17): p. 2417-24.

296. Dausse, Y., L. Grossin, G. Miralles, S. Pelletier, D. Mainard, P. Hubert, D. Baptiste, P. Gillet, E. Dellacherie, P. Netter, and E. Payan, *Cartilage repair using new polysaccharidic biomaterials: macroscopic, histological and biochemical approaches in a rat model of cartilage defect.* Osteoarthritis Cartilage, 2003. **11**(1): p. 16-28.
297. Allemann, F., S. Mizuno, K. Eid, K.E. Yates, D. Zaleske, and J. Glowacki, *Effects of hyaluronan on engineered articular cartilage extracellular matrix gene expression in 3-dimensional collagen scaffolds.* J Biomed Mater Res, 2001. **55**(1): p. 13-9.
298. Liao, E., M. Yaszemski, P. Krebsbach, and S. Hollister, *Tissue-engineered cartilage constructs using composite hyaluronic acid/collagen I hydrogels and designed poly(propylene fumarate) scaffolds.* Tissue Eng, 2007. **13**(3): p. 537-50.
299. Takeuchi, R., T. Saito, H. Ishikawa, H. Takigami, M. Dezawa, C. Ide, Y. Itokazu, M. Ikeda, T. Shiraishi, and S. Morishita, *Effects of vibration and hyaluronic acid on activation of three-dimensional cultured chondrocytes.* Arthritis Rheum, 2006. **54**(6): p. 1897-905.
300. Tognana, E., A. Borrione, C. De Luca, and A. Pavesio, *Hyalograft C: hyaluronan-based scaffolds in tissue-engineered cartilage.* Cells Tissues Organs, 2007. **186**(2): p. 97-103.
301. Park, S.H., S.R. Park, S.I. Chung, K.S. Pai, and B.H. Min, *Tissue-engineered cartilage using fibrin/hyaluronan composite gel and its in vivo implantation.* Artif Organs, 2005. **29**(10): p. 838-45.

11 Appendix A: Cell-to-Cell Distance Calculation

Variables:

x = # of chondrocytes per alginate bead
R_A = radius of alginate bead = 1500 μm
R_C = radius of chondrocyte = 7.5μm
$R_V = R_C + R_{boundary}$

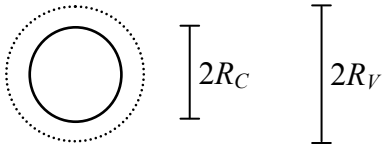

Equations:

$$V_{\text{alginate}} = \frac{4}{3}\pi R_A^{\,3}$$

$$V_{\text{void}} = \frac{4}{3}\pi R_V^{\,3}$$

Find Cell to Cell Distance:

$$V_{\text{void}} = \frac{V_{\text{alginate}}}{x}$$

$$\frac{4}{3}\pi R_V^{\,3} = \frac{\left(\frac{4}{3}\pi R_A^{\,3}\right)}{x}$$

$$R_V = \left(\frac{R_A^{\,3}}{x}\right)^{\frac{1}{3}}$$

Cell to Cell Distance = $2\left(R_V - R_C\right)$